UNIVERSITY OF BIRMINGHAM

Controlled Release of Automatic Dishwashing Detergent Ingredients

by

Thomas Mark Fenton

A thesis submitted to
University of Birmingham

for the degree of

DOCTOR OF PHILOSOPHY

University of Birmingham

School of Chemical Engineering

College of Engineering and Physical Sciences

October 2022

Abstract

Dishwashers are a ubiquitous appliance in almost every modern household in the United Kingdom. Millions of people everyday load their dishwasher with their dirty crockery and glassware, insert a tablet or pouch and run a washing cycle without consideration of if the cleaning performance of their dishwasher could be improved. The familiar compressed powdered or liquid detergent capsules have been a mainstay of the supermarket aisles for decades, with only minor improvements made in their formulation characteristics and performance in this time period. The primary issue which still plagues current formulations is the inherent incompatibility between several of the detergent ingredients, caused by mixing harsh chemical reagents such as bleach, with sensitive ingredients such as non-ionic surfactants and enzymes. Current formulations offer only rudimentary ways of separating these incompatible ingredients in storage and during the wash cycle. The focus of this thesis was to create a way of encapsulating these ingredients such that good segregation would be achieved during storage and in the wash cycle, whereby the release profile of the ingredient would be well-understood and tuneable to the consumer requirements. To carry out this task, a variety of hydrocolloid gels were investigated for their ability to encapsulate and selectively release an enzyme and surfactant which are sustainable, renewable and non-toxic materials. It was shown that both kappa carrageenan and low acyl gellan with tamarind seed xyloglucan could form suitable gels for this purpose. The encapsulation of sodium hypochlorite bleach was more difficult due to its low molecular weight giving a consequentially high diffusivity, and its harsh chemical

nature. Hence, paraffin wax and soy wax were successfully employed as chemical resistant encapsulation materials with very low porosity. Three different techniques were employed to encapsulate the bleach within wax capsules, the most efficient and effective of these was a novel method "freeze dropped" method proposed in this thesis which produced wax capsules which were more stable to leakage and were produced at a higher encapsulation efficiency than other tested methods previously proposed in literature.

In summary this thesis proposed various methods and materials for the encapsulation and thermoselective release of automatic dishwashing detergent ingredients, as well as exploring the nature of any interactions between the detergent ingredients and the encapsulation materials. It is possible that the work proposed in this thesis could be used to develop a temperature-activated detergent capsule. Additionally, work regarding the interaction between detergent ingredients and encapsulation materials, particularly those concerning biopolymer gels, could be useful in other fields where mixtures of these ingredients are also common, such as food, cosmetics and pharmaceuticals. And finally, the novel gel formulation of low acyl gellan gum with tamarind seed xyloglucan could see potential as a gelatine replacement in the food and pharmaceutical industry due to its high mechanical strength combined with its low melting point, which is a rare property in biopolymer gels.

Acknowledgements

This thesis would simply not be possible without the dedication and support of many friends and colleagues who have helped me along this journey – too many to name, however, I will do my best to highlight those whose contributions are appreciated upmost.

Firstly, I would like to say a humungous thank you to Prof. Eddie Pelan. I was his first PhD student and have fond memories of trying to catch a quick meeting with him before his flight back home to the Netherlands during my first few months at Birmingham. With his wry smile, quick wit and sharp scientific mind, Eddie took to his supervisory role like a duck to water and has always made time to chat about science and my thesis, but more importantly, Formula 1. We may not agree on whether Max Verstappen is 'talented', or simply a 'jumped-up Dutch playboy who couldn't drive a milk float', but our discussions were *always* fruitful. My time at Birmingham would simply not have been the same without you Eddie – so thanks again. And thank you to the rest of the staff at the School of Chemical Engineering who have helped guide my journey – namely, Prof. Ian Norton, Prof. Bettina Wolf, Dr Fotis Spyropoulos and Dr Tom Mills. Not to mention, the many colleagues and friends who I have met during my time at the University of Birmingham, with whom I shared many Tesco meal deal lunches on the floor of the lab corridor and offered me so much warmth and support. A special mention to Mike, Chris, Kilian, Glen, Ana, Kelsey, Peter, Alex, Amy & Nelli on this front.

I could not have written this thesis without the support of my family. Support from my parents, from Sharon & Philip, including giving me a lockdown home (which I conveniently haven't moved out from yet), from my wonderful cats Muffin & Lola but most of all from Grace. Like a pair of masochists, fresh out of doing our Master's degrees we both dived head-first in to a PhD, care-free and perhaps a little naïve of the work which lay ahead of us. Soon enough, the reality set in. By trying to emulate Grace's astonishingly brilliant academic example, she pushed me to be better, to work harder. Thank you, Grace, for all the proof-reads, all the advice and all the love, for which I will be eternally grateful. Unfotrunely you hav'ent proof-red this bit for me, so I will try to get it wright.

How did I do?

In fact, don't tell me. Next time we have any bright ideas about spending 4 years doing a PhD, maybe we should have another think and just watch television with the cats instead.

A final thanks to the School of Chemical Engineering, University of Birmingham for funding this PhD, without whom this work would have been financially impossible.

Table of Contents

List of Illustrations

List of Tables

Nomenclature – Symbols

A	Absorbance
A_0	Initial absorbance
A_t	Absorbance at time 't'
ΔA	Change in absorbance
°C	Degrees Celsius
g	Grams
G'	Storage modulus
G''	Loss modulus
k_1	Power law constant
L	Path length
m	Relaxation exponent
p	Pearson correlation coefficient
P(one-tail)	Probability value for one-tailed T-test
R^2	Coefficient of determination

SD	Standard deviation
T	Temperature
T_g	Gelling temperature
T_m	Melting temperature
$T_{coil\text{-}helix}$	Coil-helix transition temperature
$T_{helix\text{-}coil}$	Helix-coil transition temperature
T_{peak}	Peak temperature
t	Time
w/v	Weight-by-volume basis
w/w	Weight-by-weight basis
γ	Interfacial tension
Δ	Change in (*prefix*)
δ	Phase angle
σ	Conductivity
$\sigma_{initial}$	Initial conductivity
σ_{final}	Final conductivity
σ_t	Conductivity at time 't'
τ	Turbidity
ω	Angular frequency

Nomenclature – Abbreviations

ADD	Automatic dishwashing detergent
CL	Capsule leakage
ca.	*Circa* (approximately)
CD	Cold dropping
CAC	Critical aggregation concentration
CMC	Critical micelle concentration
D36	Dehypon LS 36
DI	Deionised
DSC	Differential scanning calorimetry
EE	Encapsulation efficiency
exo	Exothermic
FD	Freeze dropping
HAG	High acyl gellan gum
ιC	Iota carrageenan
kC or κC	Kappa carrageenan
λC	Lambda carrageenan
LVR	Linear viscoelastic region
LAG	Low acyl gellan gum
μDSC	Micro differential scanning calorimetry
MW	Molecular weight
MM	Moulding method

μC	Mu carrageenan
νC	Nu carrageenan
PW	Paraffin wax
PGPR	Polyglycerol polyricinoleate
PLA	Polylactic acid
PTFE	Polytetrafluoroethylene
rpm	Revolutions per minute
SW	Soy wax
TSX	Tamarind seed xyloglucan
TA	Texture analysis
θC	Theta carrageenan
T20	Tween 20
UV/Vis	Ultraviolet/Visible Light

1

Introduction

1.1 Abstract

The following section will seek to discuss the background information and the motivation for this thesis, putting the importance of the work in the wider context of the academic field and industrial importance. It will also seek to lay out the aims and objectives of the thesis and provide information on the proceeding thesis structure. Furthermore, publications in academic journals and presentations at academic conferences as a result of the work covered in this thesis will be listed.

1.2 Background Information and Motivation

Automatic dishwashing has revolutionised the way cleaning of crockery and glassware is done, both domestically and industrially: cleaning has become easier, more thorough, more energy and water efficient, and quicker than what was previously possible by hand washing. Effective cleaning with a dishwasher occurs through a combination of mechanical, thermal, and chemical factors to remove food soils. The mechanical and thermal cleaning aspects are dictated by the design of the dishwasher and is therefore not something that the consumer or operator can easily change or adjust, apart from the small choice of pre-set wash cycles. However, the chemical cleaning is carried out by the dishwasher tablet, and the consumers' choice of tablet can heavily dictate the cleaning performance.

Currently available consumer-grade dishwasher tablets consist of either compacted powder or liquid 'gels' stored in water-soluble pouches (industrial dishwashers are typically 'fed' by large detergent containers). The ingredients within dishwasher tablets present certain formulation challenges, as there is a mixture of harsh chemicals with sensitive cleaning agents – both of which are necessary for successful cleaning. However, neither compacted powder nor liquid pouch-type dishwasher tablets present a good way of separating the storage and release of ingredients during storage, and more importantly, the wash cycle.

Controlled release is an area of formulation science which is growing exponentially, and deservedly so. In general, controlled release describes an approach to formulation which involves encapsulating or immobilising an active ingredient in a matrix, or inside a capsule. The properties of the matrix or the capsule can be tuned and designed in order to achieve the desired release profile. In the pharmaceutical industry, this formulation approach is a common method to delay the release of drugs over time, or to contain and subsequently rapidly release drugs in certain locations, for example, the stomach. However, controlled-release tactics are now being applied to other industries, such as food and fast moving consumer goods.

1.3 Aims and Objectives

The primary objective of this thesis was to design a method - or several methods - that could be capable of producing controlled-release vehicles which contained key automatic dishwashing detergent ingredients. Dishwashers gradually increase the water temperature over the duration of the wash cycle from ambient up to 60 – 70 °C, hence it was surmised that the controlled release vehicle should show burst-type release in response to a temperature trigger, whilst effectively containing the ingredient prior to release. Additionally, it was a key objective to understand and characterise the effect that the dishwashing ingredient had on the structure and properties of the encapsulating material. And finally, it was planned to devise experiments which could quantify the rate of release of the active ingredient in to a simulated dishwashing environment.

1.4 Thesis Layout

The proceeding thesis follows the *alternative thesis* format endorsed by the University of Birmingham, and references are provided in each chapter. In addition to a literature review, the results chapters will consist of published journal articles, journal articles currently under review in peer-reviewed journals or completed manuscripts awaiting submission to a journal. *Chapter 2* consists of the literature review covering an introduction to detergency and controlled release, with a particular focus on the use of hydrocolloids and waxes as controlled release

materials. *Chapter 3* is the first experimental chapter and examines the use of kappa carrageenan to encapsulate non-ionic surfactants. The influence that the surfactant has on the structure and properties of the carrageenan is investigated using rheology and calorimetry (Fenton, Kanyuck, Mills, & Pelan, 2021). *Chapter 4* builds on the work set out in the previous chapter and discusses the use of low acyl gellan with tamarind seed xyloglucan to encapsulate non-ionic surfactants. Through intradepartmental collaboration, this formulation was manufactured using additive manufacturing to create novel, printed structures. The structure and the physical properties of the gel was investigated in a similar manner to kappa carrageenan in the previous chapter – using rheology and calorimetry (Fenton, Gholamipour-Shirazi, Daffner, Mills, & Pelan, 2021). *Chapter 5* moves the focus away from non-ionic surfactants and towards α-amylase as the encapsulated active ingredient, with the encapsulation materials and methods similar to those in previous chapters – using gelling hydrocolloids. In this chapter, special attention is given to determining the amylase activity, which increases the complexity beyond the release of surfactant. *Chapter 6* focuses on the use of waxes and manufacturing techniques to encapsulate bleach inside sealed wax capsules. Three methods are presented to manufacture these wax capsules, whereby two methods are reported in the literature, and one is novel to this thesis. Texture analysis and calorimetry are key techniques used to characterise the waxes and capsules respectively. *Chapter 7* will seek to bring forth the major conclusions and findings from this thesis and makes suggestions for future avenues of research.

1.5 Publications

Fenton, T., Gholamipour-Shirazi, A., Daffner, K., Mills, T., & Pelan, E. (2021). Formulation and additive manufacturing of polysaccharide-surfactant hybrid gels as gelatine analogues in food applications. *Food Hydrocolloids*, 106881. https://doi.org/10.1016/j.foodhyd.2021.106881

Fenton, T., Kanyuck, K., Mills, T., & Pelan, E. (2021). Formulation and characterisation of kappa-carrageenan gels with non-ionic surfactant for melting-triggered controlled release. *Carbohydrate Polymer Technologies and Applications*, *2*, 100060. https://doi.org/10.1016/j.carpta.2021.100060

1.6 Manuscripts awaiting submission for publication

Fenton, T., Mills, T. & Pelan, E. Encapsulation of α-amylase in polysaccharide gels for detergency applications.

Fenton, T., Mills, T. & Pelan, E. Thermoresponsive wax encapsulation of bleaching salts for detergency applications.

1.7 Presentations

Fenton, T., Kanyuck, K., Mills, T., & Pelan, E. (2021). Formulation and characterisation of kappa-carrageenan gels with non-ionic surfactant for melting-triggered controlled release, *The International Conference on Formulations in Food and Healthcare,* Birmingham, 2021.

2

An academic review of biopolymer and wax-based temperature-mediated controlled release systems

2.1 Abstract

The purpose of the following chapter is to examine the background scientific information pertinent to the proceeding experimental chapters, with a specific focus on materials and mechanisms surrounding temperature-mediated controlled release. There are two material classes which will be discussed as controlled-release vehicles: biopolymer gels and waxes. Additionally, the composition and function of automatic dishwashing detergent formulations will be stated to provide context for the choice of encapsulated ingredients in the experimental work.

2.2 Hydrocolloids and biopolymer gels

Gelling biopolymers are a type of hydrocolloid - a water-containing structure - which have uses across many industries including food, pharmaceutical and beyond as thickening or gelling agents. Generally, gelling biopolymers are polysaccharides or proteins, and are derived from animal, plant or microbial sources. The gelling properties of biopolymers originates from the ability of the individual polymers to trap water, either through swelling or the formation of crosslinks which results in a dramatic change in the viscosity of the solution. The following sub-chapters will discuss the biopolymers relevant to the experimental chapters, with inclusion of kappa carrageenan, low acyl gellan gum, tamarind seed xyloglucan and gelatine. Additionally, a selection of other biopolymers gels will be discussed in order to give a broader background to hydrocolloids and will reinforce the choice for which biopolymers were used in the experimental chapters.

2.2.1 Kappa carrageenan and the carrageenan family

Carrageenans are a group of naturally-occurring anionic polysaccharides that originate from *Rhodophycae* seaweed (Imeson, 2000). The name for carrageenan derives from the Irish word for seaweed, "carrageen" meaning "little rock" (Campo, Kawano, Silva, & Carvalho, 2009). There are three commercial types of carrageenan: kappa (κC), iota (ιC) and lambda carrageenan (λC), and each has slight differences in their chemical structure – namely, the number of sulphate groups present on the chain: this is shown in Figure 2.2. The differing chemical structures consequently results in different physical properties and gelling behaviours of the carrageenans. There are many other forms of carrageenan – such as mu (μC), nu (νC) and theta (θC) carrageenan. μC and νC are the naturally-obtained precursors to κC and ιC respectively, and θC is obtained through chemical treatment of λC, however the chemical properties of the precursors make them of limited commercial use (Campo et al., 2009).

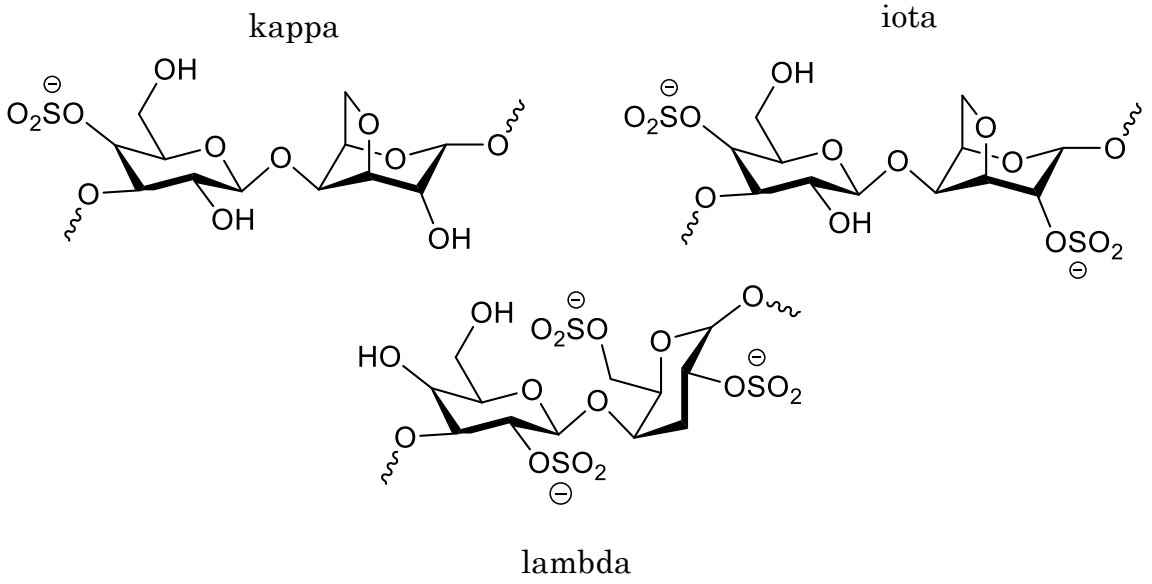

Figure 2.1 - Chemical structures of kappa, iota and lambda carrageenan. Structures represent idealised structures of one idealised repeat unit of the polymer.

Gelation of kappa and iota carrageenan is achieved by dissolution of an appropriate mass of carrageenan - above a critical concentration (Diañez et al., 2019) – in sufficiently hot water (temperature is variable depending on carrageenan concentration, type etc.), allowing the carrageenan to fully hydrate, followed by subsequent cooling in the presence of a suitable concentration of cations – potassium, sodium and calcium are common examples (Imeson, 2000). The influence of specific cations on the gelation of different carrageenans is covered later in this chapter. To form a self-supporting gel, the concentration of kappa carrageenan used is generally between 0.5 and 3% w/w (Saha & Bhattacharya, 2010). A diagrammatic representation of the mechanism of carrageenan (specifically kappa, but it also applies to iota) gelation is shown in Figure 2.2. Carrageenan exists in random coil form when the solution is sufficiently hydrated

and hot (this state is termed a “sol”), and these random coils transform to double helices upon cooling. The helices then aggregate on additional cooling and the presence of cations to form junction zones, and hence a gel network. The existence of cations is necessary to reduce electrostatic repulsion between adjacent negatively charged helices, to enable aggregation of the helices and therefore the formation of junction zones (Norton *et al.*, 1983).

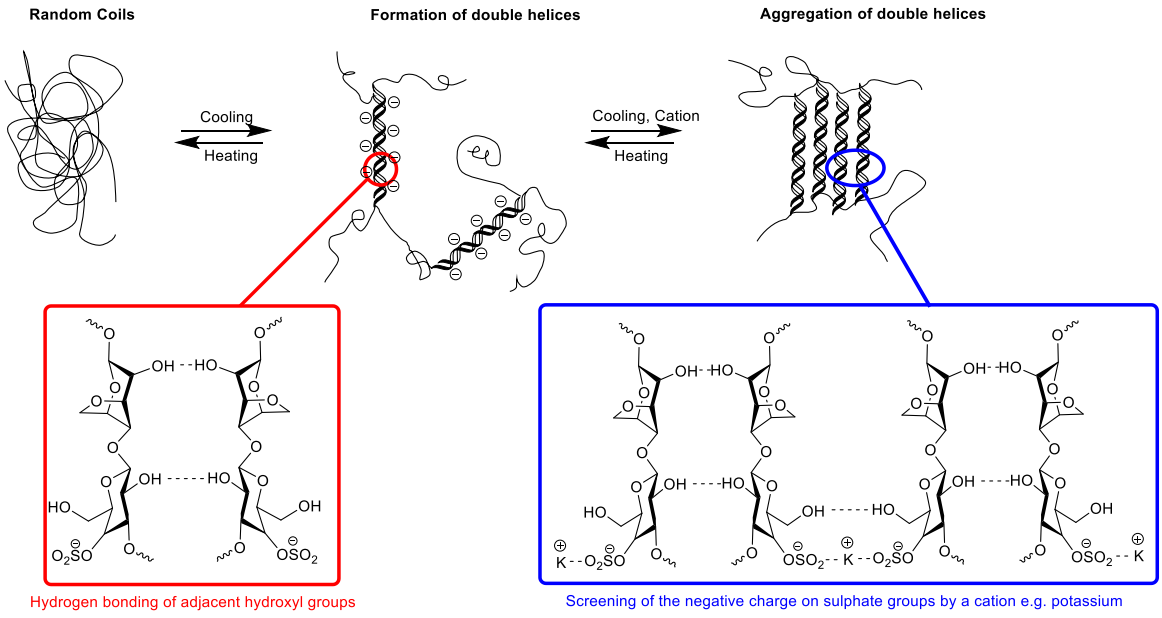

Figure 2.2 - The gelling mechanism of carrageenan. In this example, kappa carrageenan is used. Random coils form double helices upon cooling, due to hydrogen bonding of adjacent hydroxyl groups. These helices aggregate upon further cooling and the presence of an appropriate gelling cation to form the gel network.

After gelation, kappa carrageenan forms strong, brittle gels, iota carrageenan forms soft, elastic gels (Geonzon, Bacabac, & Matsukawa, 2019). Despite the fact

it cannot gel, lambda carrageenan instead forms a viscous solution (Running, Falshaw, & Janaswamy, 2012). This can be explained by examining the chemical structures in Figure 2.2: kappa carrageenan has only one sulphate group, hence there are fewer negative charges along its chain so intermolecular repulsion is lower and helical aggregation is more favourable. On the other hand, iota carrageenan has one extra sulphate group, hence gel formation is repressed due to increased intermolecular repulsions between adjacent sulphate groups (Hossain, Miyanaga, Maeda, & Nemoto, 2001). Lambda carrageenan has yet another sulphate group which inhibits any gel formation: specifically the inward facing sulphate group prevents helix formation in the first instance (Running et al., 2012).

The differing number of sulphate groups between carrageenan types also dictates which cation is the most effective at promoting gelation for the different carrageenan types: kappa carrageenan with **one** sulphate group shows preference for **mono**valent cations, and iota carrageenan with **two** sulphate groups shows preference for **di**valent cations. More specifically, kappa carrageenan gels the most effectively with K^+ ions and iota carrageenan with Ca^{2+} ions (Núñez-Santiago & Tecante, 2007). According to Thrimawithana *et al.* (2010), this is because potassium can form a "secondary electrostatic bond with the anhydro-bridge oxygen atom of the adjacent galactose residue" of kappa carrageenan, whereas sodium and lithium ions are too small to achieve this, explaining the preference of kappa carrageenan for K^+. Calcium ions are the most effective ions for iota carrageenan gelation due to the formation of intermolecular Ca^{2+} bridges

(Thrimawithana et al., 2010). Furthermore, it has been shown that if the gel-promoting cation for any carrageenan type is extremely bulky, such as tetramethylammonium cations (a quaternary ammonium salt), inter-helical aggregation, and therefore gelation, is prevented (S. Ikeda, Morris, & Nishinari, 2001). In almost all cases, an increase in salt concentration triggers an increase in viscosity, and if gelation occurs it will lead to a stronger gel (Hermansson, Eriksson, & Jordansson, 1991) that forms at a higher temperature (Imeson, 2000). This is due to more effective screening of the negative charges on the carrageenan chains which reduces the repulsion between adjacent chains and hence promotes aggregation.

Carrageenan gels are 'thermoreversible' (Dianez et al., 2019), which means that the transition between sol and gel is reversible and controlled by temperature: this is made possible by virtue of the fact that during gelation no covalent bonds are formed. The mechanism of melting takes place in steps, with increasing temperature causing more extensive breakdown of the carrageenan network as junction zones of greater thermal stability break down. Upon further heating, all the carrageenan helical aggregates become broken, and the double helices unwind to reform random coils (Liu, Huang, & Li, 2016). Carrageenan gels show 'thermal hysteresis', which means that the gelling temperature (T_g) is lower than the melting temperature (T_m), and this difference increases with increasing carrageenan and salt concentration (Kara, Tamerler, Bermek, & Nder Pekcan, 2003). Thermal hysteresis arises from the fact that helical aggregation gives rise

to structures which are thermodynamically stabilised to higher temperatures than those that they are formed at (E. R. Morris, Nishinari, & Rinaudo, 2012). The gelling and melting temperatures of kappa carrageenan range dramatically due to many factors including the concentration of carrageenan and counter-ions, carrageenan source and processing and the addition of other interacting species. For example, Núñez-Santiago and Tecante (2007) studied the thermal behaviour of 0.5% kappa carrageenan, and reported that gelling temperatures ranged from ca. 10 – 50 °C and the melting temperatures ranged from 15 – 65 °C as the concentration of KCl was increased from 0 to 80 mM. Another property of carrageenan gels is that they show syneresis, which is the formation of a water layer on the top surface of the gel (Thrimawithana et al., 2010), which tends to be more prevalent under shear. This phenomenon can make rheological measurements difficult, since it leads to slip, so serrated geometries are often used (Thrimawithana et al., 2010).

2.2.2 Gellan gum

Gellan gum is a negatively charged polysaccharide, produced by a species of bacteria called *Sphingomonas elodea* (syn. *Auromonas elodea* or *Pseudomonas elodea*) (Jansson, Lindberg, & Sandford, 1983). Gelation in gellan gum occurs via a very similar mechanism to that of carrageenan: dissolution of gellan gum in hot water (> 85 °C, typically) yields a solution of random coil polymers, which then form double helices upon cooling. Upon further cooling and the existence of

appropriate counter-ions, the helices aggregate to form junction zones and therefore a gel network (Yuguchi, Urakawa, & Kajiwara, 1997).

In its native form, the gellan gum polymer exists in the high acyl gellan (HAG) form, however, to increase commercial value – by increasing gel strength – hot alkali treatment is used to convert the gellan into a low acyl (LAG) form. Idealised chemical structures of both polymers are given in Figure 2.3. As can be seen, the hot alkali treatment partially hydrolyses the sterically bulky side groups, resulting in a change in gel properties from a soft, elastic gel in the high acyl form, to a hard, brittle gel in the low acyl form (Grasdalen & Smidsrød, 1987). In both gellan gum types, the carboxylic acid side groups deprotonate in solution, giving the polysaccharide chains a negative charge.

The gelation process relies on the aggregation of negatively charged polysaccharide helices in a similar manner to carrageenan, hence the degree of aggregation and consequently gel properties such as gel strength, gelling temperature and melting temperature are also strongly dependent on factors such as pH and the existence of gelling counter-ions (E. R. Morris et al., 2012). Gellan gels most effectively with divalent cations (such as Mg^{2+}, Ca^{2+}) but can also form gels in the presence of monovalent cations (Na^{+}, K^{+}) (Milas & Rinaudo, 1996). The mechanism of melting in gellan gum is analogous to that previously described for carrageenan and involves the gradual breakdown of junction zones of increasing thermal stability.

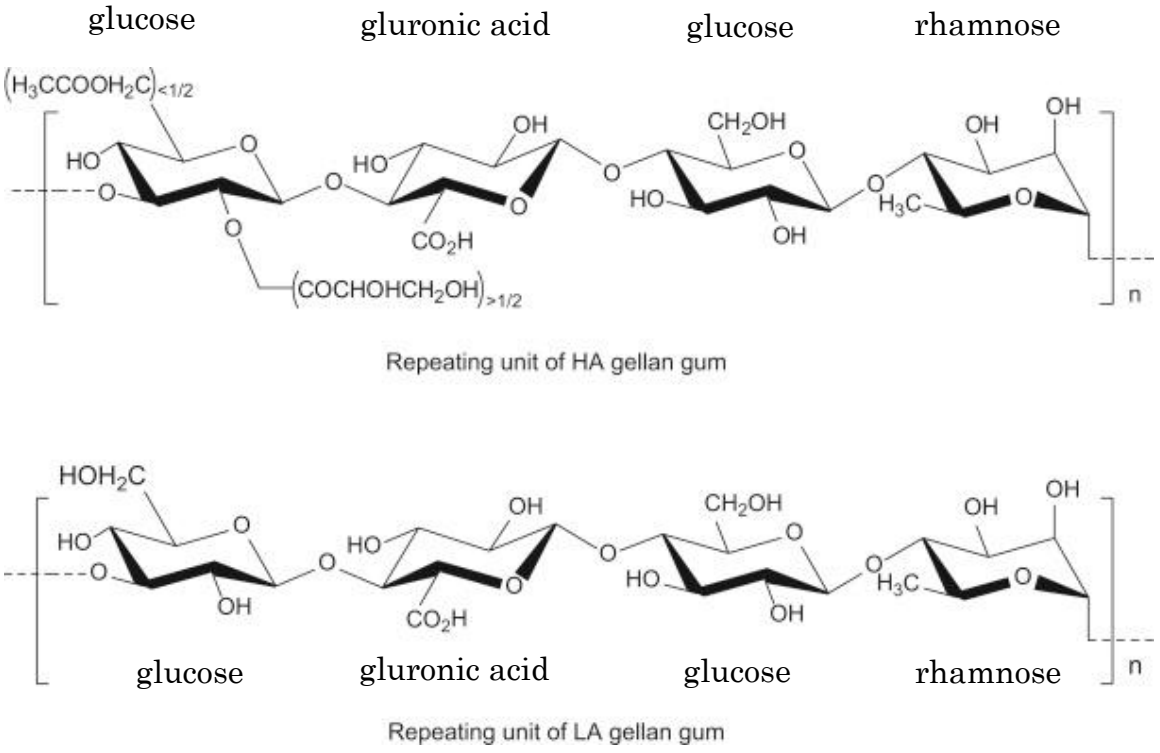

Figure 2.3 - Idealised chemical structures of high acyl (HAG) gellan gum and low acyl (LAG) gellan gum. Figure taken from Chen (2019).

2.2.3 Tamarind Seed Xyloglucan

Tamarind seed xyloglucan (TSX) is an uncharged polysaccharide obtained from the seeds of the tamarind tree, *Tamarindus indica* (Kozioł, Cybulska, Pieczywek, & Zdunek, 2015). Xyloglucans are present in the cell walls of many dicotyledons, where they influence the orientation of cellulose microfibrils, act as a storage polysaccharides and increase the rigidity of the cell wall (Hayashi, 1989). Tamarind seeds are particularly abundant in xyloglucan content, hence it is a common commercial source to obtain xyloglucan (Kozioł et al., 2015). According to Freitas *et al.* (2005), the structure of xyloglucan is reported to be a "cellulose-like (1→4)-linked ß-glucan backbone to which single α-D-Xylp substituents are attached at O-6. Some Xylp residues are further substituted at O-2 by β-D-Galp

(Hayashi, 1989)". Approximately three in every four glucose residues are 1,6-α-D-Xylp substituted, however the degree of 1,2-β-D-Galp substitution depends on the xyloglucan source (Kozioł et al., 2015). The idealised chemical structure of xyloglucan is shown in Figure 2.4.

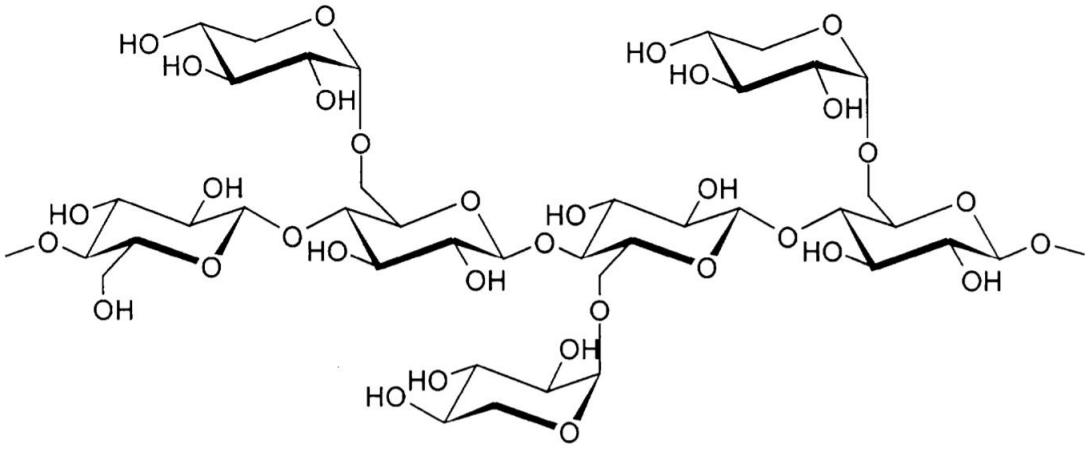

Figure 2.4 - Idealised chemical structure of xyloglucan. Figure taken from Ebringerová *et al.* (2013).

In solution, xyloglucan adopts a double helical conformation, however, the physical and chemical properties, such as water solubility and gelation behaviour, of the xyloglucan depends on the degree of backbone substitution (Kozioł et al., 2015). These helical macromolecules are not fully water soluble and tend to form helical aggregates in solution, even in very dilute solutions (Kozioł et al., 2015; Picout, Ross-Murphy, Errington, & Harding, 2003), however the aggregates are soluble. Xyloglucan is used most often in industry as a thickener or stabiliser, as it forms a viscous solution which is stable to heat, pH and shear (Nitta et al., 2003).

2.2.4 Gelatine

Gelatine is a proteinaceous molecule which has important uses in the food industry and beyond as a gelling agent. It is particularly useful in food formulations as it has a melting temperature of approximately body temperature (ca. 35 °C), therefore can provide melt-in-the-mouth release of flavourings and other encapsulated molecules (Osorio *et al.*, 2007). Gelatine is derived from denatured collagen, a common structural protein. The collagen, commonly obtained from bovine or porcine sources, undergoes unfolding of its helical structure when hydrolysed with acid or base under heat to result in random coils of gelatine molecules with a range of molecular weights. The variation in the gelatine molecular weights originates from differing degrees of hydrolysis of the collagen; typically, the higher molecular weight gelatines are more desirable and are produced at lower temperatures as less hydrolysis is typically experienced (Ledward, 2000). In general, gelatine gels are considered relatively soft and flexible compared to other more brittle biopolymer gels, such as kappa carrageenan or low acyl gellan gum.

Industrially, gelatine is characterised by its gel strength, and to do so a parameter called 'Bloom strength' was introduced. Bloom strength is calculated using a standard Bloom method based on the compressibility of a gelatine sample, and it is necessary to characterise gelatine in this way due to the variability in mechanical strength resulting from different molecular weights of the gelatine chains. Typically, Bloom values range between 50 – 300 g Bloom, where a higher

Bloom value indicates a stronger gel. Manufacturers generally supply various gelatine samples with a range of Blooms. Frustratingly, there is no direct correlation between Bloom values and molecular weight distribution of gelatine molecules as different combinations of gelatines of differing molecular weights can lead to gelatines with the same Bloom strength (Ledward, 2000).

Gelation in gelatine occurs through dispersing the gelatine powder in hot water, which results in gelatine molecules existing as random coils. Upon cooling, the triple helices from the parent collagen partially reform, and then adjacent helices interact at junction zones via hydrogen bonding: this is illustrated in Figure 2.5. The gelation process in gelatine is fully thermoreversible, which in practice means that it is initiated by cooling down from an elevated temperature, but this can be reversed by reheating the set gel. An interesting and relatively unique property of gelatine is that it has very little thermal hysteresis: its gelling and melting temperatures are often very similar (Osorio, Bilbao, Bustos, & Alvarez, 2007). However, the gelation mechanism of gelatine is further complicated by the fact that it continually reorganises at a molecular level to form new junction zones of increasing thermodynamic stability over time.

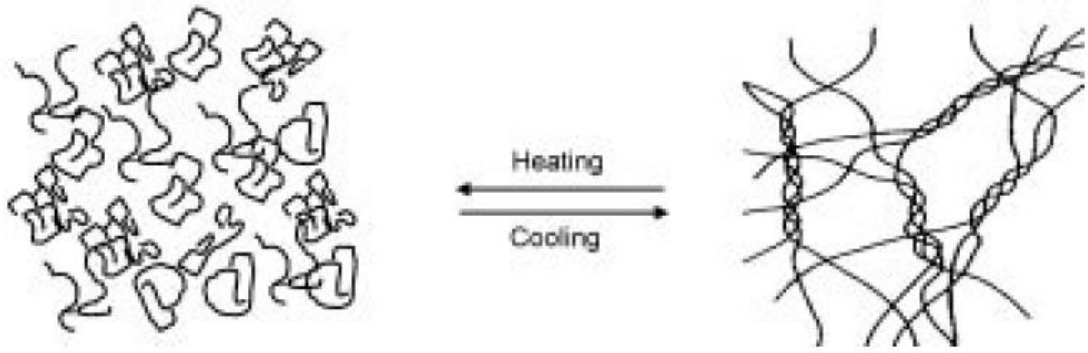

Figure 2.5 - A diagram depicting gelatine gelation mechanism. Random coils form triple helices upon cooling. Figure taken from Ledward (2000).

The result of this is that gelatine continually gets firmer with time and rarely, if ever, reaches an equilibrium value. Although this implies that gelatine can obtain infinite firmness given enough time, in reality the rate of firmness increase follows a logarithmic profile by where the rate of increase in firmness approaches zero given enough time, hence a pseudo-equilibrium is obtained (Williams & Phillips, 2000).

2.2.5 Other hydrocolloids and biopolymer gels

Starches are hugely versatile structural ingredients, enabling the manufacture of a multitude of different foodstuffs including bread, pasta, confectionery items, soups and sauces. Starches are a general class of polysaccharides and are extracted from a variety plant sources, most commonly maize, wheat, rice, tapioca and potato (Ai & Jane, 2015). On a molecular level, starches exist as a combination of two different polymers, amylose and amylopectin (Bertoft, 2017). After extraction

starches exist as discrete, insoluble granules which can be irreversibly swollen in hot water in a process called starch gelatinisation (Tester, Qi, & Karkalas, 2006), which typically occurs at temperatures of approximately 60 – 70 °C (Perry & Donald, 2002). Once gelatinised, the starch "traps" large quantities of water and forms a viscous gel structure which cannot be reversed by heating i.e. gelatinised starch does not melt (Arocas, Sanz, & Fiszman, 2009). Gelatinisation in starch also makes it much more susceptible to enzymatic or chemical hydrolysis compared to ungelatinised starch (Tester et al., 2006). Although the gelatinisation reaction is irreversible, some of the gelatinised starch will naturally recrystallise over time in a process called starch retrogradation, which is the process responsible for bread staling (Arocas et al., 2009). The final starch gel properties are mostly dependent on the ratio of amylose to amylopectin, with high amylose contents giving strong gels; high amylose maize starch has among the highest amylose contents of any starch and consequently forms one of the strongest starch gels (Li, Li, Zhu, & Ai, 2021). There are many chemically-modified starches which are designed to have high gel strengths, long shelf lives and high resistance to retrogradation through the formation of chemical crosslinks (Ai & Jane, 2015).

Agar is a strongly gelling hydrocolloid derived from marine algae sources, and its earliest recorded usage as a gel is the oldest of all biopolymer gels, dating back to 17th Century Japan (Armisen & Galatas, 2009). In a similar manner to starch, agar was found to consist as a combination of two different polysaccharide molecular fractions: agarose (a linear polysaccharide) and agaropectin (a branched

polysaccharide), as described in the work of Araki (1937). The gelation in agar solely involves the agarose fractions and is similar to that seen in carrageenans: the agarose molecules form helices from random coils upon cooling which then aggregate via hydrogen bonding under further cooling to result in a firm gel (Armisen & Galatas, 2009). Due to the high thermal stability of agar, the melting temperature is usually considerably higher than the gelling temperature: agar shows a high thermal hysteresis (Mohammed, Hember, Richardson, & Morris, 1998).

Alginate is a negatively charged polysaccharide derived from brown seaweed, in which it is used to provide both rigidity and flexibility (Lahaye, 2001). It is most widely utilised in its sodium salt form - sodium alginate. It differs from most gels by being a 'cold set' gel, which is to say temperature does not induce or reverse gelation in alginate. Instead, gelation is promoted by the introduction of cations, particularly calcium ions (K. Y. Lee & Mooney, 2012). Because it is extremely difficult to introduce calcium ions uniformly under no shear conditions, this can result in the formation of "fish eyes" or gel lumpiness during gel formation as the alginate gels only where calcium ions are present (Williams & Phillips, 2000). Alginates are very heat stable due to the strong crosslinking, which makes them popular gelling agents in hot foodstuffs where heat resistance is desirable (Draget, 2009).

2.2.6 Combinations of hydrocolloids

Aside from using a single type of hydrocolloid to form a gel, two or more different hydrocolloids can be combined for this purpose in a mixed system. When a mixed biopolymer system has uniquely different gel properties than any of the constituent species, this can be termed a 'synergistic combination', and allows the development of novel, interesting and useful formulations (Williams & Phillips, 2000). Such gel properties could be gelling temperature, melting temperature, gel strength or texture.

The combination of two or more different polymers leads to either a coupled or a phase separated morphology (E. R. Morris, 2009). In the former case, a coupled system is the result of the polymers directly bonding through the formation of covalent and/or non-covalent interactions (E. R. Morris, 2009). Coupling of two polymers can lead to either gelation or precipitation: for gelation, this involves the formation of homotypic junction zones, and precipitation is typically the result of two oppositely charged polymers binding to form an electrostatically neutral complex which consequently becomes much less soluble due to a reduction in ion-dipole interactions and the complex precipitates out of solution (Williams & Phillips, 2000). In the latter case of a phase separated system, the more common of the two cases, this arises as a result of unfavourable polymer-polymer interactions between the two different polymers, and is therefore often described as a 'water-in-water emulsion' (E. R. Morris, 2009). The microstructure of a water-in-water emulsion arising from phase separation of two biopolymer solutions is

similar to that of conventional oil/water emulsions, however they differ in the aspect that the two phases show slight miscibility in each other, which leads to a very small interfacial tension (Wolf, Scirocco, Frith, & Norton, 2000). Additionally, as both phases are water-continuous, the density of each phase is very similar hence the rate of creaming or sedimentation is much slower than for a water and oil emulsion. The formation of a water-in-water emulsion can be detected by an increase in turbidity due to the existence of small polymer "droplets" in solution (E. R. Morris, 2009). Additionally, provided that at least one of the biopolymers in a biopolymer mixture is gelling, this can lead to a phase separated microstructure which is much more dominated by kinetic factors rather than thermodynamic, in contrast to traditional oil/water emulsions as gelation enables 'trapping' of a microstructure. The thermodynamic driving force for phase separation of the two polymers is to maximise heterotypic polymer-polymer interactions (E. R. Morris, 2009).

Understanding and predicting the microstructure and properties of a mixed biopolymer system is extremely complex – to illustrate this point, there is an academic journal *Biopolymer Mixtures*, dedicated solely to this topic. Much of the formative work in the area of understanding and characterising mixed biopolymer systems was carried out in the latter part of the 20th Century by pioneers such as Prof. Vic Morris and co-workers [(Cairns, Miles, & Morris, 1986; Cairns, Morris, Miles, & Brownsey, 1986; Miles, Morris, & Carroll, 1984; V. J. Morris & Chilvers, 1984)] and Prof. Lennart Piculell [(Piculell & Lindman, 1992)]. Since its inception,

studies into the properties and characterisation of mixed biopolymer systems have grown exponentially; at the time of writing an internet search concerning mixtures or combinations of hydrocolloids or biopolymer gels yielded over 147,000 results.

Thousands of different combinations of biopolymers have been studied in the past 50 years or so, however a special case of biopolymer synergism will form the content for the remainder of this section – the case of helical polysaccharides - such as carrageenan, xanthan gum, gellan gum - with ß(1→4) linked polysaccharides based on a cellulosic backbone (termed 'galactomannans') - such as guar gum, locust bean gum and xyloglucans (Nishinari, Kim, Fang, Nitta, & Takemasa, 2006). One example study by Grisel *et al.* (2015) investigated synergistic interactions between xanthan gum and guar gum, and it was found that the nature of the interaction between the two polymers was dependent on the degree of substitution of the guar gum – this is shown in Figure 2.6. In this work, Grisel *et al.* (2015) discuss that the mechanism of synergy between xanthan gum and guar gum originates from attractive homotypic (involving more than one polymer type) interactions leading to the formation of homotypic junction zones, rather than the more common case of repulsive interactions leading to structural changes through volume exclusion effects (the water-in-water emulsion model). It was reported that the xanthan gum and guar gum both must have molecular "smooth", unsubstituted areas to be able to form these homotypic junction zones. The net result of the synergy in this case, was that the intrinsic viscosity was lower-than-expected, due to a decrease in hydrodynamic volume.

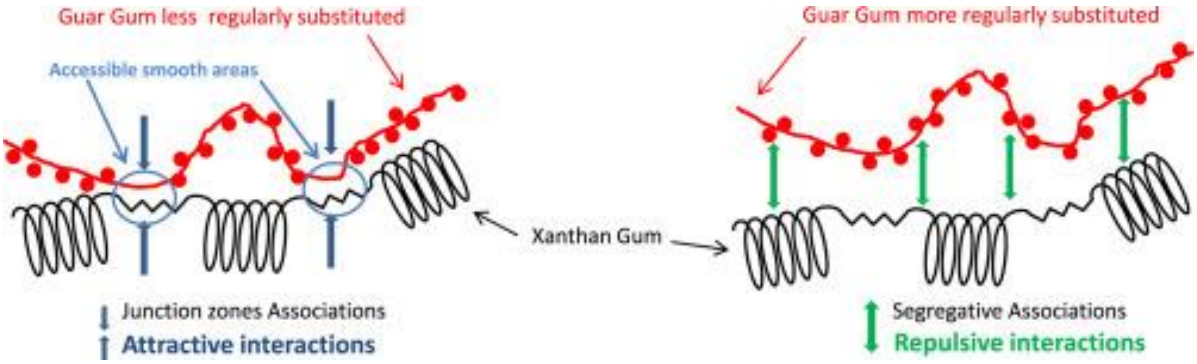

Figure 2.6 - A diagram showing how guar gum substitution influences homotypic polymer interactions in a xanthan/guar gum mixture. Figure taken from Grisel *et al.* (2015).

Aside from the xanthan and guar gum mixture, other similar examples of reported synergies are: kappa carrageenan with locust bean gum (Fernandes, Gonçalves, & Doublier, 1991; Stading & Hermansson, 1993; Williams & Langdon, 1998), gellan gum with xyloglucan (Shinya Ikeda et al., 2004; Nitta et al., 2003) and xanthan gum with locust bean gum (Copetti, Grassi, Lapasin, & Pricl, 1997).

2.3 Lipid-based controlled release systems

The following section will discuss lipid-based controlled-release systems: their chemistry and structure, their origins, their properties and methods to manufacture novel, functional vessels for controlled-release applications. Specifically, it will focus on the use of fats and waxes.

2.3.1 Introduction to waxes

Waxes are a class of hydrophobic organic molecules which are typically solid at ambient temperatures, and derive from animal, vegetable, petroleum or synthetic sources. Characteristic to all waxes is a long, highly-saturated hydrocarbon chain with an ester linkage formed by the condensation of a fatty acid to a fatty alcohol, however, there are many different moieties that may additionally appear on this chain: ketone, alcohol, ester, aldehyde, carboxylic acid and aromatic groups are all common in waxes (Soleimanian, Goli, Shirvani, Elmizadeh, & Marangoni, 2020). As an example, the chemical structure of a common wax, cetyl palmitate, is given in Figure 2.7. Along with the long chain ester molecule, also present in naturally-derived waxes are numerous other organic components in varying concentrations such as carboxylic acids, alcohols, ketones, terpenes, mono-, di- and tri-acylglycerols, free fatty acids, aliphatic and aromatic molecules (Matthies, 2001; Soleimanian et al., 2020).

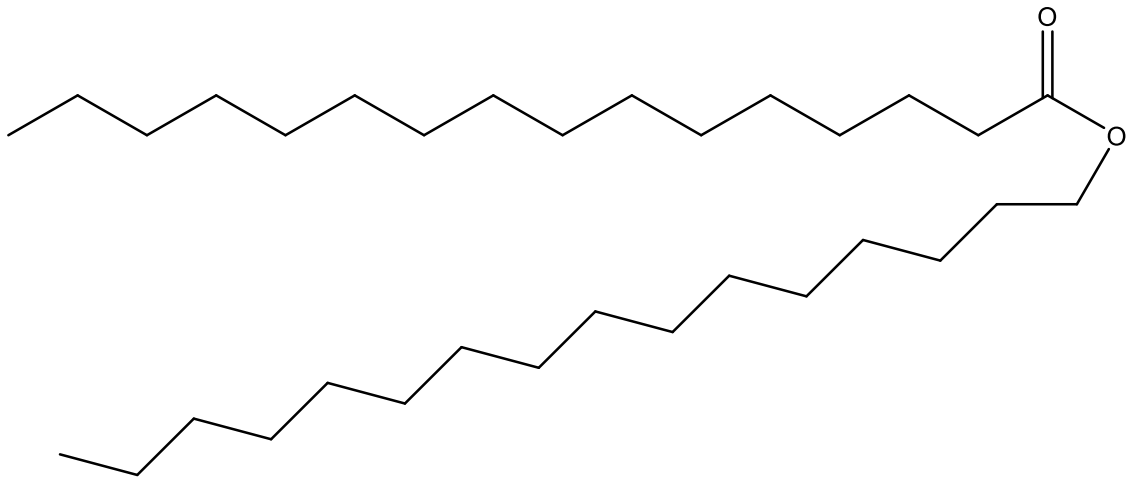

Figure 2.7 - An example chemical structure of a wax: the displayed wax is cetyl palmitate.

There are many different waxes available in nature and synthetically. Common examples of waxes are beeswax, carnauba wax, paraffin wax, shellac wax, and sunflower petroleum jelly. In nature, plant and animal waxes are used to impart a hydrophobic coating on to surfaces which provide a protective barrier against water loss, UV radiation and predation (Matthies, 2001). Humans have utilised waxes since as early as 4200 B.C. as food preservation agents, candle wax and skincare agents (Matthies, 2001). The chemical structure of waxes, being mostly long chain, saturated organic molecules, leads waxes to be hydrophobic and chemically inert to many chemicals including strong alkalis and acids (Rosiaux, Jannin, Hughes, & Marchaud, 2014). In solid form, waxes also possess a very dense microstructure which typically halts the diffusion of even small molecules (MW < 1 kDa) across the waxy layer and provides high mechanical strength. Additionally, due to their hydrophobicity, waxes are especially effective at containing the

diffusion of water-based mixtures. A comparison of the diffusion barrier properties of oils, fats and waxes is shown in Figure 2.8.

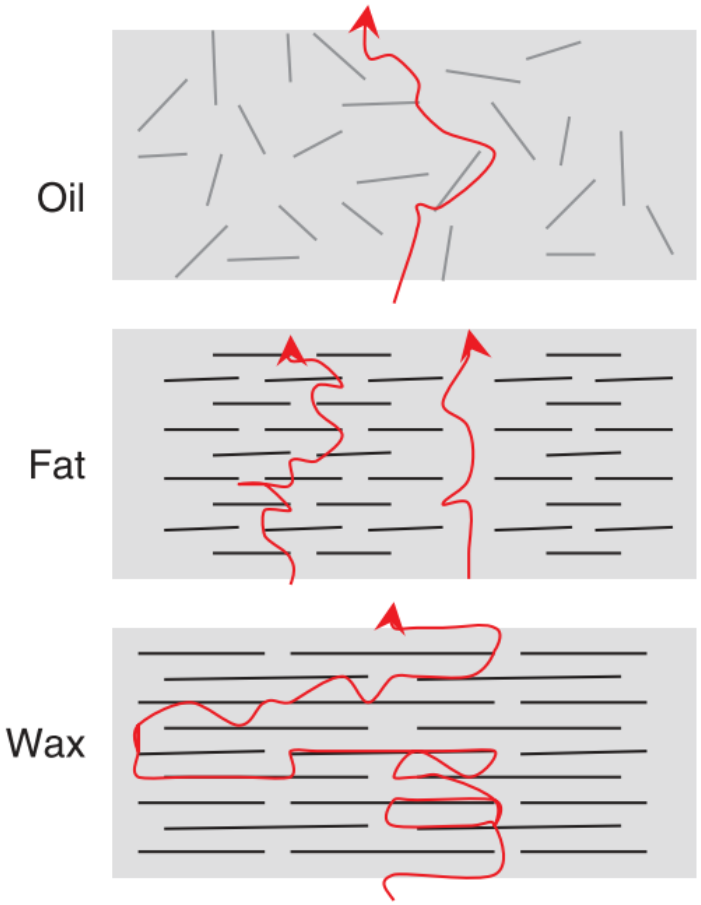

Figure 2.8 - Diffusion barrier properties of oils, fats and waxes, in order of decreasing permeability. Figure taken from Mellema et al. (2006a).

Waxes also have a very well-defined melting temperature, which varies between different waxes, however it is commonly between 40 to 70 °C whereby an increasing in fatty chain length generally leads to an increase in melting temperature (Goertz, Demella, Thompson, White, & Raghavan, 2019a). A list of some common waxes and their melting points is given in Table 2.1. One important item to note is that as the carbon chain length of the waxes is increased, so does the melting point. The

naturally derived waxes (paraffin, beeswax and carnauba wax) are a mixture of waxes with different carbon chain lengths and so have a broader melting point range compared to pure or synthetic waxes with a well-defined carbon chain length, which consequently have a much more well-defined melting point.

Table 2.1 - Melting points and carbon chain lengths of some common waxes.

Wax	Melting Point (°C)	Carbon Chain Length	Reference
n-tetraocasane	50.4	24	(Allan, Kaminski, Bertrand, Head, & Sunderland, 2009)
Paraffin	53 - 55	20 - 30	(Khan, Ali, Obaydullah, & Wadud, 2019; Speight, 2019)
Beeswax	61 - 63	27 - 33	(Fratini, Cilia, Turchi, & Felicioli, 2016; Khan et al., 2019)
n-octacosane	61.1	28	(Allan et al., 2009)
n-hexatriacontane	75.8	36	(Allan et al., 2009)
Carnauba	80 - 87	~ 50	(Khan et al., 2019; Zhang et al., 2016)
Soy	15 - 55	16 - 18	(Collins & Sedgwick, 1959; L. Wang & Wang, 2007)

2.3.2 Methods for production of wax-based controlled release systems

On the surface, waxes appear to be good candidates for creating controlled-release vehicles: they are effective at containing active ingredients for long periods of time by limiting diffusion, they are chemically inert to most species, they have a high mechanical strength and have a well-defined melting temperature. Furthermore,

compared to solid fats, waxes are ductile and have less tendency to crack under stress, and also have a denser microstructure which inhibits diffusion (Mellema, Van Benthum, Boer, Von Harras, & Visser, 2006a). In contrast, aqueous gels, such as were discussed in the previous section, have a much bigger mesh size in the polymer network and hence encapsulated materials, particularly of small molecular weights (MW < 1 kDa) can diffuse out of the gel over time if the gel is placed in a sufficient solvent (usually water). This slow leaching of encapsulated ingredients over time can be advantageous in the case of drug delivery, for example (Kamlow, Vadodaria, Gholamipour-Shirazi, Spyropoulos, & Mills, 2021), however in many cases long-term retention of an active ingredient inside the encapsulate is preferable. Despite this, there are very limited studies which examine the use of waxes for the purpose of controlled release. Work by Goertz *et al.* (2019) noted this 'literature vacuum' and so work was published which presented two different methods for creating wax-based controlled release systems with an encapsulated aqueous phase. The first method detailed by Goertz *et al.* (2019) involved either dropping a cold aqueous solution or hydrogel beads in to a container of molten wax held just above its melting temperature and incubating for a small period of time (5 to 20 seconds) before manually removing the newly formed wax capsule. The difference in temperature between the water droplet/gel bead caused any molten wax it came in to contact with to immediately solidify, hence a complete hard shell was formed around the droplet/gel bead. A second method detailed by Goertz *et al.* (2019) involved pouring molten wax in to a mould and stamping out a central cavity before leaving the hollow shell to solidify. Following this, either an aqueous

solution or hydrogel beads were added to the cavity and the shell was then sealed by pouring more molten wax on top of the capsule. These methods are shown in Figure 2.9.

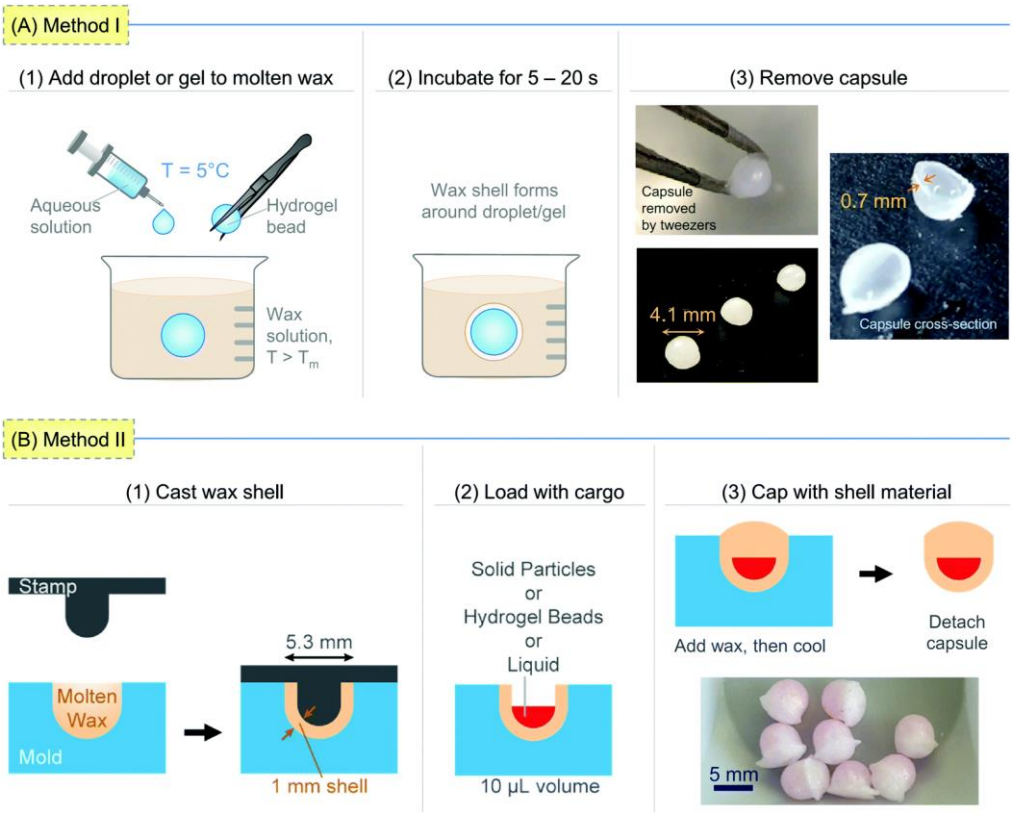

Figure 2.9 - Methods reported by Goertz et al. (2019) for creating thermoresponsive, hermetically sealed wax capsules. Figure taken from Goertz et al.(2019).

Mellema *et al.* (2006) have utilised wax encapsulation in the context of creating controlled-release food systems. The work presents two more techniques for the manufacture of wax capsules with an encapsulated aqueous phase, termed 'solid' and 'liquid' methods, and these are described visually in Figure 2.10.

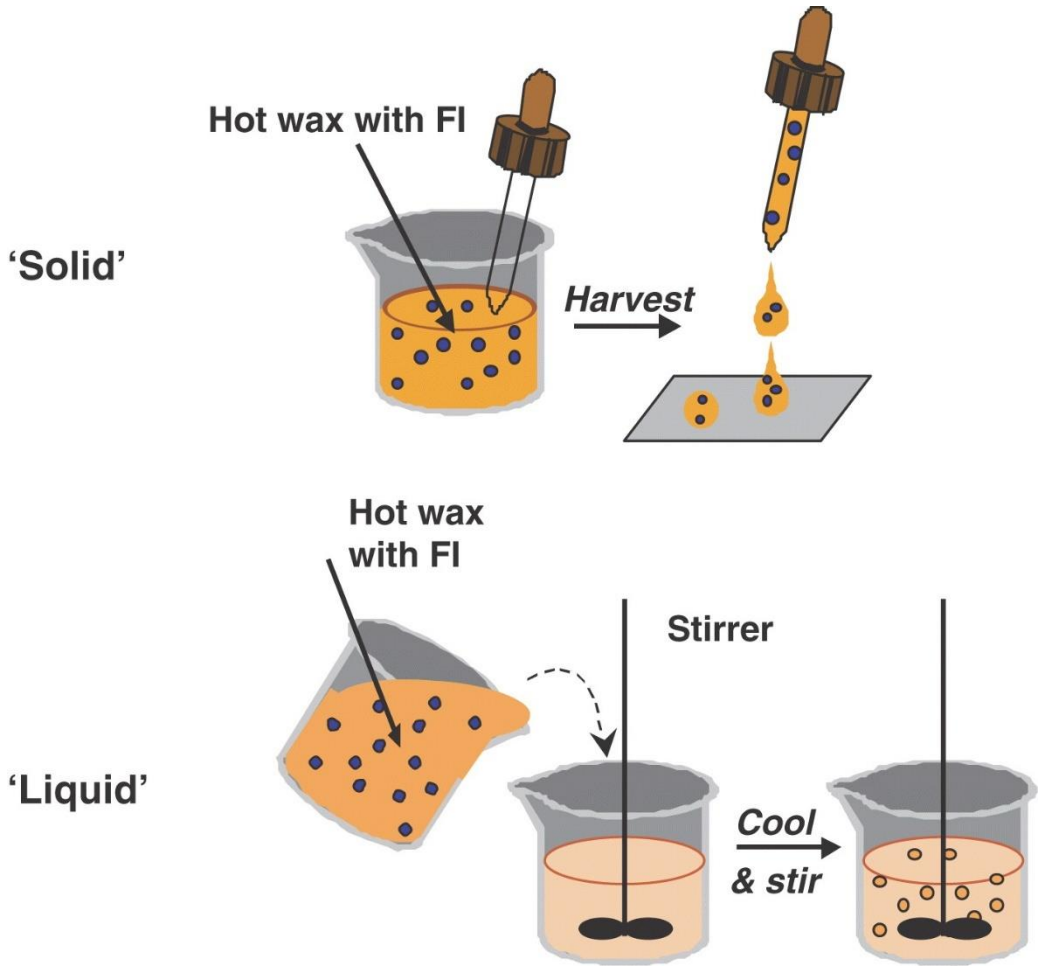

Figure 2.10 - Methods for the wax encapsulation of an aqueous phase proposed by Mellema et al. (2006). The 'Solid' method involves depositing a hot wax emulsion on to a plate. The 'Liquid' method involves mixing hot wax with a function ingredient (FI) and adding this to cold oil under high shear mixing. Figure taken from Mellema et al. (2006a).

For the 'solid' preparation technique water droplets were formed in a molten wax phase, and lecithin or polyglycerol polyricinoleate (PGPR) were used as emulsifiers to form a stable water-in-oil emulsion. This hot mixture could then be deposited on a cool surface where upon cooling the wax solidified hence trapping the dispersed water droplets. This 'solid' preparation technique gave wax capsules of a size in the order of 0.1 to 1 cm, with the dispersed water droplets measuring

approximately 1 – 5 μm. A water-soluble colourant was dissolved into the water phase in order to examine leakage from the capsules by dispersing the wax capsules in water at room temperature and using UV/Vis spectroscopy to examine the increase in absorbance at the peak absorbance wavelength for the specific colourant. It was found that leakage from the tablets was approximately 30% over a period of 16 weeks immersed in room temperature water. Because of the need to form a water-in-oil emulsion there is a relatively large amount of wax required (> 40% w/w) leading to a relatively low encapsulation efficiency. It was proposed that the mechanism of leaking from the tablets was due to the difference in osmotic pressure between the inside and outside of the capsule: this was evidenced by the fact that the rate of leakage from the capsules was greater as the concentration of salt or acid was increased. Additionally local imperfections can be formed during deposition of the hot wax emulsion.

For the 'liquid' preparation technique, the first step also involved forming a water-in-oil emulsion with a dispersed aqueous phase and a continuous hot wax phase. However, the next step involved pouring the hot wax emulsion into a beaker of cold oil under high shear. Upon contact with the cold oil the wax capsules immediately solidify, and the high shear environment limits the size of the capsules to 150 – 500 μm. Using this preparation method, the leakage from the tablets was measured at approximately 40% over a time period of 1 week in room temperature water, which was also examined using colourimetric analysis. The reduced

stability of the capsules was purported to be that the smaller capsules are more sensitive to structural inhomogeneities.

A patent filed by Gabriel *et al.*, (1989) discussed a novel technique for the encapsulation of powdered bleach within paraffin wax using fluidisation techniques. The bleach powder was placed in a fluidised bed at room temperature (or slightly above), and molten wax was sprayed on to the bleach, resulting in paraffin wax to rapidly solidify around pockets of bleach powder. This results in bleach particles with an outer paraffin wax layer 100 – 1000 μm thick. The paraffin wax forms approximately 40 – 50% of the particle weight, resulting in an encapsulation efficiency of 50 – 60%. It was shown that when placed in aqueous-based media, the bleach capsules did not leak any bleach over the experimental time period of 56 days, indicating good stability to leakages.

2.3.3 Pickering controlled release systems containing fat or wax

Aside from forming macroscopic wax capsules for the purpose of controlled release, there have been several publications detailing the use of crystalline fats (Frasch-Melnik, Norton, & Spyropoulos, 2010; Le Révérend, Taylor, & Norton, 2011; I. T. Norton, Spyropoulos, & Cox, 2009; J. E. Norton, Fryer, Parkinson, & Cox, 2009) or waxes (Soleimanian et al., 2020) to form a hard coating around water droplets in a water-in-oil emulsion. As with the wax capsules previously discussed, the waxes and fats have well-defined melting temperatures and so temperature-mediated controlled release of the water droplets can be achieved by melting.

First described by Spencer Pickering in 1907, an emulsion can be stabilised by the addition of 'Pickering particles': these are solid particles which adsorb at the oil-water interface and prevent coalescence by providing a physical (steric) barrier against droplet-droplet interactions (Pickering, 1907) – a diagram illustrating Pickering stabilisation of emulsions is shown in Figure 2.11. Typically the enthalpy of adsorption for particles at the interface is extremely high, and so can be considered essentially irreversible (Frasch-Melnik et al., 2010). To enable the adsorption of particles at the interface, the solid particle needs to be amphiphilic to some degree; surfactants are often added to encourage the adsorption of solid particles at the interface by enhancing particle polarity (Frasch-Melnik et al., 2010).

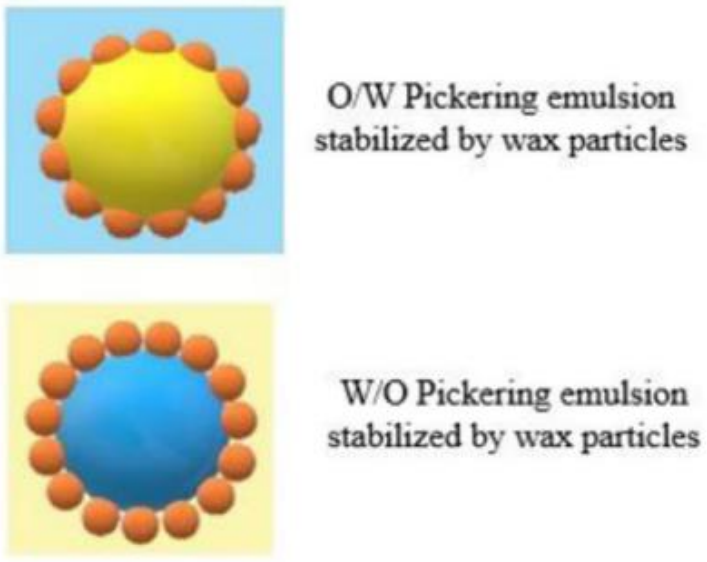

Figure 2.11 - Mechanism of Pickering stabilisation of emulsions. Solid particles adsorb at the interface and prevent droplet coalescence by providing a steric barrier. Figure taken from Soleimanian et al., (2020).

Some of the most common materials for creating Pickering-stabilised emulsions are mono- and triglycerides: these are amphiphilic ester molecules based on the combination of free fatty acid(s) with glycerol – an example is shown in Figure 2.12. Monoglycerides and triglycerides have the advantage of being naturally amphiphilic therefore show good adsorption at interfaces even in liquid form. Monoglycerides particularly show good interface adsorption however the single fatty chain results in poor steric stabilisation of droplets compared to triglycerides.

If monoglycerides and triglycerides are mixed and added in liquid form ($T > T_m$) to an emulsion, the liquid monoglycerides will migrate to the interface where they will adsorb however the triglycerides tend to stay in solution. As the temperature is cooled below the crystallisation temperature of the monoglycerides and triglycerides, the monoglycerides crystallise, which then creates nucleation points for triglycerides to crystallise at the interface. The net result of this is that sub-micron particles of mono/triglycerides are seeded directly at the interface (Frasch-Melnik et al., 2010).

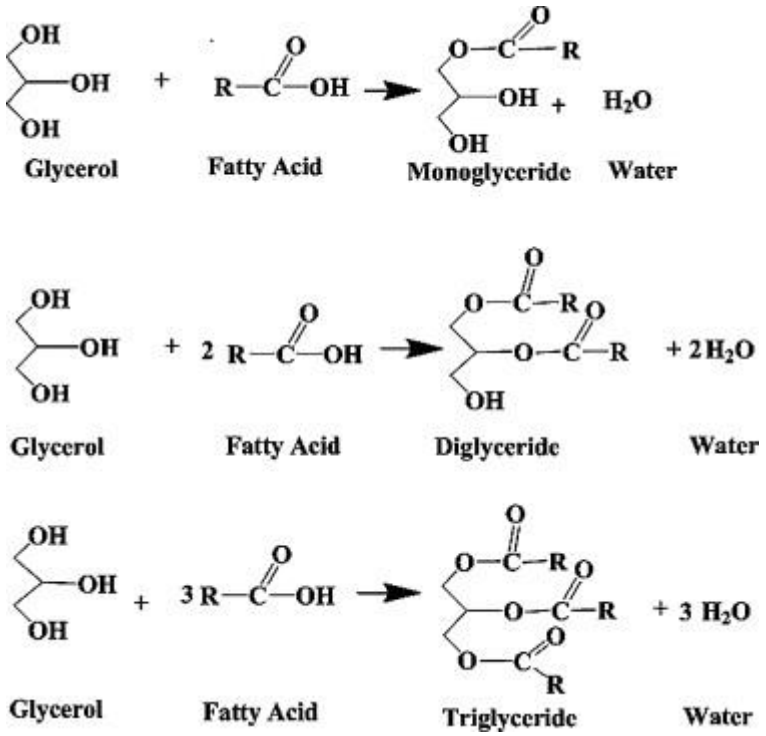

Figure 2.12 - Illustration of how mono, di and triglycerides are formed from glycerol and free fatty acids. Figure taken from Hermida, Abdullah and Mohamed (2011).

Rapid cooling decreases the crystal size of the mono/triglycerides, which increases the effectiveness with which they can adsorb at the interface and therefore increases emulsion stability (Hodge & Rousseau, 2005). Similar Pickering stabilised emulsion systems have been created with combinations of waxes and surfactants (Hodge & Rousseau, 2003; Soleimanian et al., 2020). Much of the formative work in this area was conducted by Hodge and Rousseau (2003) who investigated the influence of paraffin wax on the stability of water-in-oil emulsions. It is reported that the formation of paraffin wax crystals at the water-oil interface resulted in an increase in emulsion stability (with respect to sedimentation and coalescence).

A primary issue with many of the Pickering emulsion encapsulation methods is that the encapsulation efficiency is low, since the active ingredient must be contained in the dispersed phase, rather than in the continuous phase. In contrast, the macroscopic wax capsules discussed previously do not require an external continuous phase to be dispersed in, and hence the encapsulation efficiency can be much higher. Many of the Pickering-stabilised emulsion systems are relevant to food applications and involve the controlled release of salt, nutrients and flavourings and hence only a small loading of active ingredient is required. In these cases, the external continuous phase already forms a necessary part of the food structure, for example, mayonnaise has a water-continuous phase and dispersed oil droplets, and butter has a fat-continuous morphology with dispersed water droplets. If it is simply required to encapsulate one active ingredient, then there may be no requirement to have an outer continuous phase and having this second phase would lower the encapsulation efficiency of the active ingredient.

2.4 Automatic dishwashing detergent formulations

The following section will seek to discuss the ingredients and formulation techniques currently employed during the manufacture of automatic dishwashing detergents.

2.4.1 Overview of automatic dishwashing detergent formulations

As an introduction to the classes of ingredients that are contained within automatic dishwashing detergent (ADD) formulations, a table giving a list of common ADD ingredients along with their function, concentration and chemical examples is shown in Table 2.2. As can be seen, it is a complex list of ingredients, each of which adds a useful function to the formulation. The bulk of the tablet is made from the builders, corrosion inhibitors and alkali source which are all mostly sodium salts. Some of the more 'complex' ingredients are the surfactants, enzymes and bleaches. Each of these ingredients will be examined in further detail in the following sections.

Table 2.2 - Main ADD ingredients, concentration and function. Information from (Ahmed, 2009)

Ingredient	Approximate Concentration (% w/w)	Ingredient Function	Example(s)
Surfactants	5	Lowers interfacial tension between oil and water to encourage emulsification of fatty deposits.	Non-ionic surfactants, most are common alcohol ethoxylates
Builders	30	Salts which bind to water hardness minerals (calcium and magnesium). Also increases alkalinity which aids soil removal.	Sodium tripolyphosphate, sodium citrate, sodium carbonate, sodium citrate
Corrosion inhibitors	30	Protects glassware, dishes and machine parts from corrosion.	Sodium silicate, zinc salts, bismuth salts.
Alkalis	15	Aids emulsification of fatty and oily deposits.	Sodium carbonate, sodium tripolyphosphate, caustic soda
Enzymes	1	Enzymatically digests starchy, proteinaceous or fatty deposits into smaller molecules which are easier to wash away.	Amylase, lipase, protease.
Bleaches	15	Aids emulsification of proteinaceous deposits, sanitises and removes staining.	Sodium hypochlorite, sodium percarbonate
Fragrance, colours and other additives	4	Used to create an appealing appearance and user experience	Any common fragrances and colourings.

2.4.2 Interfacial phenomena and surfactants

An interface is defined by the Oxford English Dictionary as "a point where two systems, subjects, organisation, etc. meet and interact". Such is true for a colloidal interface: this is the point where two heterotypic phases meet and interact with one another. Immiscibility between two different fluids arises because homotypical molecular interactions (with other molecules of the same type) are more favourable than heterotypical (with different molecules) (E. R. Morris, 2009); for example, in a mixture of oil and water, oil-oil and water-water interactions are more thermodynamically favourable than oil-water interactions. The attractiveness or repulsiveness of heterotypic molecular interactions depends on the polarity of the two molecules: polar molecules such as water, prefer to interact with other polar molecules, and vice-versa for non-polar molecules, such as oil (Williams & Phillips, 2000). The compatibility of one phase with another can be quantified by the interfacial tension (γ), and it is calculated based on the energy required to form surface area, and hence has units of joules per metre squared, or more often the equivalent unit of Newtons per metre (Poce-Fatou, 2006). Surface tension describes a case where one phase is air, rather than liquid, leading to the formation of a gas/air interface, rather than a liquid/liquid interface.

Surfactants, or 'surface-active agents' decrease the interfacial tension between mixtures of incompatible fluids. On a molecular level, a surfactant comprises of two distinct regions: a hydrophobic region and a hydrophilic region. The hydrophobic region (tail) is often a variant of an alkyl chain, which is fatty in

nature and consequently is much more soluble in non-polar rather than polar solvents. Contrastingly, the hydrophilic (head) region is either directly charged/ionisable or is polar, hence it is much more soluble in polar solvents than non-polar solvents (Poce-Fatou, 2006). Surfactants are classified according to the chemical nature of their headgroup and there are four types: non-ionic, cationic, anionic and zwitterionic (Nakama, 2017). These differences in solvent preferences in separate parts of the same molecule give the surfactants their surface-active properties: when an interface is present between two incompatible (a polar with a non-polar) species, the surfactants will migrate to the interface and partially adsorb into each phase which lowers the interfacial tension across the interface and hence encourages mixing of the two incompatible phases (Poce-Fatou, 2006). Adsorption is the molecular process of attachment to a surface or interface, and is not the same as absorption, which is a bulk process.

Non-ionic surfactants are a vital addition to automatic dishwashing detergent (ADD) formulations since they aid in the emulsification of fat and oil-based deposits in to the wash water (Gambogi, Kennedy, & Ambundo, 2009), whilst producing comparatively little foam compared to cationic and anionic surfactants, which increases the efficiency of the wash process (Chun, Theiler, Baumgarten, & Gabriel, 1990). Non-ionic surfactants are added to ADD formulations at a quantity of between 0.5 and 10 wt% (but more often around 5 wt%), and can be solid or liquid at room temperature depending on the tablet type (Chun et al., 1990). Mixtures of different surfactants typically outperform one single surfactant

(Griffiths & Cheung, 2003), and therefore anionic surfactants are commonly mixed with non-ionic surfactants due to their low cost and excellent detersive properties (Oldenhove de Guertechin, 1999). Additionally, a 'rinse-aid surfactant' will often be incorporated, which causes water to run off crockery at the end of the wash cycle, and so avoids water spotting and gives a sparkling appearance: however, for this to be effective the rinse aid should be released at the end of the cycle (Gambogi et al., 2009).

A potential issue with using non-ionic surfactants in dishwashing is that commercially-available non-ionic surfactants (and also enzymes, to be discussed in section 2.4.4) can be deactivated in the presence of sodium hypochlorite bleach, a common ADD ingredient, especially in liquid formulations where the surfactant and bleach reside in the same phase (Gambogi et al., 2009). Additionally, the reduced foaming ability of non-ionic surfactants comes at the cost of reduced emulsification ability compared to anionic surfactants (Gambogi et al., 2009).

2.4.3 Enzymes in ADD formulations

Enzymes are proteinaceous biological catalysts which speed up specific chemical reactions without being consumed themselves. In the context of ADD formulations, they are added in order to break down and digest common food soils in to smaller, easier to clean molecules (Ahmed, 2009). The most common enzymes used for this purpose are amylases, lipases and proteases, which digest starch-based, lipid-

based and protein-based soils respectively (Olsen & Falholt, 1998). The introduction of enzymes to ADD formulations allowed a reduction in harsh cleaning agents such as bleaches and alkalis (Olsen & Falholt, 1998).

Enzymes rely on retaining a specific molecular confirmation in order to carry out their catalytic function, and therefore if the molecular confirmation is altered in any way, the function of the enzyme will be greatly reduced or removed all together. The process of irreversible structural changes in enzymes is referred to as 'denaturation', and this process occurs in the presence of a high temperature or chemically deactivating species. Temperatures above 50 °C reduce the activity of proteases (Tang, Wu, Ying, & He, 2010) and lipases (Rajakumara, Acharya, Ahmad, Sankaranaryanan, & Rao, 2008), however amylases tend to be more resilient to high temperatures, showing denaturation at temperatures over 70 °C (Singh, Shandilya, Kundu, & Kayastha, 2015). Temperature-resistant enzymes have been developed which can withstand temperatures greater than 100 °C (Daniel, Dines, & Petach, 1996), however these enzymes are more expensive than their unmodified analogues. Sodium hypochlorite bleach is particularly deactivating to enzymes as the hypochlorite ions hydrolyse the protein chain (K. E. Olson, 1989). Additionally the presence of high salt concentrations, introduced by the ADD formulation, can lead to protein aggregation and precipitation (Ahmed, 2009).

2.4.4 Bleaches in ADD formulations

Bleaches are key ingredients in ADD formulations for their excellent cleaning, stain-removing and sanitising properties (Ahmed, 2009). Commonly, ADD formulations use one of two different bleaches: sodium hypochlorite (chlorine bleach) or sodium percarbonate (oxygen bleach) (Chun et al., 1990). Chlorine bleach is an excellent cleaning agent however it is highly chemically deactivating towards enzymes and non-ionic surfactants. In contrast, oxygen bleach shows much better compatibility with enzymes and non-ionic surfactants, however, the cleaning performance is inferior to chlorine bleach (Chun et al., 1990).

2.5 Biopolymer-surfactant interactions

The following section will discuss literature surrounding biopolymer-surfactant interactions as this is a complex phenomenon which requires special consideration when formulating some of the controlled-release systems in the later experimental chapters.

According to Grządka (2015) it is known that surfactants have the capacity to interact with polymers in a variety of mechanisms including "electrostatic, dipole-dipole, hydrophobic and hydrogen bonding". This is important since any interaction between the surfactant and a gelling biopolymer may alter the biopolymer's solubility, gelling and melting temperature, gel strength and texture. The nature of these surfactant-polymer interactions can be complex and hence a

significant volume of literature has been published in this area, including many publications on carrageenan-surfactant interactions (Bonnaud, Weiss, & McClements, 2010; Grządka, 2015; Rosas-Durazo et al., 2011; Shtykova et al., 2000; Tomašić, Tomašić, & Filipović-Vinceković, 2002; Marko Vinceković, Bujan, Šmit, & Filipović-Vinceković, 2005; Yin et al., 2014). However, these are limited to only studying charged surfactants, and no literature could be found relating to the interaction of carrageenan with non-ionic surfactants. It is stated by Griffiths and Cheung (2003) that when the polymer and/or surfactant is non-ionic, any polymer-surfactant interactions are relatively weak, which is plausible since Coulombic interactions are significantly stronger than intermolecular interactions based on dipoles, such as hydrogen bonding. Hence, it has been reported by several authors that mixtures of carrageenan and cationic surfactants can form complexes, termed "polyelectrolyte-surfactant complexes" (Bonnaud et al., 2010; Tomašić et al., 2002; Marko Vinceković et al., 2005; Yin et al., 2014). It is reported that initially surfactant monomers adsorb on to the carrageenan chain, and then on increasing surfactant concentration micelles begin to form at a concentration below the critical micelle concentration (CMC): this new concentration is termed the critical aggregation concentration (CAC) (Tomašić et al., 2002), as is determined by noting an abrupt change in the conductivity of the solution (Chang, Hwang, Lin, Chen, & Lin, 1998; Tomašić et al., 2002).

Piculell and Lindman (1992) state that similarly charged mixtures of polymers and surfactants show 'segregative' phase separation, when two distinct phases form,

each that is almost wholly comprised of an individual species. In contrast, when the polymer and surfactant have opposite charges, associative phase separation occurs, by where the polymer and surfactant become precipitate away from the solvent. Furthermore, it was shown by Vinceković *et al.* (2011) that addition of a cationic surfactant to carrageenan caused a decrease in solution viscosity which corresponds to chain collapse, as the cationic micelles screen the negative charges on the carrageenan and therefore intramolecular and intermolecular electrostatic repulsion disappears. This is in contrast to the behaviour reported by Griffiths and Cheung (2003), when investigating the properties of mixtures of gelatine and surfactants, they reported that upon the addition of surfactant the viscosity of the solution increased, owing to the expansion of the polymer upon surfactant adsorption. This disparity between seemingly similar systems illustrates the depth and complexity of polyelectrolyte-surfactant interactions.

2.6 Automatic dishwashing detergent formulation challenges and proposed solution

A major potential issue with ADD formulations is that some of the materials are chemically and/or biologically incompatible with others. Primarily it is the sensitive enzymes and non-ionic surfactants which become deactivated in the presence of chlorine bleach (sodium hypochlorite), a strong chemical oxidising agent (Chun et al., 1990). Hence, if all three ingredients are released into the wash

cycle at the same point, then the efficacy of the surfactants and the enzymes may be reduced if they become deactivated by the bleach. Therefore, it would be theoretically advantageous to have sensitive ingredients such as enzymes and surfactants released earlier in the wash cycle where many enzymes show a maximum in activity. This is followed by the bleach later in the wash cycle, by which point the enzymes and surfactants have had time to perform their function and cleaning performance could be improved.

ADD products exist as either compressed powder or in liquid form. A compressed powder formulation could allow pseudo-controlled release as dissolution of the tablet happens over time, and if the enzymes and surfactants were at the outer layer of the tablet and bleach at the middle, this could separate out the ingredients in the wash. However, a time-based dissolution is difficult to control as the length of wash cycles varies with manufacturer and programs, and compacted powder tablets have a tendency to absorb water over time (Esteban, Moxon, Simons, Bakalis, & Fryer, 2017), leading to a short shelf life. Additionally, some dishwashing ingredients such as enzymes are difficult and expensive to use in powdered form, compared to liquid form (US7125828B2, 2000). Current liquid-based ADD products do not have any aspect of controlled-release, hence deactivation of ingredients is possible, both in the wash and during storage (Gambogi et al., 2009). There have been various methods devised to circumvent this deactivation issue, as reported in the patent literature. A brief description of some of these patents is given in Table 2.3.

Table 2.3 - Patent information surrounding novel methods to counteract ingredient deactivation.

Patent Content	Reference
A multilayer tablet which contains different ingredients in each layer, and dissolves over time. The thickness of the layers can be used to control release times.	(Chun et al., 1990)
Multi-compartment pouches to deliver controlled release of dishwasher ingredients made from partially-hydrolysed polyvinylacetate/polyvinyl alcohol as the pouch material.	(US20040235697A1, 2000)
A water-soluble pouch containing a combination of liquid and solid components separated out into multiple compartments.	(US7125828B2, 2000)
Capsule-in-capsule detergent delivery system consisting of concentric water-soluble pouches, which dissolve over time.	(WO2018169421A1, 2017)
An outer shell of bleach with an inner core of double-encapsulated enzymes. The outer layer is a time-delay substance and the inner layer is a bleach-deactivating substance.	(US4965012A, 1987)
Encapsulation of bleach with silicates to release bleach later in the cycle allowing enzymes to work first.	(US20170121645A1, 2012)

Use of organosilica gels to form a host matrix in which to encapsulate and immobilise an active ingredient e.g. enzymes. Upon dissolution into the wash cycle the enzymes can rapidly diffuse from the matrix.	(US2013115176 (A1), 2013)

The aforementioned patent literature in Table 2.3 provides some interesting information on how previous work has attempted to solve some of the incumbent problems in current ADD products. Time-based controlled release appears to be a popular choice for easily separating ingredients in the wash cycle, however for the reasons previously discussed, it is less flexible with different wash cycle program lengths. The primary focus of this thesis is to formulate methods for the encapsulation and controlled release of these ingredients. The controlled release aspect will be utilised to allow the sensitive ingredients to be released prior to the deactivating ingredients. The release of the ingredients should be triggered by temperature to account for different wash cycle lengths, and methods should be devised for accurately monitoring the release of these ingredients into a simulated dishwashing environment. Based on the literature search performed for this work, the encapsulation materials will either be gelling biopolymers or waxes. A secondary objective of this thesis is to understand the physical properties of the encapsulate materials that influence the release profiles, and to quantify the effect that the encapsulated ingredients have on these physical properties. It is expected that the melting temperature of the encapsulate will be important to characterise,

as release is to be triggered by temperature, and also the mechanical strength of the encapsulated system.

2.7 References

Ahmed, F. U. (2009) 'Part E: Applications - Industrial and Institutional Cleaning', in Zoller, U. (ed.) *Handbook of Detergency*. Boca Raton, FL: CRC Press Taylor & Francis Group, p. 380.

Ai, Y. and Jane, J. L. (2015) 'Gelatinization and rheological properties of starch', *Starch/Staerke*. John Wiley & Sons, Ltd, pp. 213–224. doi: 10.1002/star.201400201.

Allan, K. M. *et al.* (2009) 'Laminar smoke points of wax candles', *Combustion Science and Technology*, 181(5), pp. 800–811. doi: 10.1080/00102200902935512.

Araki, C. (1937) 'Acetylation of agar like substance of Gelidium amansii', *J. Chem. Soc. Japan*, 58, pp. 1338–1350.

Armisen, R. and Galatas, F. (2009) 'Agar', in Phillips, G. O. and Williams, P. A. (eds) *Handbook of Hydrocolloids*. 2nd edn. Boca Raton, FL, pp. 82–107.

Arocas, A., Sanz, T. and Fiszman, S. M. (2009) 'Influence of corn starch type in the rheological properties of a white sauce after heating and freezing', *Food Hydrocolloids*. Elsevier, 23(3), pp. 901–907. doi: 10.1016/j.foodhyd.2008.05.009.

Babelek, Z. (2017) 'Complex capsule-in-capsule detergent'. WIPO. Available at: https://patents.google.com/patent/WO2018169421A1/en?q=~patent%2FUS200201 37648A1&sort=new&page=2 (Accessed: 6 July 2022).

Bakul, D. (2013) 'Materials for dissolution-controlled release'. EPO. Available at: https://worldwide.espacenet.com/publicationDetails/description?CC=US&NR=201 3115176A1&KC=A1&FT=D&ND=3&date=20130509&DB=&locale=en_EP (Accessed: 6 July 2022).

Bertoft, E. (2017) 'Understanding Starch Structure: Recent Progress', *Agronomy*, 7(3), p. 56. doi: 10.3390/agronomy7030056.

Bonnaud, M., Weiss, J. and McClements, D. J. (2010) 'Interaction of a food-grade cationic surfactant (Lauric Arginate) with food-grade biopolymers (pectin, carrageenan, xanthan, alginate, dextran, and chitosan)', *Journal of Agricultural and Food Chemistry*, 58(17), pp. 9770–9777. doi: 10.1021/jf101309h.

Cairns, P. *et al.* (1986) 'Comparative studies of the mechanical properties of mixed gels formed by kappa carrageenan and tara gum or carob gum', *Topics in Catalysis*, 1(1), pp. 89–93. doi: 10.1016/S0268-005X(86)80010-8.

Cairns, P., Miles, M. J. and Morris, V. J. (1986) 'X-ray diffraction studies of kappa carrageenan-tara gum mixed gels', *International Journal of Biological Macromolecules*, 8(2), pp. 124–127. doi: 10.1016/0141-8130(86)90011-5.

Campo, V. L. *et al.* (2009) 'Carrageenans: Biological properties, chemical modifications and structural analysis - A review', *Carbohydrate Polymers*, pp. 167–180. doi: 10.1016/j.carbpol.2009.01.020.

Catlin, T. M. L. A. *et al.* (2000) 'Detergent products, methods and manufacture'. USPTO. Available at: https://patents.google.com/patent/US7125828B2/en?q=~patent%2FUS20020137648A1 (Accessed: 6 July 2022).

Chang, H. C. *et al.* (1998) 'Measurement of critical micelle concentration of nonionic surfactant solutions using impedance spectroscopy technique', *Review of Scientific Instruments*. American Institute of Physics, 69(6), pp. 2514–2520. doi: 10.1063/1.1148951.

Chen, Y. (2019) *Hydrogels based on natural polymers*, *Hydrogels Based on Natural Polymers*. Elsevier. doi: 10.1016/C2018-0-00171-1.

Chun, K. W. *et al.* (1990) 'US5133892'. Available at: https://patents.google.com/patent/US5133892A/en (Accessed: 1 April 2019).

Copetti, G. *et al.* (1997) 'Synergistic gelation of xanthan gum with locust bean gum: A rheological investigation', *Glycoconjugate Journal*. Glycoconj J, 14(8), pp. 951–961. doi: 10.1023/A:1018523029030.

Daniel, R. M., Dines, M. and Petach, H. H. (1996) 'The denaturation and degradation of stable enzymes at high temperatures', *Biochemical Journal*, pp. 1–11. doi: 10.1042/bj3170001.

Diañez, I. *et al.* (2019) '3D printing in situ gelification of κ-carrageenan solutions: Effect of printing variables on the rheological response', *Food Hydrocolloids*. Elsevier, 87, pp. 321–330. doi: 10.1016/j.foodhyd.2018.08.010.

Draget, K. I. (2009) 'Alginates', in Phillips, G. O. and Williams, P. A. (eds) *Handbook of Hydrocolloids*. 2nd edn. Boca Raton, FL, pp. 807–828.

Ebringerová, A. and Hromádková, Z. (1999) 'Xylans of Industrial and Biomedical Importance', *Biotechnology and Genetic Engineering Reviews*. Taylor & Francis Group, 16(1), pp. 325–346. doi: 10.1080/02648725.1999.10647982.

Esteban, J. *et al.* (2017) 'Understanding and Modeling the Liquid Uptake in Porous Compacted Powder Preparations', *Langmuir*. American Chemical Society, 33(28), pp. 7015–7027. doi: 10.1021/acs.langmuir.7b01334.

Fernandes, P. B., Gonçalves, M. P. and Doublier, J. L. (1991) 'Phase diagrams in kappa-carrageenan/locust bean gum systems', *Food Hydrocolloids*, 5(1), pp. 71–73. Available at: https://repositorio.ucp.pt/bitstream/10400.14/6655/3/Phase diagrams in kappa carrageenan locust bean gum systems.pdf (Accessed: 25 February 2019).

Frasch-Melnik, S., Norton, I. T. and Spyropoulos, F. (2010) 'Fat-crystal stabilised w/o emulsions for controlled salt release', *Journal of Food Engineering*. Elsevier, 98(4), pp. 437–442. doi: 10.1016/j.jfoodeng.2010.01.025.

Fratini, F. *et al.* (2016) 'Beeswax: A minireview of its antimicrobial activity and its application in medicine', *Asian Pacific Journal of Tropical Medicine*. No longer published by Elsevier, pp. 839–843. doi: 10.1016/j.apjtm.2016.07.003.

Freitas, R. A. *et al.* (2005) 'Physico-chemical properties of seed xyloglucans from different sources', *Carbohydrate Polymers*, 60(4), pp. 507–514. doi: 10.1016/J.CARBPOL.2005.03.003.

Gabriel, R. *et al.* (1989) 'Wax encapsulated bleach particles and method for making same'. European Patent Office. Available at: https://patents.google.com/patent/EP0436971A2 (Accessed: 28 June 2022).

Gambogi, J., Kennedy, S. and Ambundo, E. (2009) 'Part E: Applications - Dishwashing with Detergents', in Zoller, U. (ed.) *Handbook of Detergency*. Boca Raton, FL: CRC Press Taylor & Francis Group, pp. 39–65.

Geonzon, L. C., Bacabac, R. G. and Matsukawa, S. (2019) 'Network structure and gelation mechanism of kappa and iota carrageenan elucidated by multiple particle tracking', *Food Hydrocolloids*, 92, pp. 173–180. doi: 10.1016/j.foodhyd.2019.01.062.

Goertz, J. P. *et al.* (2019) 'Responsive capsules that enable hermetic encapsulation of contents and their thermally triggered burst-release', *Materials Horizons*. Royal Society of Chemistry, 6(6), pp. 1238–1243. doi: 10.1039/c9mh00309f.

Grasdalen, H. and Smidsrød, O. (1987) 'Gelation of gellan gum', *Carbohydrate Polymers*. Elsevier, 7(5), pp. 371–393. doi: 10.1016/0144-8617(87)90004-X.

Griffiths, P. C. and Cheung, A. Y. F. (2003) 'Interaction between surfactants and gelatine in aqueous solutions', *Materials Science and Technology*, 18(6), pp. 591–599. doi: 10.1179/026708302225003587.

Grisel, M. *et al.* (2015) 'Impact of fine structure of galactomannans on their interactions with xanthan: Two co-existing mechanisms to explain the synergy', *Food Hydrocolloids*. Elsevier, 51, pp. 449–458. doi: 10.1016/j.foodhyd.2015.05.041.

Grządka, E. (2015) 'Interactions between kappa-carrageenan and some surfactants in the bulk solution and at the surface of alumina', *Carbohydrate Polymers*. Elsevier, 123, pp. 1–7. Available at: https://www.sciencedirect.com/science/article/pii/S014486171500048X?via%3Dihub (Accessed: 28 February 2019).

Hayashi, T. (1989) 'Xyloglucans in the Primary Cell Wall', *Annual Review of Plant Physiology and Plant Molecular Biology*. Annual Reviews, 40(1), pp. 139–168. doi: 10.1146/annurev.pp.40.060189.001035.

Hermansson, A. M., Eriksson, E. and Jordansson, E. (1991) 'Effects of potassium, sodium and calcium on the microstructure and rheological behaviour of kappa-

carrageenan gels', *Carbohydrate Polymers*, 16(3), pp. 297–320. doi: 10.1016/0144-8617(91)90115-S.

Hermida, L., Abdullah, A. Z. and Mohamed, A. R. (2011) 'Synthesis of monoglyceride through glycerol esterification with lauric acid over propyl sulfonic acid post-synthesis functionalized SBA-15 mesoporous catalyst', *Chemical Engineering Journal*. Elsevier, 174(2–3), pp. 668–676. doi: 10.1016/j.cej.2011.09.072.

Hodge, S. M. and Rousseau, D. (2003) 'Flocculation and coalescence in water-in-oil emulsions stabilized by paraffin wax crystals', *Food Research International*. Elsevier, 36(7), pp. 695–702. doi: 10.1016/S0963-9969(03)00036-X.

Hodge, S. M. and Rousseau, D. (2005) 'Continuous-phase fat crystals strongly influence water-in-oil emulsion stability', *Journal of the American Oil Chemists' Society 2005 82:3*. Springer, 82(3), pp. 159–164. doi: 10.1007/S11746-005-5166-4.

Hossain, K. S. *et al.* (2001) 'Sol-gel transition behavior of pure ι-carrageenan in both salt-free and added salt states', *Biomacromolecules*. American Chemical Society, 2(2), pp. 442–449. doi: 10.1021/bm000117f.

Ikeda, S. *et al.* (2004) 'Single-phase mixed gels of xyloglucan and gellan', *Food Hydrocolloids*. Elsevier, 18(4), pp. 669–675. doi: 10.1016/j.foodhyd.2003.11.005.

Ikeda, S., Morris, V. J. and Nishinari, K. (2001) 'Microstructure of aggregated and nonaggregated κ-carrageenan helices visualized by atomic force microscopy', *Biomacromolecules*. American Chemical Society, 2(4), pp. 1331–1337. doi: 10.1021/bm015610l.

Imeson, A. (2000) 'Carrageenan', in Williams, P. A. and Phillips, G. O. (eds) *Handbook of Hydrocolloids*. 2nd edn. Cambridge, UK: Woodhead Publishing Limited, pp. 87–101.

Jansson, P. E., Lindberg, B. and Sandford, P. A. (1983) 'Structural studies of gellan gum, an extracellular polysaccharide elaborated by Pseudomonas elodea', *Carbohydrate Research*. Elsevier, 124(1), pp. 135–139. doi: 10.1016/0008-6215(83)88361-X.

Kamlow, M. A. *et al.* (2021) '3D printing of edible hydrogels containing thiamine and their comparison to cast gels', *Food Hydrocolloids*. Elsevier, 116, p. 106550. doi: 10.1016/j.foodhyd.2020.106550.

Kara, S. *et al.* (2003) 'Hysteresis During Sol-Gel and Gel-Sol Phase Transitions of-Carrageenan: A Photon Transmission Study', *Journal of Bioactive and Compatible Polymers*, 18, pp. 33–44. doi: 10.1177/088391103032793.

Khan, K. A. *et al.* (2019) 'Production of candle using solar thermal technology', *Microsystem Technologies*. Springer Verlag, 25(12), pp. 4505–4515. doi: 10.1007/s00542-019-04390-7.

Kozioł, A. *et al.* (2015) 'Evaluation of Structure and Assembly of Xyloglucan from

Tamarind Seed (Tamarindus indica L.) with Atomic Force Microscopy', *Food Biophysics*. Springer, 10(4), pp. 396–402. doi: 10.1007/s11483-015-9395-2.

Lahaye, M. (2001) 'Chemistry and physico-chemistry of phycocolloids', *Cahiers de Biologie Marine*, 42(1–2), pp. 137–157. doi: 10.21411/cbm.a.a7aade12.

Ledward, D. A. (2000) 'Gelatine', in Phillips, G. O. and Williams, P. A. (eds) *Handbook of Hydrocolloids*. 2nd edn. Cambridge, UK: Woodhead Publishing Limited, pp. 67–86.

Lee, K. Y. and Mooney, D. J. (2012) 'Alginate: Properties and biomedical applications', *Progress in Polymer Science (Oxford)*. NIH Public Access, pp. 106–126. doi: 10.1016/j.progpolymsci.2011.06.003.

Li, J. *et al.* (2021) 'Utilization of maltogenic α-amylase treatment to enhance the functional properties and reduce the digestibility of pulse starches', *Food Hydrocolloids*. Elsevier, 120, p. 106932. doi: 10.1016/j.foodhyd.2021.106932.

Liu, S., Huang, S. and Li, L. (2016) 'Thermoreversible gelation and viscoelasticity of κ-carrageenan hydrogels', *Journal of Rheology*. Society of Rheology, 60(2), pp. 203–214. doi: 10.1122/1.4938525.

Matthies, L. (2001) 'Natural montan wax and its raffinates', *European Journal of Lipid Science and Technology*, 103(4), pp. 239–248. doi: 10.1002/1438-9312(200104)103:4<239::aid-ejlt239>3.3.co;2-r.

Mellema, M. *et al.* (2006) 'Wax encapsulation of water-soluble compounds for application in foods', *Journal of Microencapsulation*. Taylor & Francis, 23(7), pp. 729–740. doi: 10.1080/02652040600787900.

Miles, M. J., Morris, V. J. and Carroll, V. (1984) 'Carob Gum-x-Carrageenan Mixed Gels: Mechanical Properties and X-ray Fiber Diffraction Studies', *Macromolecules*, 17(11), pp. 2443–2445. doi: 10.1021/MA00141A041.

Mohammed, Z. H. *et al.* (1998) 'Kinetic and equilibrium processes in the formation and melting of agarose gels', *Carbohydrate Polymers*. Elsevier, 36(1), pp. 15–26. doi: 10.1016/S0144-8617(98)00011-3.

Morris, E. R. (2009) 'Functional Interactions in Gelling Biopolymer Mixtures', in *Modern Biopolymer Science*. Elsevier Inc., pp. 167–198. doi: 10.1016/B978-0-12-374195-0.00005-7.

Morris, E. R., Nishinari, K. and Rinaudo, M. (2012) 'Gelation of gellan - A review', *Food Hydrocolloids*. Elsevier, pp. 373–411. doi: 10.1016/j.foodhyd.2012.01.004.

Morris, V. J. and Chilvers, G. R. (1984) 'Cold setting alginate-pectin mixed gels', *Journal of the Science of Food and Agriculture*, 35(12), pp. 1370–1376. doi: 10.1002/jsfa.2740351215.

Nakama, Y. (2017) 'Surfactants', *Cosmetic Science and Technology: Theoretical Principles and Applications*. Elsevier, pp. 231–244. doi: 10.1016/B978-0-12-802005-0.00015-X.

Nishinari, K. *et al.* (2006) 'Rheological and related study of gelation of xyloglucan in the presence of small molecules and other polysaccharides', *Cellulose*. Springer, 13(4), pp. 365–374. doi: 10.1007/s10570-005-9041-0.

Nitta, Y. *et al.* (2003) 'Synergistic gel formation of xyloglucan/gellan mixtures as studied by rheology, DSC, and circular dichroism', *Biomacromolecules*, 4(6), pp. 1654–1660. doi: 10.1021/bm034103w.

Norton, I. T., Spyropoulos, F. and Cox, P. W. (2009) 'Effect of emulsifiers and fat crystals on shear induced droplet break-up, coalescence and phase inversion', *Food Hydrocolloids*. Elsevier, 23(6), pp. 1521–1526. doi: 10.1016/j.foodhyd.2008.09.014.

Norton, I. T. *et al.* (1983) 'Role of cations in the conformation of the iota and kappa carrageenan', *Journal of the Chemical Society, Faraday Transations 1: Physical Chemistry in Condensed Phases,* 79(10), pp. 2475–2488. doi: 10.1039/F19837902475

Norton, J. E. *et al.* (2009) 'Development and characterisation of tempered cocoa butter emulsions containing up to 60% water', *Journal of Food Engineering*. Elsevier, 95(1), pp. 172–178. doi: 10.1016/j.jfoodeng.2009.04.026.

Núñez-Santiago, M. del C. and Tecante, A. (2007) 'Rheological and calorimetric study of the sol-gel transition of κ-carrageenan', *Carbohydrate Polymers*. Elsevier, 69(4), pp. 763–773. doi: 10.1016/j.carbpol.2007.02.017.

Oldenhove de Guertechin, L. (1999) 'Part A: Properties - Surfactants: Classification', in Broze, G. and Zoller, U. (eds) *Handbook of Detergency*. New York: Marcel Dekker, Inc., pp. 7–47.

Olsen, H. S. and Falholt, P. (1998) 'The role of enzymes in modern detergency', *Journal of Surfactants and Detergents*, 1(4), pp. 555–567. doi: 10.1007/s11743-998-0058-7.

Olson, K. (1987) 'Water insoluble encapsulated enzymes protected against deactivation by halogen bleaches'. USPTO. Available at: https://patents.google.com/patent/US4965012A/en?q=~patent%2FUS2002013764 8A1&sort=new&page=2 (Accessed: 6 July 2022).

Olson, K. E. (1989) 'Water insoluble encapsulated enzymes protected against deactivation by halogen bleaches'. Available at: https://patents.google.com/patent/US4965012A/en?q=~patent%2FUS2002013764 8A1&sort=new&page=2 (Accessed: 1 April 2019).

Osorio, F. A. *et al.* (2007) 'Effects of concentration, bloom degree, and pH on gelatine melting and gelling temperatures using small amplitude oscillatory rheology', *International Journal of Food Properties*, 10(4), pp. 841–851. doi: 10.1080/10942910601128895.

Perry, P. A. and Donald, A. M. (2002) 'The effect of sugars on the gelatinisation of starch', *Carbohydrate Polymers*. Elsevier, 49(2), pp. 155–165. doi: 10.1016/S0144-8617(01)00324-1.

Pickering, S. U. (1907) 'CXCVI. - Emulsions', *Journal of the Chemical Society, Transactions*, 91, pp. 2001–2021.

Picout, D. R. *et al.* (2003) 'Pressure cell assisted solubilization of xyloglucans: Tamarind seed polysaccharide and detarium gum', *Biomacromolecules*. Biomacromolecules, 4(3), pp. 799–807. doi: 10.1021/bm0257659.

Piculell, L. and Lindman, B. (1992) 'Association and segregation in aqueous polymer/polymer, polymer/surfactant, and surfactant/surfactant mixtures: similarities and differences', *Advances in Colloid and Interface Science*. Elsevier, 41, pp. 149–178. doi: 10.1016/0001-8686(92)80011-L.

Poce-Fatou, J. A. (2006) 'A Superficial Overview of Detergency', *Journal of Chemical Education*, 83(8), pp. 1147–1151. doi: 10.1021/ed083p1147.

Rajakumara, E. *et al.* (2008) 'Structural basis for the remarkable stability of Bacillus subtilis lipase (Lip A) at low pH', *Biochimica et Biophysica Acta - Proteins and Proteomics*. Biochim Biophys Acta, 1784(2), pp. 302–311. doi: 10.1016/j.bbapap.2007.10.012.

Le Révérend, B. J. D., Taylor, M. S. and Norton, I. T. (2011) 'Design and application of water-in-oil emulsions for use in lipstick formulations', *International Journal of Cosmetic Science*. John Wiley & Sons, Ltd, 33(3), pp. 263–268. doi: 10.1111/j.1468-2494.2010.00624.x.

Rosas-Durazo, A. *et al.* (2011) 'Gelation processes in the non-stoichiometric polylectrolyte-surfactant complex between κ-carrageenan and dodecyltrimethylammonium chloride in KCl', *Soft Matter*. The Royal Society of Chemistry, 7(5), pp. 2103–2112. doi: 10.1039/c0sm00663g.

Rosiaux, Y. *et al.* (2014) 'Solid lipid excipients - Matrix agents for sustained drug delivery', *Journal of Controlled Release*. Elsevier, pp. 18–30. doi: 10.1016/j.jconrel.2014.06.004.

Running, C. A., Falshaw, R. and Janaswamy, S. (2012) 'Trivalent iron induced gelation in lambda-carrageenan', *Carbohydrate Polymers*. Elsevier, 87(4), pp. 2735–2739. doi: 10.1016/j.carbpol.2011.11.018.

Saha, D. and Bhattacharya, S. (2010) 'Hydrocolloids as thickening and gelling agents in food: A critical review', *Journal of Food Science and Technology*. Springer, pp. 587–597. doi: 10.1007/s13197-010-0162-6.

Shtykova, E. *et al.* (2000) 'SAXS Study of ι-Carrageenan−Surfactant Complexes', *Langmuir*, 16(12), pp. 5284–5288. doi: 10.1021/la991357n.

Singh, K. *et al.* (2015) 'Heat, acid and chemically induced unfolding pathways, conformational stability and structure-function relationship in wheat α-amylase', *PLoS ONE*. Public Library of Science, 10(6). doi: 10.1371/journal.pone.0129203.

Smith, D. *et al.* (2000) 'Dishwashing Method'. USPTO. Available at: https://patents.google.com/patent/US20040235697A1/en?q=Sharma%2C&invento

r=kinloch&oq=Sharma%2C+kinloch (Accessed: 6 July 2022).

Soleimanian, Y. *et al.* (2020) 'Wax-based delivery systems: Preparation, characterization, and food applications', *Comprehensive Reviews in Food Science and Food Safety*. John Wiley & Sons, Ltd, 19(6), pp. 2994–3030. doi: 10.1111/1541-4337.12614.

Souter, P. F., Jackson, M. and Magennis, E. J. (2012) 'Detergent composition with silicate coated bleach'. USPTO. Available at: https://patents.google.com/patent/US20170121645A1/en?q=detergent&q=controlled&q=release&q=dishwashing&assignee=The+Procter+%26+Gamble+Company&before=publication:20190101&after=publication:20160101 (Accessed: 6 July 2022).

Speight, J. G. (2019) *Handbook of industrial hydrocarbon processes*, *Handbook of Industrial Hydrocarbon Processes*. Elsevier. doi: 10.1016/C2015-0-06314-6.

Stading, M. and Hermansson, A. M. (1993) 'Rheological behaviour of mixed gels of κ-carrageenan-locust bean gum', *Carbohydrate Polymers*. Elsevier, 22(1), pp. 49–56. doi: 10.1016/0144-8617(93)90165-Z.

Tang, X. Y. *et al.* (2010) 'Biochemical properties and potential applications of a solvent-stable protease from the high-yield protease producer pseudomonas aeruginosa PT121', *Applied Biochemistry and Biotechnology*, 160(4), pp. 1017–1031. doi: 10.1007/s12010-009-8665-1.

Tester, R. F., Qi, X. and Karkalas, J. (2006) 'Hydrolysis of native starches with amylases', *Animal Feed Science and Technology*. Elsevier, pp. 39–54. doi: 10.1016/j.anifeedsci.2006.01.016.

Thrimawithana, T. R. *et al.* (2010) 'Texture and rheological characterization of kappa and iota carrageenan in the presence of counter ions', *Carbohydrate Polymers*. Elsevier, 82(1), pp. 69–77. doi: 10.1016/j.carbpol.2010.04.024.

Tomašić, V., Tomašić, A. and Filipović-Vinceković, N. (2002) 'Interactions Between Dodecylammonium Chloride and ι-Carrageenan', *Journal of Colloid and Interface Science*, 256(2), pp. 462–471. doi: 10.1006/jcis.2002.8687.

Vinceković, M. *et al.* (2005) 'Phase behavior in mixtures of cationic surfactant and anionic polyelectrolytes', *Colloids and Surfaces A: Physicochemical and Engineering Aspects*. Elsevier, 255(1–3), pp. 181–191. Available at: https://www.sciencedirect.com/science/article/pii/S0927775704009719 (Accessed: 20 August 2019).

Vinceković, M. *et al.* (2011) 'Interactions between dodecylammonium chloride and carrageenans in the semidilute regime', *Colloids and Surfaces A: Physicochemical and Engineering Aspects*. Elsevier, 384(1–3), pp. 739–748. doi: 10.1016/j.colsurfa.2011.05.056.

Williams, P. A. and Langdon, M. J. (1998) 'The influence of locust bean gum and dextran on the gelation of κ-carrageenan', *Biopolymers*. John Wiley & Sons, Ltd,

38(5), pp. 655–664. doi: 10.1002/(SICI)1097-0282(199605)38:5<655::AID-BIP9>3.0.CO;2-R.

Williams, P. A. and Phillips, G. O. (2000) 'Introduction to Food Hydrocolloids', in Williams, P. A. and Phillips, G. O. (eds) *Handbook of Hydrocolloids*. 2nd edn. Cambridge, UK: Woodhead Publishing Limited, p. 15.

Wolf, B. *et al.* (2000) 'Shear-induced anisotropic microstructure in phase-separated biopolymer mixtures', *Food Hydrocolloids*. Elsevier, 14(3), pp. 217–225. doi: 10.1016/S0268-005X(99)00062-4.

Yin, T. *et al.* (2014) 'The interactions of ι-carrageenan with cationic surfactants in aqueous solutions', *Soft Matter*. The Royal Society of Chemistry, 10(23), pp. 4126–4136. doi: 10.1039/c4sm00322e.

Yuguchi, Y., Urakawa, H. and Kajiwara, K. (1997) 'Structural Characteristics of Crosslinking Domain in Gellan Gum Gel', *Macromolecular Symposia*. John Wiley & Sons, Ltd, 120(1), pp. 77–89. doi: 10.1002/masy.19971200110.

Zhang, Y. *et al.* (2016) 'Plasticisation of carnauba wax with generally recognised as safe (GRAS) additives', *Polymer*, 86, pp. 208–219. doi: 10.1016/j.polymer.2016.01.033.

3

Formulation and characterisation of kappa-carrageenan gels with non-ionic surfactant for melting triggered controlled release

Originally published in:

Fenton, T., Kanyuck, K., Mills, T., & Pelan, E. (2021). Formulation and characterisation of kappa-carrageenan gels with non-ionic surfactant for melting-

triggered controlled release. Carbohydrate Polymer Technologies and Applications, 2, 100060. https://doi.org/10.1016/j.carpta.2021.100060

3.1 Abstract

Kappa carrageenan was identified as a possible gel for melting-triggered release at 30 – 40 °C with the inclusion of a non-ionic surfactant for use in detergency or food-related applications. The gel formulation was kappa carrageenan (0.6 – 3% w/w) and either Tween 20 or Dehypon LS 36: two different non-ionic surfactants (0 – 5% w/w). Rheology and micro differential scanning calorimetry (μDSC) found that the addition of either non-ionic surfactant had a significant increase in the gelling and melting temperatures, however the gelling and melting enthalpies remained unchanged with additional surfactant. Additionally, the elastic modulus, increased by up to an order of magnitude upon addition of the surfactant. Surface tension measurements showed that the critical micelle concentration of both non-ionic surfactants did not change with the addition of carrageenan, indicating no electrostatic interactions. The mechanism of interaction between carrageenan and non-ionic surfactants is suggested to be hydrophobic interactions leading to electrostatic shielding, which enhances carrageenan aggregation. Melting measurements of kappa-carrageenan gels with non-ionic surfactant proved that temperature-mediated release at 40 °C was achieved.

3.2 Introduction

The gelling capacity of hydrocolloids has been exploited for decades as a texture modifier in foodstuffs (Saha & Bhattacharya, 2010), however, attention has since been given to hydrocolloids for their controlled release properties (Burey, Bhandari, Howes, & Gidley, 2008; Gulrez, Saphwan, & Phillips, 2011; Patil & Speaker, 1998). Hydrocolloids can make ideal controlled release vehicles by helping to solubilise insoluble or volatile species (Chakraborty, 2017) and controlled release can be obtained by formulating biopolymers to have burst release in response to an external stimuli such as a change in temperature, pH, or salt concentration, or a more steady, diffusion/erosion-mediated release (Pal, Paulson, & Rousseau, 2009).

Carrageenan, an algae-derived polysaccharide originating from *Rhodophycae* seaweed, is one such hydrocolloid that has been highlighted for its potential as a controlled release agent. It is a negatively-charged polyelectrolyte consisting of a sulphated polysaccharide chain, hence its structure is sensitive to its ionic environment, most notably, the pH and cation concentrations (Imeson, 2000). The degree of chain substitution with sulphate groups, and hence the physical properties of the resultant gels, is used to classify common carrageenans into three types: kappa-carrageenan (κC), iota-carrageenan (ιC) and lambda-carrageenan (λC), which have one, two and three sulphate groups per idealised repeat unit respectively. Under suitable cation conditions, gelation in carrageenans is possible and is attributed to the formation and subsequent aggregation of double helices.

The degree of carrageenan aggregation, and hence the resulting gel structure, is strongly salt dependent, particularly potassium salts for kappa carrageenan and calcium salts for iota carrageenan (Imeson, 2000). Cations interact with the anionic carrageenan helices and screen the negative charges on the chain, reducing interchain repulsion and encouraging aggregation. The process of gelation in carrageenans is fully thermally-reversible, therefore release can be theoretically triggered through melting of gelled structures upon the application of heat (Liu et al., 2016).

Surfactants, or surface-active agents, are amphiphilic molecules which adsorb at interfaces, lowering the interfacial tension. Surfactant molecules have a hydrophobic and a hydrophilic region, which gives them the ability to adsorb across interfaces formed when mixing two phases of differing polarities. They are known to form ordered structures called micelles once the concentration of surfactant reaches or exceeds the critical micelle concentration CMC. Once the CMC is reached, it is characteristic that the surface tension does not decrease further. The presence of a surfactant makes the two phases more compatible with each other and results in wetting or emulsification due to a decrease in interfacial tension. It is this principle that allows cleaning of soiled clothes and crockery in detergency applications. Non-ionic surfactants, produce little foam, are tolerant of a range of water hardnesses, and are generally safer to handle and consume in edible formulations (Blagojević, & Pejić, 2016), hence they are the preferred choice in automatic dishwashing detergent (ADD) and food-grade formulations.

The combination of gelling hydrocolloids with surfactants has been featured widely in literature for the past several decades (Piculell and Lindman, 1992; Griffiths and Cheung, 2003; Wang *et al.*, 2006; Moonprasith *et al.*, 2008; Pepić, Filipović-Grčić and Jalšenjak, 2009; Bonnaud, Weiss and McClements, 2010b; Vinceković *et al.*, 2010; Sreejith, Nair and George, 2010; Vinceković *et al.*, 2011; Rosas-Durazo *et al.*, 2011; Fasolin *et al.*, 2013; Picone and Cunha, 2013; Yin *et al.*, 2014; Grządka, 2015). The majority of this literature is concerned with structures formed between a polyelectrolyte and a surfactant -often with each species having opposing electrical charges - termed polyelectrolyte-surfactant complexes, which interact through electrostatic interactions. Upon complexation, the critical micelle concentration (CMC) of a surfactant can decrease in the presence of a polymer due to complexation of the polymer and the surfactant, sometimes by several orders of magnitude (Jain et al., 2004). This new concentration can be denoted the critical aggregation concentration (CAC) and is a useful indicator of polyelectrolyte-surfactant binding. For polymers and surfactants without opposing charges, hydrophobic interactions can occur between the two species also resulting in some level of complexation, however, if this interaction is weak then the CMC and CAC of the surfactant are very similar (Yang & Pal, 2020).

Understanding the mechanical and thermal properties of a sample is central to predicting how that material will perform as a controlled release product, and also how easily the product can be handled and can withstand shear before irreversibly breaking. Oscillatory rheology is a powerful tool for elucidating these properties,

since it can determine gelling (T_g) and melting (T_m) temperatures by the cross-over of G' and G" (Warner, Norton, & Mills, 2019), and a frequency sweep can predict if the sample is solid-like or liquid-like by examining the values of G' and G", and their dependence on frequency. Micro differential scanning calorimetry (μDSC) also examines thermal transitions by measuring the heat produced or absorbed upon bond formation or breakage. μDSC is more sensitive than conventional differential scanning calorimetry, as well as being able to perform scans at much slower heating and cooling rates.

The purpose of this work was to quantify and understand the change in mechanical and thermal properties of kappa-carrageenan when formulated in combination with non-ionic surfactant, and to determine whether the resulting formulation is suitable for temperature-triggered release at temperatures of 30 – 40 °C. This temperature was chosen to provide melt-in-the-mouth release in food formulations, or early release in a dishwasher cycle, which would avoid deactivation by surfactant-deactivating species, such as bleaches, if formulated in tandem with a higher melting point gel (50 – 60 °C). Kappa carrageenan was chosen due to its desirable thermal, mechanical and environmental properties; it forms thermoreversible firm gels, derived from renewable natural resources. The surfactants used were Tween 20, a common, edible non-ionic surfactant, and Dehypon LS 36 (D36), a fatty alcohol-type non-ionic surfactant used in detergent formulations. The gelling and melting temperatures were determined using rheology and micro-differential scanning calorimetry (μDSC), which also provided

mechanical properties and thermal transition enthalpies respectively. Turbidity measurements were performed to investigate any change to the size and number of carrageenan aggregates. The CMC (only surfactant and water) and CAC (surfactant, water and carrageenan) of the non-ionic surfactants were determined using tensiometry. The melting performance of the gels were elucidated using conductivity in a custom, temperature-controlled setup by detecting the release of ions in water from the carrageenan gels.

3.3 Experimental

3.3.1 Materials

Genugel® CG-130 (batch no. SK30005409), a commercially available carrageenan was kindly gifted by CP Kelco (USA) – from this point on, Genugel® CG-130 shall be referred to as Genugel®, κC or kappa-carrageenan. The ^{13}C NMR spectrum of Genugel® is given in Figure 3.9 shows that Genugel® can be treated as 'pure' kappa carrageenan as there is only one peak at ca. 95 ppm, corresponding to the α-anomeric carbon of κC (Villanueva, Mendoza, Rodrigueza, Romero, & Montaño, 2004). The ion content of Genugel® was determined by Inductively Coupled Plasma-Optical Emission Spectroscopy (PerkinElmer Optima 8000) as (% w/w): Na^+ = 0.332, K^+ = 2.20, Mg^{2+} = 0.0191, Ca^{2+} = 1.15. Tween 20 was purchased from Merck (Germany). Dehypon LS 36 was purchased from BASF (Germany). All water used was purified using a reverse-osmosis Millipore® unit. All materials were used without any further purification.

3.3.2 Methods

3.3.2.1 Preparation of carrageenan and carrageenan-surfactant solutions.

An appropriate mass of Genugel® was added to hot distilled water (ca. 80 °C), covered to prevent evaporation and was allowed to fully disperse and hydrate under agitation from a magnetic stirrer bar for 2 hours. If required, an appropriate mass of surfactant (0.1 – 5% w/w) was added to the hot carrageenan solution, and this was stirred at a reduced speed for a further 30 minutes at ca. 80 °C to minimise foam formation. Solutions were removed from heat and kept at room temperature overnight. Prior to measurement, samples were re-heated to ca. 80 °C under agitation until isothermal. Solutions were formulated at 0.6, 1, 2, and 3% w/w carrageenan with 0, 1, 2, 3, 4 and 5% w/w surfactant.

3.3.2.2 Rheological measurements

A MCR 302 rheometer (Anton Paar, Austria) equipped with a PP50-TG parallel plate geometry (D = 50.0 mm) and a P-PTD200/62/TG roughened lower plate geometry (D = 62.0 mm) was used to characterise the rheology of the samples. In all measurements, samples were loaded in sol form (80 °C) and trimmed to a gap of 1 mm, with the geometry pre-heated to 70 °C. A thin layer of silicone oil was immediately added to the outer edge of the samples to prevent evaporation and a Peltier hood (H-PTD-200) was lowered. For samples with a gelling temperature of below 20 °C, for the frequency and amplitude sweeps, after loading samples were initially cooled to 5 °C for 10 minutes, before heating back to 20 °C to ensure gelation had taken place. The TruGap™ setting ensured the rheometer gap

adjusted due to any thermal expansion or contraction by the measurement geometry.

3.3.2.3 Amplitude sweep to determine the linear viscoelastic region (LVR)

An amplitude sweep was performed from 0.01 to 100% strain, at a frequency of 6.28 rad s^{-1} (1 Hz) and a temperature of 20 °C. The linear viscoelastic region was determined as the range of strain values which showed no significant degradation (± 1%) in the value of the storage (G') modulus. This data was only used to determine strain values in proceeding oscillatory rheology and is not presented in this manuscript.

3.3.2.4 Temperature sweep to determine the gelling and melting temperatures

A temperature sweep was performed from 70 °C to 10 °C and from 10 °C back to 70 °C to record gelling and melting temperatures respectively, and this was performed in triplicate for each sample. Strain values were chosen to be within the LVR of the samples, and all sweeps were performed at a frequency of 6.28 rad s^{-1} (1 Hz). The rate of temperature change was 1 °C per minute. T_g and T_m were determined by the crossover point of the elastic modulus (G') and viscous modulus (G") (Warner et al., 2019).

3.3.2.5 Frequency sweep to determine the mechanical spectra

A frequency sweep was performed in triplicate, with the frequency varying between 10 rad s^{-1} to 0.1 rad s^{-1} (1.59 Hz to 0.0159 Hz), at strain within the LVR of the samples. The measurements were performed at 20 °C.

3.3.2.6 μDSC measurements

A Setaram evo3 differential scanning calorimeter was used to record the thermal transitions of the prepared samples. An appropriate mass (0.6 – 0.8 g) of melted sample was loaded into a screw-top, stainless steel cell using a pipette, and this was mass-balanced to within ± 0.005 g with deionised water in the reference cell. Both cells were sealed with a new o-ring gasket. After an initial hold at 20 °C for 30 minutes to allow for sample equilibration, samples were cooled down to -5 °C, followed by a heating step to 90 °C. In all cases, the rate of change of temperature was kept constant at 1 °C per minute. Each heating and cooling cycle was performed a total of 3 times per sample, with a 5 minute isothermal hold between each cycle.

3.3.2.7 Tensiometry measurements - Critical Micelle Concentration (CMC) and Critical Aggregation Concentration (CAC) determination

A drop shape Sinterface PAT1M Tensiometer was used to measure CMC and CAC aqueous solutions of non-ionic surfactant without and with additional carrageenan respectively. Sample preparation involved performing serial dilutions of a surfactant with deionised water or a solution of 0.6% w/w Genugel®, to achieve final concentrations of surfactant of 0.001 – 0.01% w/w (10 to 100 mg L^{-1}). Measurements were performed at room temperature (22 °C). The samples containing carrageenan were not gelled, which was necessary for the measurements. The tensiometric measurement was continued until the surface tension reached a steady value (± 1%), with each experiment being performed in triplicate. The droplets were formed as pendant drops, and were kept at a constant area of 25 mm^2, extruded from a capillary with a 3mm diameter. Density values were previously obtained as 0.997 g cm^{-3} and 1.002 g cm^{-3} for the surfactant-water and surfactant-water-carrageenan samples respectively. The density of air was assumed as 0.0012 g cm^{-3}.

3.3.2.8 Turbidity Measurements

A Thermo Scientific Orion AquaMate 8000 UV-Vis spectrometer was used to determine turbidity by measuring absorbance at a wavelength of 600 nm. Hot melted samples were poured in to 10 mm disposable plastic cuvettes, cooled to below their gelling temperature and subsequently stored overnight at room

temperature until measurement. Measurements were performed in triplicate at room temperature and distilled water was used as a blank.

3.3.2.9 Melting of gels in water using conductivity

A Mettler Toledo SevenEasy conductivity meter was used monitor conductivity. The gel formulations were 0.6% w/w Genugel® with 3% w/w Tween 20 or Dehypon LS 36, and 10 g of this hot solution was added to a silicone ice tray (dimensions 27 mm × 27 mm × 21mm) in order to form duplicate cubes. The gel cubes were covered and stored at 5 °C overnight. Prior to measurement, the gels were weighed to ensure no evaporative losses had taken place and were allowed to come to room temperature. A conductivity probe was inserted in to a 1 dm^3 beaker containing 900 g of distilled water through a hole in a custom 3D-printed lid: this ensured that the relative position of the probe to the sample was fixed. The gel cubes were placed in a porous net attached to the lid and the endpoint of the release measurement was determined once the conductivity value was steady (±0.01 mS cm^{-1}) for a period of 5 minutes. The water was kept isothermal at either 20, 30 or 40 °C using a thermostatic probe connected to a stirrer hotplate, and the solution was agitated at a constant rate of 200 rpm with a magnetic stirrer bar. Conductivity was logged via Mettler Toldedo LabX Direct-pH software, which recorded the conductivity once per second until it was manually stopped.

3.3.2.10 Statistical Analysis

Gelling and melting temperatures and enthalpies, and turbidity measurements were analysed by calculating the Pearson correlation coefficient (ρ): a positive correlation is indicated if $0 < \rho \leq 1$, and a negative correlation if $-1 \leq \rho < 0$, whereby the strength of the correlation increases as ρ moves away from 0. The CMC and CAC values were compared using the two-sample T-test in the Analysis TookPak for Microsoft Excel, and the two populations were considered to have equal means if t Stat < t Critical two-tail.

3.4 Results

3.4.1 Rheological characterisation of Genugel® with non-ionic surfactant

3.4.1.1 Determination of the gelling and melting temperatures

A temperature sweep was used to determine the gelling and melting temperatures of samples by noting the temperature at which the elastic and viscous moduli are equal: an example of this is given in Figure 3.10. This data was gathered for Genugel® samples at the aforementioned concentrations, formulated in tandem with non-ionic surfactants, and this data is plotted in Figure 3.1. There are three variables in these temperature sweep data: the concentration of carrageenan (and hence the concentration of gelling cations), the concentration of non-ionic surfactant and the type of the non-ionic surfactant, and each will be examined in turn for its influence on the gelling and melting temperatures of the carrageenan gels.

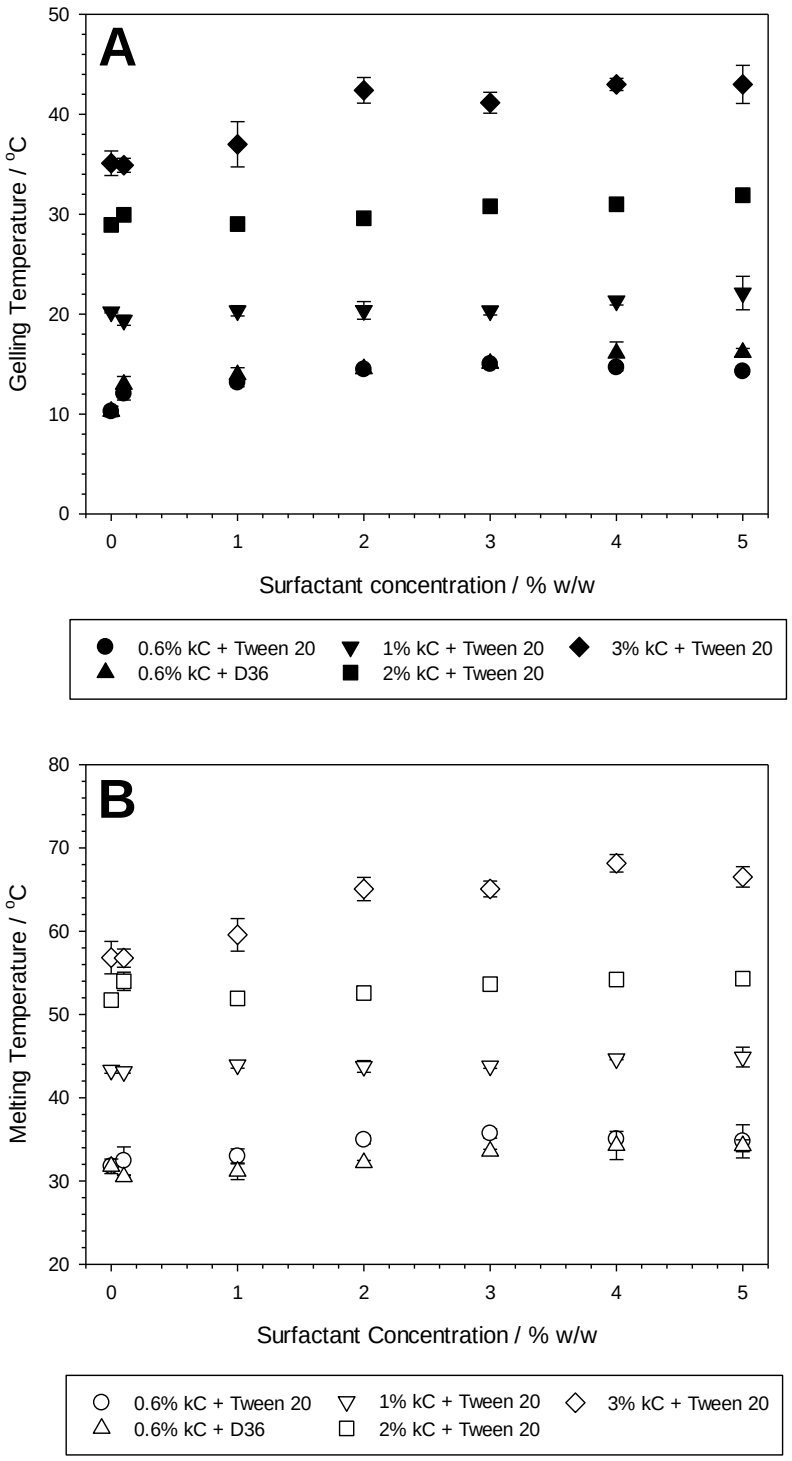

Figure 3.1 - Temperature sweep data for Genugel® solutions at with different concentrations of added surfactants. (A) shows data for the gelling temperature, (B) shows data for the melting temperature, both of which were obtained by the crossover of G' and G".

As the concentration of carrageenan was increased, the gelling and the melting temperatures both increased, with gelling temperatures increasing from ca. 10 °C to 35 °C, and melting temperatures increasing from ca. 30 °C to 55 °C as the concentration of carrageenan increased from 0.6 to 3% w/w. The increase in gelling and melting temperatures of carrageenan can be attributed to more effective screening of negative charges on the polysaccharide chain of carrageenan reducing the intermolecular repulsion between chains and encouraging aggregation of double helices Norton *et al.* (1983). The magnitude of the thermal hysteresis – the numerical difference between the gelling and the melting temperatures – also increased slightly from ca. 20 °C for 0.6% w/w carrageenan, to ca. 25 °C for 2 and 3% w/w carrageenan. This rise in thermal hysteresis with increasing carrageenan concentration suggests that the gel structure became more thermally stable – and therefore more aggregated (Liu et al., 2016). Thermal hysteresis is a well-known phenomenon for κC (Diañez *et al.*, 2019), and the magnitude of the measured thermal hysteresis agreed closely with previously published literature by Lai, Wong and Lii (2000), who reported an average thermal hysteresis of 22.5 °C of 1.5 g / dL κC in water.

The introduction of non-ionic surfactant led to an increase in gelling and melting temperatures across all tested carrageenan concentrations. As surfactant concentration was increased from 0 to 5% w/w, the gelling and melting temperatures increased by approximately 5 °C, regardless of the concentration of. Furthermore, the Pearson correlation coefficient values, shown in Table 3.1, were

$0.77 \leq \rho \leq 0.93$, indicating a statistically strong positive relationship between gelling & melting temperatures and the concentration of surfactant. There was very little difference between the phase transition temperatures measured between the Tween 20 and Dehypon LS 36-containing formulations, which provides evidence that similar changes may be seen with many other non-ionic surfactants in similar formulations. With regards to the most effaceable concentration for controlled release, the measured melting temperatures of the carrageenan-non-ionic surfactant gels suggest that 0.6% w/w Genugel® would be ideal for release at 30 – 40 °C since it was the only formulation that melted in this temperature range, regardless of the presence of any surfactant.

Table 3.1 - Pearson correlation coefficient values (ρ) for the gelling (Tg) and melting (Tm) temperature data vs. surfactant concentration.

Formulation	**$\rho(T_g)$**	**$\rho(T_m)$**
0.6% κC + Tween 20	0.90	0.87
0.6% κC + D36	0.84	0.85
1% κC + Tween 20	0.89	0.93
2% κC + Tween 20	0.79	0.76
3% κC + Tween 20	0.78	0.77

3.4.1.2 Determination of the mechanical spectra

A frequency sweep was performed to examine the frequency dependence and the viscoelastic moduli of the carrageenan-non-ionic surfactant gels: this data is shown in Figure 3.2. For clarity only frequency sweep data at surfactant concentrations of 0, 1, 3 and 5% w/w are plotted. The remaining frequency sweep data at surfactant concentrations of 0.1, 2 and 4% w/w are plotted in Figure 3.11.

The first observation is that as the concentration of carrageenan was increased, the values of G' increased markedly: the difference between 0.6 and 3% w/w carrageenan was approximately 3 orders of magnitude, increasing from ca. 10 Pa, to 10^4 Pa. At concentrations of 2% w/w carrageenan and above, the samples shifted from being frequency dependent to almost frequency independent, which indicated that the samples became more solid-like in nature. The value of G' at 0% w/w surfactant did not change between 2 and 3% w/w carrageenan, which suggests that a maximum in aggregation without any additional species was reached.

The addition of non-ionic surfactant to the carrageenan also resulted in a greater measured value of G', in some cases by up to an order of magnitude. Similar increases in G' were seen for both Tween 20 and D36-containing formulations. As the concentration of carrageenan was increased from 0.6 to 2% w/w the influence

that the surfactant had on the carrageenan gel strength decreased.

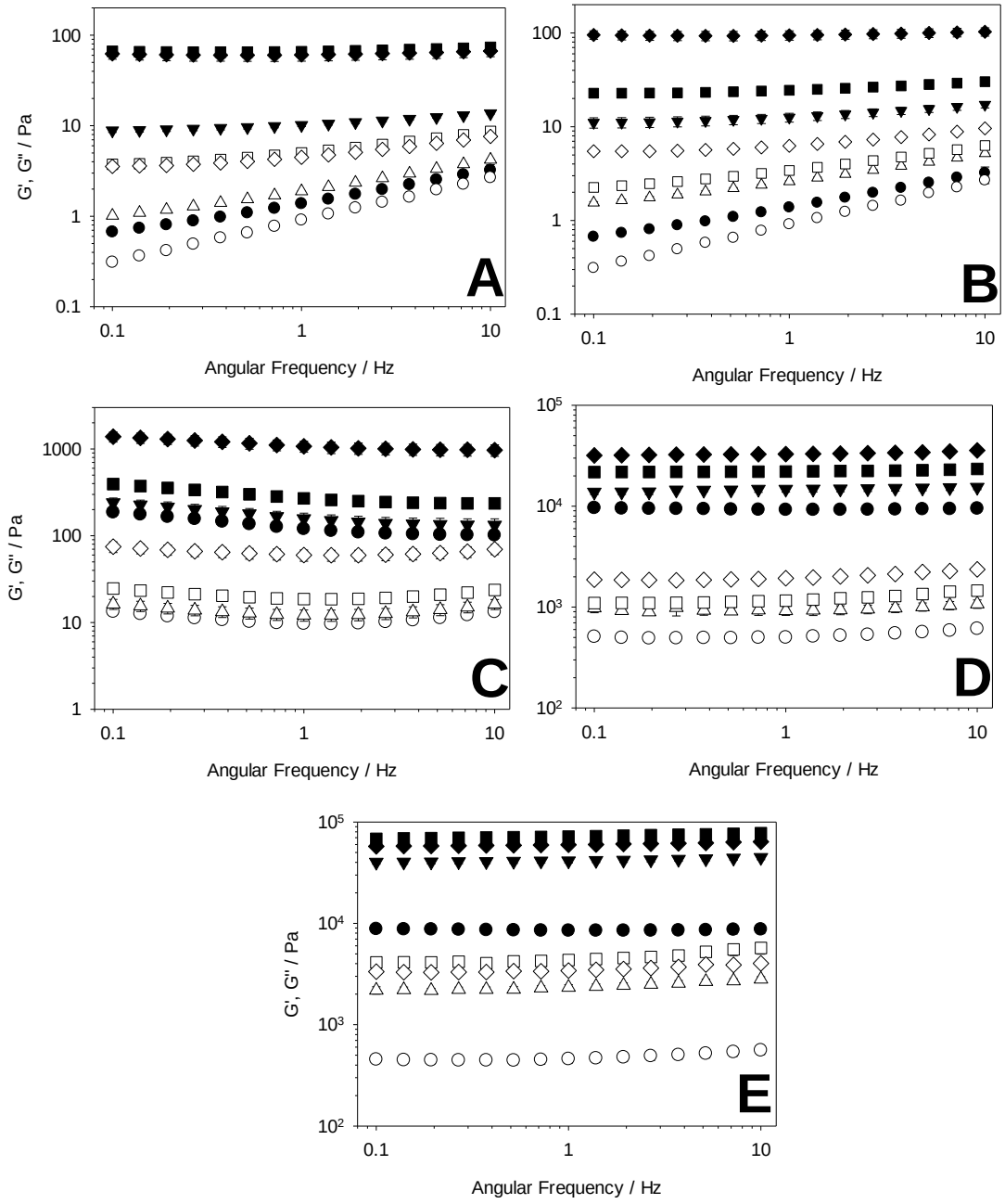

Figure 3.2 - Frequency sweep data for Genugel and surfactant solutions. (A) – 0.6% Genugel with Tween 20, (B) – 0.6% Genugel with D36, (C) – 1% Genugel with Tween 20, (D) – 2% Genugel with Tween 20 and (E) – 3% Genugel with Tween 20. Filled black symbols indicates values of G', and filled white symbols indicates values for G". Different concentrations of surfactant are denoted by the symbol shape – ● - no surfactant, ▼ - 1% surfactant, ■ - 3% surfactant, ◆ - 5% surfactant).

At 0.6% w/w carrageenan G' increased by 2 orders of magnitude across the range of surfactant concentrations tested, decreasing to 1 order of magnitude at 1% w/w carrageenan, then less than an order of magnitude at 2 and 3% w/w carrageenan. This is likely because at lower carrageenan concentrations – and therefore lower gelling cation concentrations – the gel structure is less aggregated and hence there is more potential for aggregation to increase.

Material properties are not only dictated by G', but also G'', or more specifically the phase angle. The difference between G' and G'' defines the phase angle (δ), as shown in Equation 3.1.

$$\tan(\delta) = G''/G' \tag{3.1}$$

The phase angle can predict if the gel is self-supporting, as this is essential for many applications. Work by Gholamipour-Shirazi, Norton and Mills (2019) outline the following rules: phase angles of below 3° are very firm, stiff materials; 3-15° gives semi-solid, self-supporting materials; 15-45° gives semi-solid but non-self-supporting materials and any material with a phase angle above 45° is a liquid by definition. Phase angle values were calculated at each based on frequency sweep data, and averaged, as shown in Figure 3.3.

It was found that only 0.6% w/w carrageenan gels at surfactant concentrations of 1% w/w or below can be classed as non-self-supporting, soft gels, and would therefore be unsuitable for many applications. As the surfactant concentration was increased past 1% w/w, the phase angle of 0.6% w/w carrageenan samples decreased such that all subsequent samples can be classed as self-supporting. For carrageenan at concentrations of 1% w/w or less, the addition of surfactant had a strong influence on the phase angle, whereas at carrageenan concentrations of 2% w/w and above, there was no influence on the phase angle.

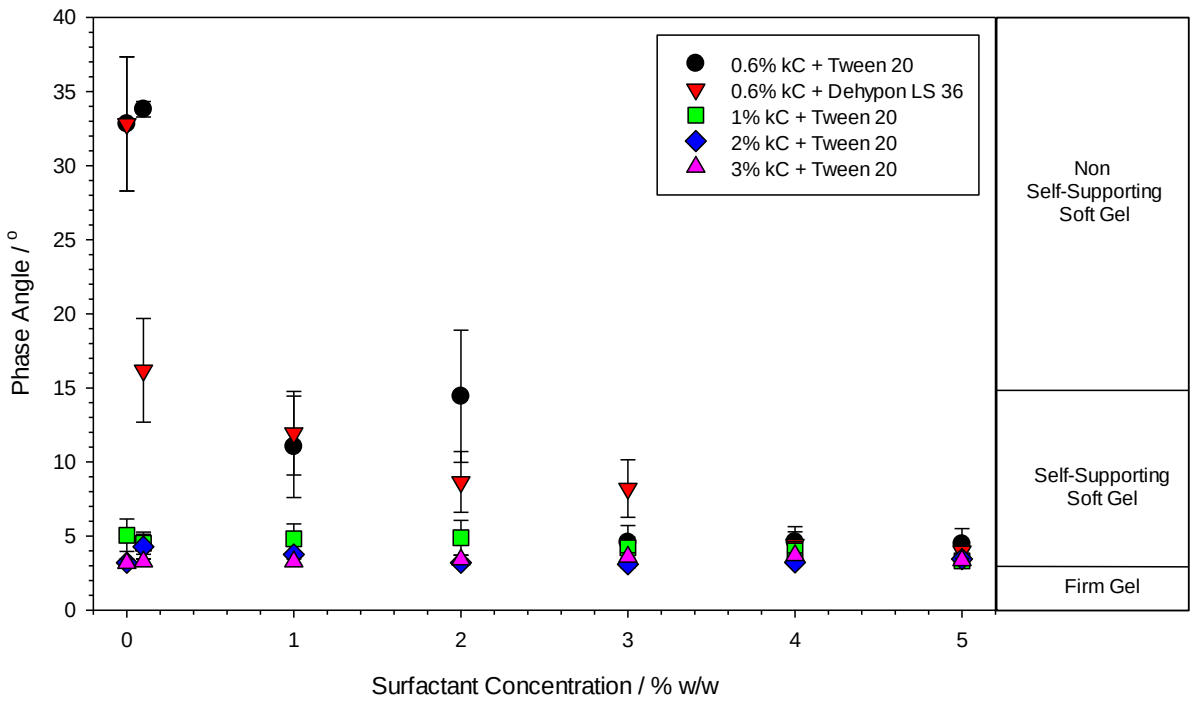

Figure 3.3 - Phase diagram for Genugel®-non-ionic surfactant systems, showing how the material properties change with carrageenan and surfactant concentration, and surfactant type. The shading of the graph background indicates the material behaviour shown (white – non-self-supporting soft gels, light grey – self-supporting soft gel, dark grey – firm gel).

3.4.2 Micro-Differential Scanning Calorimetry of Genugel® with non-ionic surfactant

Micro differential scanning calorimetry (μDSC) was performed on Genugel® samples in combination with Tween 20 at to the aforementioned concentrations. Dehypon LS 36 could not be tested due to the fact that its cloud point occurred in the temperature range tested, which masked any signal from the gelling or melting of the carrageenan: a characteristic of ethoxylated polyol surfactants. The phase transition temperatures were taken as the maximum or minimum in the heat flow for both cooling and heating cycles respectively (Núñez-Santiago & Tecante, 2007), and enthalpies were calculated from integration of the thermograms.

The phase transition temperatures were plotted as a function of increasing Tween 20 concentration, as shown in Figure 3.4, and as previously, Pearson correlation coefficients were calculated to examine if there was a statistical trend, shown in Table 3.2. When examining the phase transition temperatures, it is apparent that the values obtained using μDSC were 5- 10 °C lower than those measured with rheology, apart from 0.6% w/w Genugel® which showed good parity. Gelling values ranged from ca. 10 – 30 °C and melting values from ca. 25 – 50 °C, compared to ca. 10 – 40 °C and ca. 30 – 65 °C measured by rheology. A very strong positive correlation between surfactant concentration and phase transition temperature was measured across all carrageenan and surfactant concentrations tested ($\rho \geq 0.90$). The Pearson correlation coefficient values were generally larger than those previously calculated in the rheological data, likely because the measurements

made in the μDSC were more repeatable, hence giving less measurement variability.

Upon addition of Tween 20, measured phase transition temperatures increased in the order of 2 - 5 °C across the surfactant concentrations tested: very similar to the behaviour measured using rheology. Additionally, the value of the thermal hysteresis increased with increasing carrageenan concentration, from ca. 15 °C for 0.6 and 1% w/w carrageenan, to 20 °C for 2 and 3% w/w carrageenan: once again, very similar to that measured with rheology. The shapes of the profiles are given in the appendix Figure 3.12 - Figure 3.19, and can be seen to have a single peak in each exotherm and endotherm, indicating a single transition. If strong polyelectrolyte-surfactant complexes were formed, one would expect to see an associated enthalpy upon formation or breakage of these complexes, which was not seen. Tween 20 itself, without carrageenan, did not produce any detectable signal in the temperature range tested, hence all contributions must be due to carrageenan-associated interactions.

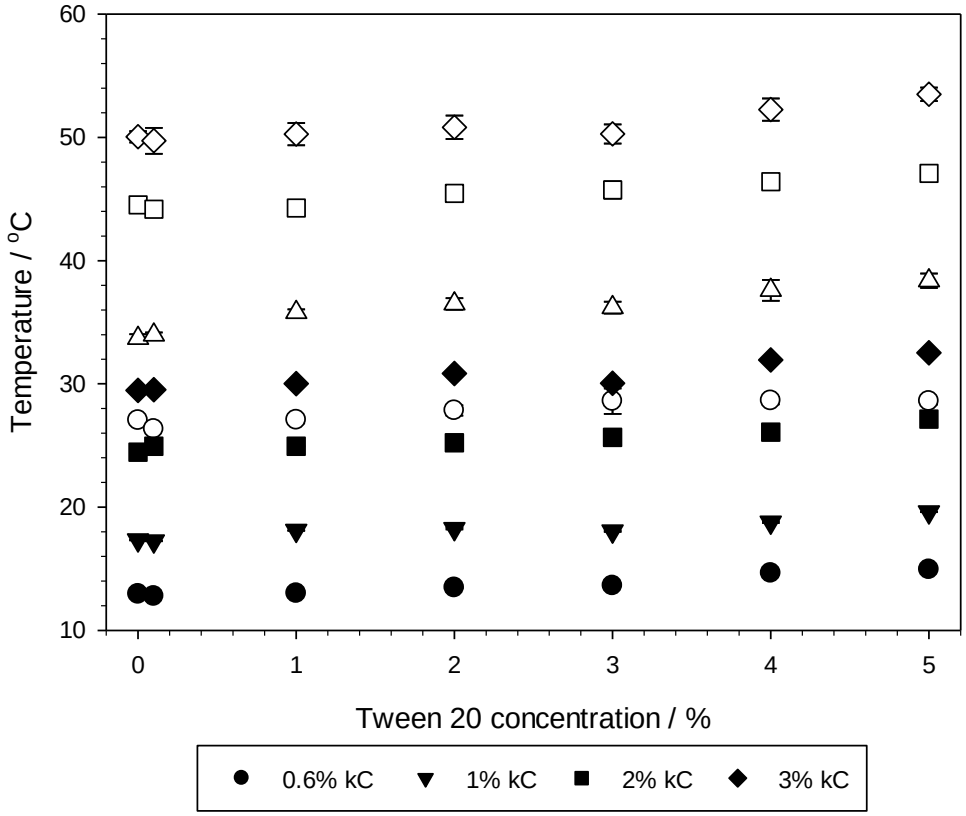

Figure 3.4 - Data for the phase transition temperatures of Genugel® samples at different concentrations of Tween 20, obtained by μDSC. Filled markers (●) indicate coil-helix temperatures, whereas unfilled markers (○) indicate helix-coil temperatures.

Table 3.2 - Statistical analysis for the μDSC phase transition temperature data.

Formulation	**$\rho(T_{coil-helix})$**	**$\rho(T_{helix-coil})$**
0.6% κC + Tween 20	0.97	0.92
1% κC + Tween 20	0.94	0.95
2% κC + Tween 20	0.96	0.99
3% κC + Tween 20	0.92	0.90

Phase transition enthalpies can be measured by integration of the heat flow-temperature curve: these data are given in Figure 3.5. It is apparent that 0.6% w/w Genugel® had the smallest phase transition enthalpy values, which is indicative of a weaker gel network, which aligns with rheological data obtained during frequency sweeps. As the concentration of carrageenan was increased, the phase transition enthalpies increased, and this trend holds for the entire range of concentrations tested. Previous literature has reported that phase transition enthalpies and κC concentration share a linear relationship (Iijima, Hatakeyama, Takahashi, & Hatakeyama, 2007; Liu et al., 2016), which appears to agree with the reported data for Genugel®. The range of enthalpy values obtained for the gelling and melting processes is ca. 0.1 – 1 J g^{-1}, which also agrees closely with previously reported data for κC (Iijima et al., 2007).

In contrast, it is apparent that the addition of non-ionic surfactant to the carrageenan gels had no measurable influence on the gelling or melting enthalpies at all concentrations tested. The Pearson correlation coefficient values were $\rho < 0.7$ (data not given) across all carrageenan concentrations tested which further evidences the lack of any strong correlation between surfactant concentration and phase transition enthalpy.

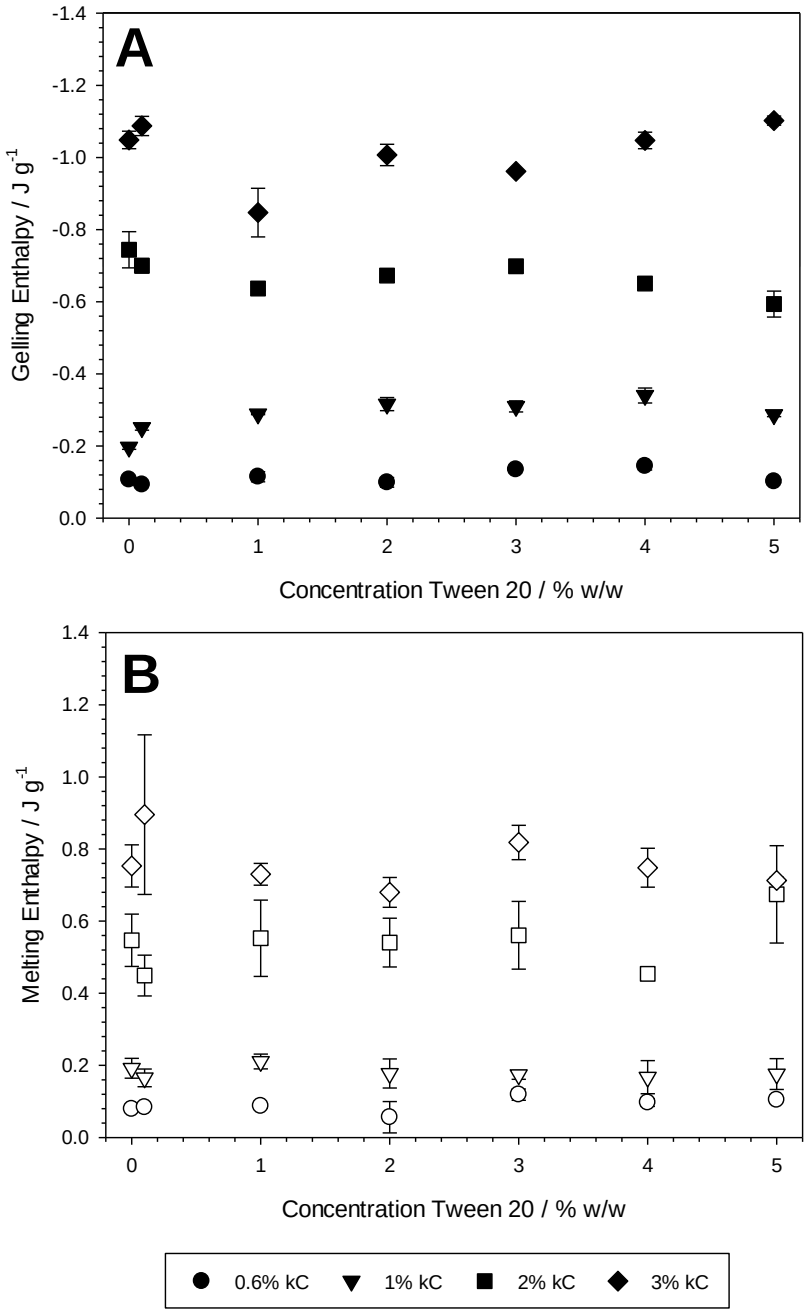

Figure 3.5 - Phase transition enthalpies measured by μDSC for Genugel®-Tween 20 gels. (A) – gelling enthalpies, (B) – melting enthalpies. Filled markers (●) indicate gelling enthalpies, whereas unfilled markers (○) indicate melting enthalpies.

3.4.3 Determination of the critical micelle and aggregation concentrations of Genugel® with non-ionic surfactants

Determining the CMC and CAC of both surfactant systems serves two purposes: firstly, it will determine a useful-dose of surfactant required in a detergent formulation, since detergency does not improve past the CMC (Poce-Fatou, 2006). Secondly, if the CAC and the CMC are very different (an order of magnitude or more), this suggests that carrageenan and non-ionic surfactants electrostatically interact. Whereas is the CAC and CMC are very similar, this indicates no interaction or weak, hydrophobic-driven interactions (Yang & Pal, 2020). Hence, the CAC and CMC was determined for Tween 20 and Dehypon LS 36 with and without Genugel® present respectively, as shown in Figure 3.6.

As can be seen from the data, the CMC values for Tween 20 and Dehypon LS 36 were both close to 60 mg / L. For Tween 20, this agrees well with previously reported values (Mittal, 1972), however for Dehypon LS 36, no literature value for the CMC could be found. Low CMC values such as these are characteristic of non-ionic surfactants. For a dishwasher of a 10 litre capacity (Bengtsson, Berghel, & Renström, 2015), this would mean that the ideal surfactant concentration would be ca. 3- 6% w/w for 10-20 g of gel, hence the previous formulations of up to 5% w/w surfactant are industrially-relevant. The relatively large error bars seen at low concentrations of Tween 20 are attributed to the heterogeneity of its formulation, which is amplified at very low concentrations, resulting in variability in the measurements. Additionally, at very low surfactant concentrations, the mobility of

the surfactant to arrive at the interface can be extremely slow, resulting in a long time to reach an equilibrium surface tension, making it difficult to determine the exact endpoint. As the concentration of Tween 20 was increased, the inhomogeneities in the Tween 20 solutions became less apparent, and the time taken to reach apparent equilibrium decreased dramatically: both of these made the surface tension measurements more repeatable.

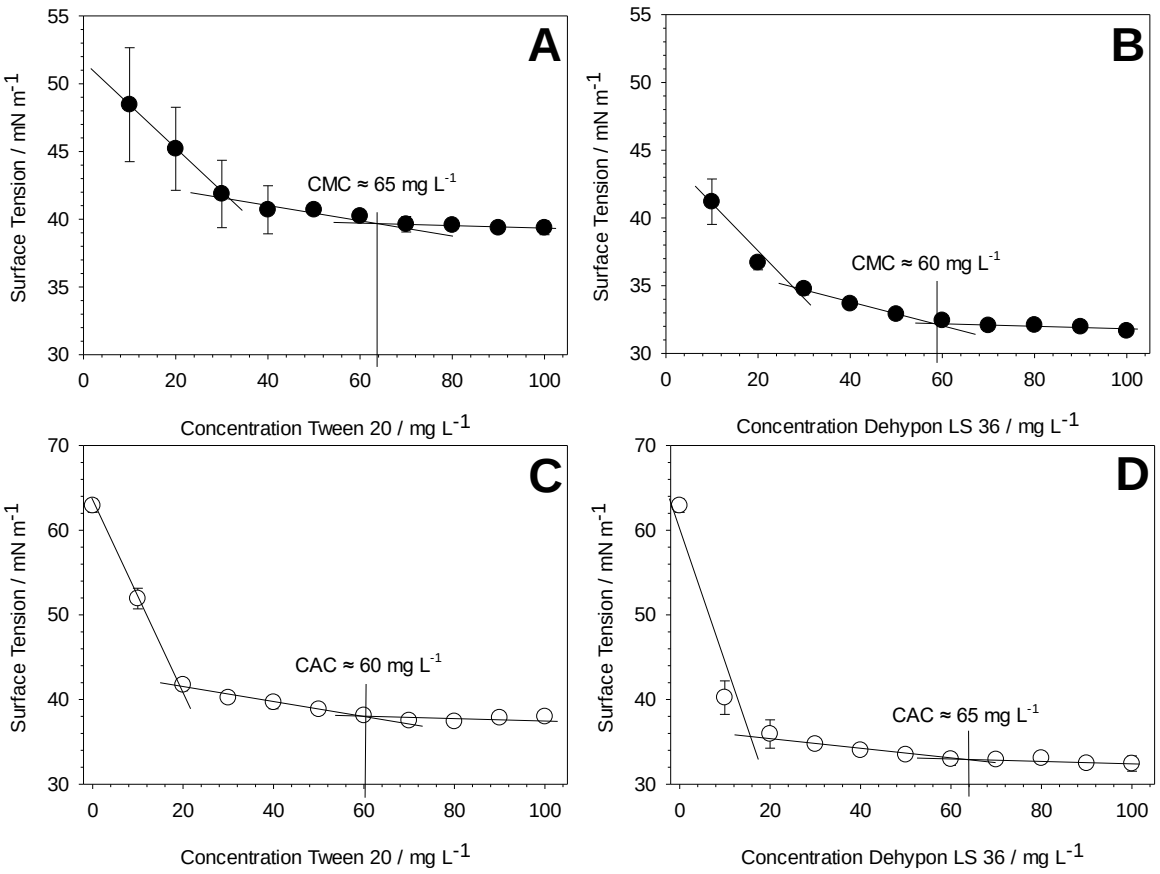

Figure 3.6 – Surface tension measurements for Tween 20 in water (A), Dehypon LS 36 in water (B), Tween 20 in 0.6% Genugel® (C) and Dehypon LS 36 in 0.6% Genugel® (D). Filled markers (●) indicate surfactant-water solutions, whereas unfilled markers (○) indicate surfactant-carrageenan solutions. The concentration at which the surface tension did not change – the CMC or CAC - is indicated on each graph. The CMC/CAC was estimated by the intersection point between a horizontal and a diagonal trendline.

The introduction of Genugel® to either surfactant mixtures had no measurable impact ($p > 0.05$) on the value of the CMC with all critical concentration values measuring as approximately 60 mg / L. If the carrageenan and non-ionic surfactant were electrostatically interacting, then one would expect to see a large difference between the CMC and CAC values, due to stabilisation of the micelles by the carrageenan chains (Griffiths & Cheung, 2003). Overall these surface tension data indicates two possibilities: weak non-ionic surfactant-carrageenan interactions, or no attractive interactions at all between the two species, which agrees with the previous μDSC data showing only one peak in the thermograms.

3.4.4 Turbidity of Genugel®-non-ionic surfactant gels

A change in turbidity of a gel suggests that a microstructural change has taken place, and so turbidity measurements were performed in order to evaluate if the addition of non-ionic surfactant to κC resulted in such a microstructural change – these results are shown in Figure 3.7. Turbidity is caused by the formation of structures that are large enough to scatter light (Bonnaud et al., 2010), and therefore an increase in turbidity can be seen as an increase in the number these structures, in this case, aggregates of carrageenan helices. A UV-Vis spectrometer can be used to determine the turbidity of gels by measuring the absorbance at 600 nm. Absorbance values (A) can be converted to turbidity values (τ / cm^{-1}) by using the path length (L / cm), as shown in Equation 3.2 (Sow et al., 2017).

$$\tau = \left(\frac{1}{L}\right) A \qquad (3.2)$$

Firstly, it was ensured that surfactant micelles were not interfering with scattering, hence Tween 20 in water was investigated without any carrageenan. As can be seen, no absorbance was detected at 600 nm, due to the fact that the small surfactant micelles are not large enough to scatter light. Hence, it was known that any change in the turbidity of carrageenan gels, in the concentration range tested, was not simply due to an increase in the number or size of surfactant micelles, and therefore it was assumed that the carrageenan aggregates must have been responsible.

Secondly, it can be noted that upon increasing the concentration of carrageenan from 0.6 to 3% w/w gave a large, steady increase in the turbidity of the gels: increasing from ca. 0.1 to ca. 0.9 cm^{-1}. It is taken that this is simply due to additional carrageenan aggregates scattering more light. Interestingly, there was a small statistical decrease in the turbidity upon the addition of non-ionic surfactant across every concentration of carrageenan tested, as shown by the negative Pearson correlation coefficient values in Figure 3.7. This indicates that the introduction of surfactant actually decreased the number of carrageenan aggregates, which seems to contradict the earlier rheological data.

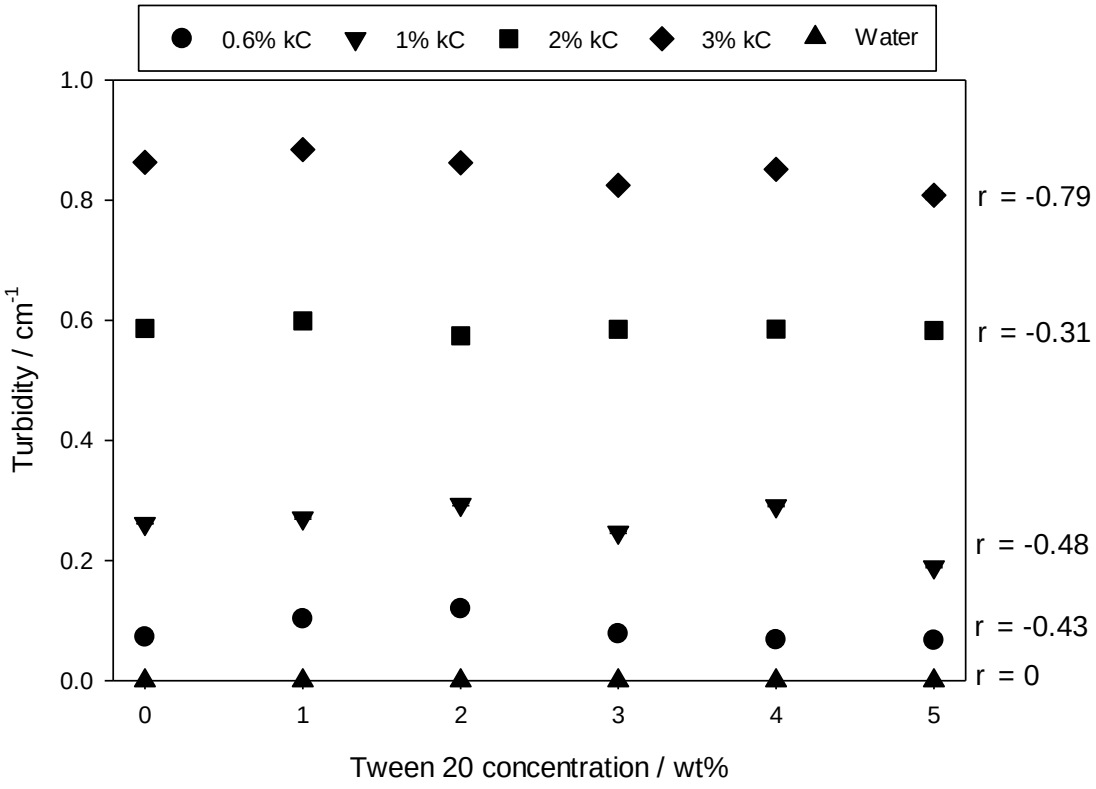

Figure 3.7 - Turbidity data obtained for kC gels at different combinations as a function of increasing Tween 20 concentration. Water was also tested as a control. Pearson correlation coefficient (ρ) values are given alongside the data.

There did not appear to be any trend in the Pearson correlation coefficient values with concentration of carrageenan, indicating that the introduction of surfactant affected each concentration of carrageenan equally, which does agree with the previously reported rheological data.

3.4.5 Measuring the melting of Genugel®-non-ionic surfactant gels in water

To estimate the release of non-ionic surfactant from κC-surfactant gels, ca. 10 cm^3 cuboid gels were placed into water and the conductivity of the water was logged over time. The solutions were stirred slowly as to homogenise the vessel, yet not so fast as to significantly shear and break the gel. The release experiments were performed at 20, 30 and 40 °C, and the corresponding release profiles are given in Figure 3.8. Carrageenan at concentrations of 0.6 and 1% w/w were initially tested due to having melting temperatures either side of 40 °C, as measured by rheology. If the release was melting-mediated (rapid at 40 °C yet much slower at 20 and 30 °C), then successful controlled release was achieved. Any successful carrageenan-Tween 20 formulations were then verified at that carrageenan concentration with Dehypon LS 36. Release was calculated as a percentage based on the difference in final conductivity of the water once melted (σ_{final}), and conductivity of the water at time *t*, *t* (σ_t), using the initial conductivity ($\sigma_{initial}$) to normalise the results as shown in Equation 3.3.

$$\text{Release (\%)} = \frac{(\sigma_t - \sigma_{initial})}{(\sigma_{final} - \sigma_{initial})} \times 100\% \quad (3.3)$$

The release data at a range of temperatures was measured, as shown in Figure 3.8. For both 0.6% w/w carrageenan-surfactant formulations, release of salt was rapid at 40 °C (ca. 5 minutes), taking considerably longer at 30 °C (ca. 30 minutes)

and longer still at 20 °C (ca. 1 – 2 hours). These data indicate that melting of the biopolymer took place. Similar release behaviour upon melting has also been reported by Mills *et al.* (2011). For 1% w/w Genugel®, even at 40 °C the release took over 30 minutes, with release at 30 °C taking ca. 100 minutes and at 20°C, nearly 3 hours, indicating that melting behaviour was not observed. In all release experiments there was no solid material left in the vessel, regardless of temperature or carrageenan concentration.

For non-melting scenarios an increase in temperature still resulted in faster release rates. This can be attributed to faster diffusion of gelling cations out of the gel, faster swelling of the carrageenan and perhaps some breakage of weaker helical aggregates: both leading to faster erosion. The melting thermograms shown in Figures 3.12 – 3.19 are relatively broad, which indicates that there is a corresponding broad distribution of aggregate strengths. Mills *et al.* (2011) found that salt release from non-swelling gels – gelatine, gellan and alginate – at a temperature well below their melting temperatures (25 °C) all occurred at nearly the same rate: this is indicative of a pure-diffusion controlled process. However, in these data there was a significant difference between the release profile for 0.6 and 1% w/w Genugel® at 20 and 30 °C, despite the fact that both of these temperatures are below the melting temperatures of both gels, which further evidences that swelling and/or erosive release was taking place.

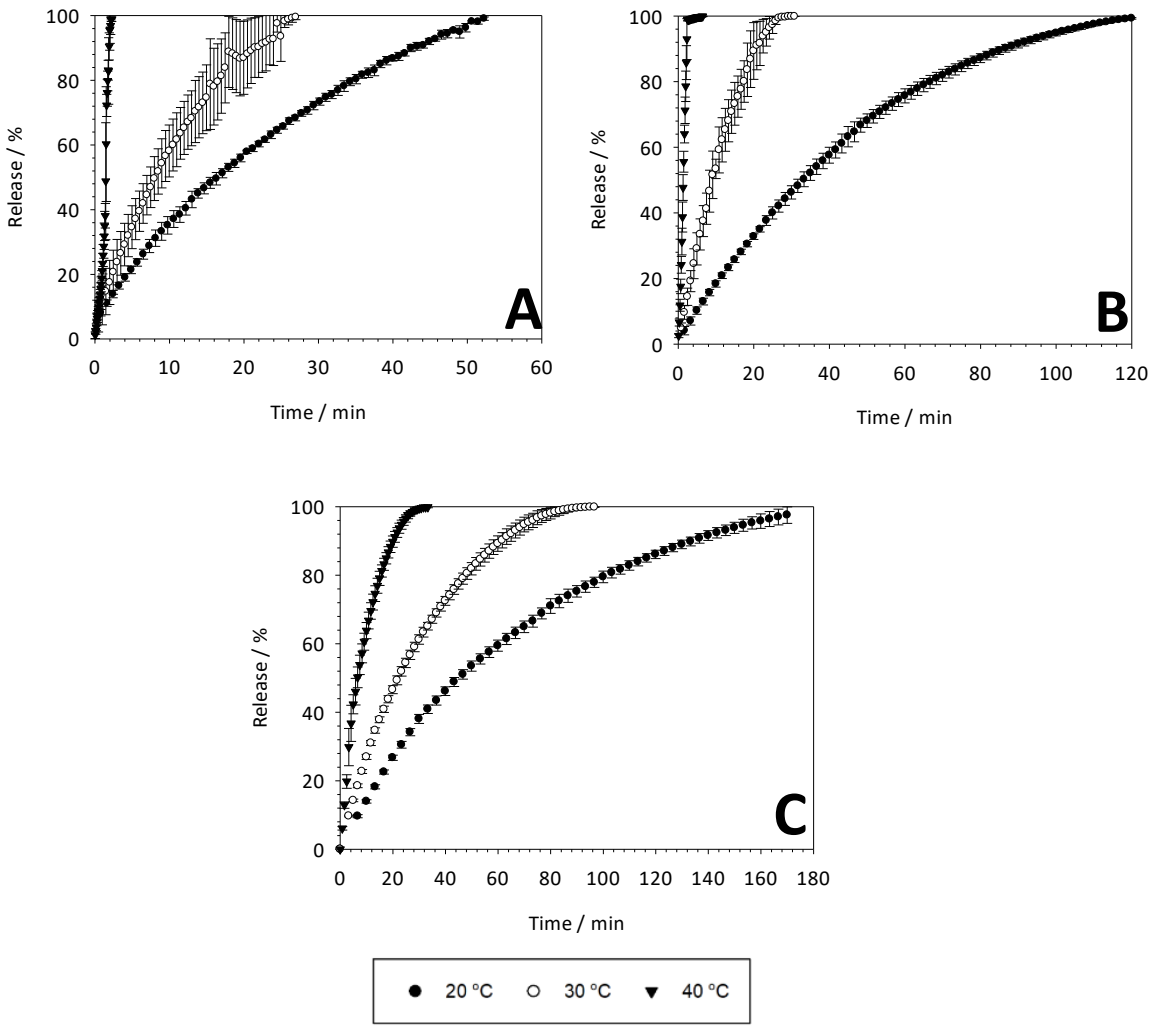

Figure 3.8 - Release profiles resulting from the melting of carrageenan-non-ionic surfactant cubes. (A) – 0.6% w/w Genugel® + 3% w/w Tween 20. (B) – 0.6% w/w Genugel® + 3% w/w D36. (C) – 1% Genugel® + 3% w/w Tween 20.

3.5 Discussion

Upon the addition of surfactant to the carrageenan, the major changes measured by rheology were an increase in the gelling and melting temperatures, and an increase in gel strength. Explaining this behaviour could take one of several mechanisms. Firstly, one must consider the influence of concentration: the

addition of surfactant meant (a) removal of water from the formulation, and (b) the introduction of a species (surfactant) that to must be hydrated, potentially leading to competition with carrageenan for water. Both of these factors would reduce the volume of water available to the carrageenan, therefore increasing the effective concentration of carrageenan and gelling cations, and hence potentially resulting in the observed increase in gelling and melting temperatures. To investigate this further, samples of carrageenan containing 5 g less of water to match the water content of the 5% w/w surfactant formulations were made and analysed in the same manner as the previous samples – data given in Table 3.3. In almost all cases there was a small increase between the regular samples and the samples with reduced water content, owed to concentration effects. However, in a large number of samples the increase did not extend to match those of the surfactant-containing samples, indicating that concentration effects were not the only driving force behind the changes measured. Additionally, one would expect to see much smaller changes in the gelling and melting temperatures at lower concentrations of carrageenan if altering the effective concentration was the sole contributor, which was not observed.

The combination of a charged polyelectrolyte, such as κC, with a non-ionic surfactant, such as Tween 20 or Dehypon LS 36, would theoretically result in no electrostatic attraction between the two species, and therefore no binding or adsorption of micelles: this is evidenced by μDSC (there were only single peaks in the thermograms) and surface tension measurements (no change in the CMC upon addition of carrageenan). The microstructure of such gels would therefore be either

a phase-separated or a bicontinuous morphology. Phase separation between the carrageenan and surfactant could explain the increase in gelling and melting temperatures due to exclusion effects leading to an increase in the effective concentration of carrageenan and salts. However the lack of an increase in turbidity on mixing – a characteristic of phase separated mixtures (M. Vinceković et al., 2011), was observed for all tested formulations, making phase separation unlikely. The exception to this were formulations with Dehypon LS 36 that were cloudy at room temperature due to the surfactant reaching its cloud point, which according to previously obtained μDSC data, was 15 – 16 °C (data not given). Phase separation was made unlikely due to the small size of the non-ionic surfactant micelles which had a consequently small enthalpy for segregation, compared to the relatively larger entropy of mixing (E. R. Morris, 2009). Therefore in this carrageenan-surfactant system, surfactant micelles were likely to have been dispersed throughout the carrageenan network forming a bicontinuous system.

Previous work by Johansson, Skantze and Löfroth (1993) has shown that there is a slight repulsive interaction between non-ionic surfactant micelles and kappa carrageenan chains, which may have made chain aggregation more thermodynamically favourable by reducing the number of carrageenan-micelle interactions. However, if the repulsion was not significant enough to trigger phase

separation, it is unlikely that repulsion of the same magnitude would lead to significant differences in carrageenan chain aggregation.

The final mechanistic explanation for these carrageenan-surfactant interactions is electrostatic shielding through hydrophobic interactions. Aggregation of helical chains in carrageenan is driven by electrostatic shielding, and so an increase in gelling and melting temperatures upon addition of surfactant indicates that the surfactant assisted the shielding of the carrageenan in some capacity beyond increasing the effective concentration of cations (as water was removed). Therefore, the authors believe that the only reasonable explanation for the change in properties must be shielding of the carrageenan chains by the non-ionic surfactant micelles since it is the only mechanism by which a similar increase in gelling and melting temperature would occur for each carrageenan concentration, and would explain why there the reduced-water samples did not match with the 5%-surfactant-carrageenan samples. In this mechanism, the surfactant micelles aggregate on the carrageenan chain through hydrophobic interactions, adding additional screening effects and therefore encouraging aggregation. Such mechanisms have been recently been reported for other anionic polymer-non-ionic surfactant systems in water (Yang & Pal, 2020).

Disparities between the gelling and melting temperatures measured by rheology and μDSC were clear throughout the presented data, with μDSC being consistently 5 – 10 °C. Such discrepancies can arise to differences in heating/cooling rate (Liu

et al., 2016), hence this was kept constant at 1 °C per minute for both rheology and μDSC. μDSC measured the energy (heat) produced or absorbed from the formation or breakage of carrageenan double helices, rather than the formation and breakage of aggregates, and the phase transition temperatures were taken as maxima and minima in the thermograms: these can be termed $T_{coil\text{-}helix}$ and $T_{helix\text{-}coil}$ to avoid confusion with T_g and T_m, measured by rheology. This is evidenced by the fact that the addition of non-ionic surfactant had no measurable change on the value of the phase transition enthalpies of carrageenan, despite the fact that the rheological data showed that surfactant increased gel strength, which indicates increased aggregation. In short, the μDSC could not measure the increase in aggregation as instead it was measuring the number of coil-helix and helix-coil transition, which did not change with surfactant concentration. In contrast, rheology measured the change in bulk material properties, which is associated with progressive aggregation of carrageenan helices, and the gelling and melting temperatures were taken at the point at which the samples changed from solid to liquid ($\delta = 45°$, G' = G'') (Miyoshi & Nishinari, 1999). Therefore, one would expect that $T_{coil\text{-}helix} \geq T_g$ and $T_{helix\text{-}coil} \geq T_m$ since during gelation, the coil-helix transition must occur *before* aggregation, and the inverse is true for the melting process. Yet this is the exact opposite of what was observed: the data collected suggests $T_{coil\text{-}helix} < T_g$ and $T_{helix\text{-}coil} < T_m$. Identical behaviour has been reported previously in carrageenan (Liu et al., 2016), however a satisfactory explanation behind its origins was not included. For formulations of carrageenan past a critical concentration the temperature difference between the formation ($T_{coil\text{-}helix}$) and aggregation (T_g) of helices becomes

so close to 0 that it is indistinguishable (Miyoshi & Nishinari, 1999). Hence this indicates an issue with either one of the measuring systems. Slip due to syneresis can lead to poor rheological measurements of carrageenan (Thrimawithana et al., 2010), however no slip was detected during the amplitude sweeps (data not given) as the value of the storage modulus did not show any reduction inside the LVR. Additionally, slip would lead to a reduction in measured melting temperatures, whereas the data presented clearly shows that rheological melting temperatures were consistently larger than those measured by μDSC. The rheological data was more accurate in predicting the onset of melting in the carrageenan samples, as proved in the release experiments. Unpicking exactly how and why this discrepancy arose in the opposite manner to which was expected is not the purpose of this publication, hence it should simply be noted that it exists and that rheology appears to be the more accurate technique for predicting melting behaviour in carrageenan.

The turbidity data indicated that the number of carrageenan aggregates decreased upon addition of non-ionic surfactant, which perhaps is the opposite of what one might expect. This information, coupled with the rheological data suggests that aggregation was enhanced by forming larger carrageenan aggregates. The turbidity decreased due to a small number of larger carrageenan aggregates

forming from a smaller number of larger carrageenan aggregates, hence explaining both the rheological and turbidity data.

The release data for the carrageenan samples showed that the 0.6% w/w carrageenan-surfactant formulations could operate as temperature-mediated controlled release vehicles in dishwashing or food-related applications. Selective rapid release was measured at 40 °C compared to much slower release at decreased temperatures. In terms of the mechanism of the release of salt there are three possible mechanisms: Fickian diffusion, swelling and erosion (melting) (Lin & Metters, 2006). For diffusion, there is no change in the matrix of the material and the release is governed simply by diffusion from the porous gel network. For swelling, gelling cations diffuse and out water penetrates the outer layer of the gel and expands to become much more porous and open, which leads to much quicker diffusion of subsequent cations via non-Fickian diffusion. And thirdly, for erosive (melting) release, the carrageenan aggregates are directly broken with heat leading to dismantling of the gel network and dispersal almost instantly in to the bulk. In this mechanism, the release rate is governed by macroscopic stirring effects and is much faster than the other two mechanisms. The erosive release model can also occur in swollen gels by where the swollen layer is sufficiently weakened that it can be eroded, however the mechanisms by which the gel is weakened are different. In swelling-mediated erosion, the release rate is governed by how fast the gelling cations diffuse out whereas in the melting scenario, heat breaks the carrageenan aggregates resulting in much quicker erosion. The fact

that no sample remained in any of the experiments indicates that at temperatures below the melting temperature, swelling followed by surface erosion took place.

3.6 Conclusions

The properties of κC-non-ionic surfactant gels were probed using rheology, μDSC, turbidity and tensiometry. These measurements showed an increase in phase transition temperatures and gel strength, a loss in turbidity whilst no measurable change in phase transition enthalpies, critical micelle concentrations. Overall there is significant evidence that kappa-carrageenan and non-ionic surfactants have a mechanism of interaction between the two species that allows for more effective shielding of the carrageenan helices during the aggregation step.

The ideal concentration of this κC for release at 30 – 40 °C was identified as 0.6% w/w, due to its relevant melting temperature and self-supporting mechanical properties. This was verified in the melting experiments where it was found that rapid melting could be achieved at 40 °C, compared to much slower degradation at 20 and 30 °C. Therefore, this gel system is appropriate for applications such as food, pharmaceuticals and automatic dishwashing detergent formulations where release at 40 °C via a rapid melting mechanism is desirable.

Future formulations could involve inclusion of an oil phase to the carrageenan gels, which would be stabilised by the presence of a non-ionic surfactant and would allow for temperature-triggered delivery of hydrophobic actives such as food flavourings or pharmaceutical ingredients. More work is needed in order to understand the reported discrepancies between phase transition temperatures measured by rheology and μDSC.

3.7 References

Bengtsson, P., Berghel, J., & Renström, R. (2015). A household dishwasher heated by a heat pump system using an energy storage unit with water as the heat source. *International Journal of Refrigeration*, *49*, 19–27. https://doi.org/10.1016/j.ijrefrig.2014.10.012

Blagojević, S. N. S. M., & Pejić, N. D. (2016). Performance and Efficiency of Anionic Dishwashing Liquids with Amphoteric and Nonionic Surfactants. *Journal of Surfactants and Detergents*, *19*(2), 363–372. https://doi.org/10.1007/s11743-015-1784-5

Bonnaud, M., Weiss, J., & McClements, D. J. (2010). Interaction of a food-grade cationic surfactant (Lauric Arginate) with food-grade biopolymers (pectin, carrageenan, xanthan, alginate, dextran, and chitosan). *Journal of Agricultural and Food Chemistry*, *58*(17), 9770–9777. https://doi.org/10.1021/jf101309h

Burey, P., Bhandari, B. R., Howes, T., & Gidley, M. J. (2008). Hydrocolloid gel particles: Formation, characterization, and application. *Critical Reviews in Food Science and Nutrition*, *48*(5), 361–377. https://doi.org/10.1080/10408390701347801

Chakraborty, S. (2017). Carrageenan for encapsulation and immobilization of flavor, fragrance, probiotics, and enzymes: A review. *Journal of Carbohydrate Chemistry*. *36(1)*, 1–19.https://doi.org/10.1080/07328303.2017.1347668

Diañez, I., Gallegos, C., Brito-de la Fuente, E., Martínez, I., Valencia, C., Sánchez, M. C., … Franco, J. M. (2019). 3D printing in situ gelification of κ-carrageenan solutions: Effect of printing variables on the rheological response. *Food Hydrocolloids*, *87*, 321–330. https://doi.org/10.1016/j.foodhyd.2018.08.010

Fasolin, L. H., Picone, C. S. F., Santana, R. C., & Cunha, R. L. (2013). Production

of hybrid gels from polysorbate and gellan gum. *Food Research International*, *54*(1), 501–507. https://doi.org/10.1016/j.foodres.2013.07.026

Gholamipour-Shirazi, A., Norton, I. T., & Mills, T. (2019). Designing hydrocolloid based food-ink formulations for extrusion 3D printing. *Food Hydrocolloids*, *95*, 161–167. https://doi.org/10.1016/J.FOODHYD.2019.04.011

Griffiths, P. C., & Cheung, A. Y. F. (2003). Interaction between surfactants and gelatine in aqueous solutions. *Materials Science and Technology*, *18*(6), 591–599. https://doi.org/10.1179/026708302225003587

Grządka, E. (2015). Interactions between kappa-carrageenan and some surfactants in the bulk solution and at the surface of alumina. *Carbohydrate Polymers*, *123*, 1–7.

Gulrez, S. K. H., Saphwan, A.-A., & Phillips, G. O. (2011). Hydrogels: Methods of Preparation, Characterisation and Applications. In A. Carpi (Ed.), *Progress in Molecular and Environmental Bioengineering - From Analysis and Modeling to Technology Applications* (pp. 126–127). InTechOpen. https://doi.org/10.5772/24553

Iijima, M., Hatakeyama, T., Takahashi, M., & Hatakeyama, H. (2007). Effect of thermal history on kappa-carrageenan hydrogelation by differential scanning calorimetry. *Thermochimica Acta*, *452*(1), 53–58. https://doi.org/10.1016/J.TCA.2006.10.019

Imeson, A. (2000). Carrageenan. In P. A. Williams & G. O. Phillips (Eds.), *Handbook of Hydrocolloids* (2nd ed., pp. 87–101). Cambridge, UK: Woodhead Publishing Limited.

Jain, N., Trabelsi, S., Guillot, S., McLoughlin, D., Langevin, D., Letellier, P., & Turmine, M. (2004). Critical aggregation concentration in mixed solutions of anionic polyelectrolytes and cationic surfactants. *Langmuir*, *20*(20), 8496–8503. https://doi.org/10.1021/la0489918

Johansson, L., Skantze, U., & Löfroth, J. E. (1993). Diffusion and interaction in gels and solutions. 6. Charged systems. *Journal of Physical Chemistry*, *97*(38), 9817–9824. https://doi.org/10.1021/j100140a045

Lai, V. M. F., Wong, P. A. L., & Lii, C. Y. (2000). Effects of cation properties on sol-gel transition and gel properties of κ-carrageenan. *Journal of Food Science*, *65*(8), 1332–1337. https://doi.org/10.1111/j.1365-2621.2000.tb10607.x

Lin, C. C., & Metters, A. T. (2006). Hydrogels in controlled release formulations: Network design and mathematical modeling. *Advanced Drug Delivery Reviews*, *58*(12-13), 1379–1408. https://doi.org/10.1016/j.addr.2006.09.004

Liu, S., Huang, S., & Li, L. (2016). Thermoreversible gelation and viscoelasticity of κ-carrageenan hydrogels. *Journal of Rheology*, *60*(2), 203–214. https://doi.org/10.1122/1.4938525

Mills, T., Spyropoulos, F., Norton, I. T., & Bakalis, S. (2011). Development of an in-vitro mouth model to quantify salt release from gels. *Food Hydrocolloids*, *25*(1), 107–113. https://doi.org/10.1016/j.foodhyd.2010.06.001

Mittal, K. L. (1972). Determination of CMC of polysorbate 20 in aqueous solution by surface tension method. *Journal of Pharmaceutical Sciences*, *61*(8), 1334–1335. https://doi.org/10.1002/jps.2600610842

Miyoshi, E., & Nishinari, K. (1999). Rheological and thermal properties near the sol-gel transition of gellan gum aqueous solutions. *Progress in Colloid and Polymer Science*, *114*, 68–82. https://doi.org/10.1007/3-540-48349-7_11

Moonprasith, N., Sa-nguanthammarong, P., Kongkaew, C., & Loykulnant, S. (2008). Effect of Surfactant on Gelation of Hydroxypropylmethyl Cellulose in Skim Natural Rubber Latex Serum. *Journal of Metals, Materials and Minerals*, *18*(2), 89–91.

Morris, E. R. (2009). Functional Interactions in Gelling Biopolymer Mixtures. In *Modern Biopolymer Science* (pp. 167–198). Elsevier Inc. https://doi.org/10.1016/B978-0-12-374195-0.00005-7

Norton, I. T., Goodall, D. M., Morris, E. R., & Rees, D. A. (1983). Role of cations in the conformation of iota and kappa carrageenan. *Journal of the Chemical Society, Faraday Transactions 1: Physical Chemistry in Condensed Phases*, *79*(10), 2475–2488. https://doi.org/10.1039/F19837902475

Núñez-Santiago, M. del C., & Tecante, A. (2007). Rheological and calorimetric study of the sol-gel transition of κ-carrageenan. *Carbohydrate Polymers*, *69*(4), 763–773. https://doi.org/10.1016/j.carbpol.2007.02.017

Pal, K., Paulson, A. T., & Rousseau, D. (2009). Biopolymers in Controlled-Release Delivery Systems. In *Modern Biopolymer Science* (pp. 519–557). Elsevier Inc. https://doi.org/10.1016/B978-0-12-374195-0.00016-1

Patil, R. T., & Speaker, T. J. (1998). Carrageenan as an anionic polymer for aqueous microencapsulation. *Drug Delivery: Journal of Delivery and Targeting of Therapeutic Agents*, *5*(3), 179–182. https://doi.org/10.3109/10717549809052033

Pepić, I., Filipović-Grčić, J., & Jalšenjak, I. (2009). Bulk properties of nonionic surfactant and chitosan mixtures. *Colloids and Surfaces A: Physicochemical and Engineering Aspects*, *336*(1–3), 135–141. https://doi.org/10.1016/j.colsurfa.2008.11.034

Picone, C. S. F., & Cunha, R. L. (2013). Formation of nano and microstructures by polysorbate-chitosan association. *Colloids and Surfaces A: Physicochemical and Engineering Aspects*, *418*, 29–38. https://doi.org/10.1016/j.colsurfa.2012.11.019

Piculell, L., & Lindman, B. (1992). Association and segregation in aqueous polymer/polymer, polymer/surfactant, and surfactant/surfactant mixtures:

similarities and differences. *Advances in Colloid and Interface Science*, *41*, 149–178. https://doi.org/10.1016/0001-8686(92)80011-L

Poce-Fatou, J. A. (2006). A Superficial Overview of Detergency. *Journal of Chemical Education*, *83*(8), 1147–1151. https://doi.org/10.1021/ed083p1147

Rosas-Durazo, A., Hernández, J., Lizardi, J., Higuera-Ciapara, I., Goycoolea, F. M., & Argüelles-Monal, W. (2011). Gelation processes in the non-stoichiometric polylectrolyte-surfactant complex between κ-carrageenan and dodecyltrimethylammonium chloride in KCl. *Soft Matter*, *7*(5), 2103–2112. https://doi.org/10.1039/c0sm00663g

Saha, D., & Bhattacharya, S. (2010). Hydrocolloids as thickening and gelling agents in food: A critical review. *Journal of Food Science and Technology*, *47*(6)*,* 587–597. *https*://doi.org/10.1007/s13197-010-0162-6

Sow, L. C., Peh, Y. R., Pekerti, B. N., Fu, C., Bansal, N., & Yang, H. (2017). Nanostructural analysis and textural modification of tilapia fish gelatine affected by gellan and calcium chloride addition. *LWT - Food Science and Technology*, *85*, 137–145. https://doi.org/10.1016/j.lwt.2017.07.014

Sreejith, L., Nair, S. M., & George, J. (2010). Biopolymer Surfactant Interactions. In M. Elnashar (Ed.), *Biopolymers*. InTech. https://doi.org/10.5772/10272

Thrimawithana, T. R., Young, S., Dunstan, D. E., & Alany, R. G. (2010). Texture and rheological characterization of kappa and iota carrageenan in the presence of counter ions. *Carbohydrate Polymers*, *82*(1), 69–77. https://doi.org/10.1016/j.carbpol.2010.04.024

Villanueva, R. D., Mendoza, W. G., Rodrigueza, M. R. C., Romero, J. B., & Montaño, M. N. E. (2004). Structure and functional performance of gigartinacean kappa-iota hybrid carrageenan and solieriacean kappa-iota carrageenan blends. *Food Hydrocolloids*, *18*(2), 283–292. https://doi.org/10.1016/S0268-005X(03)00084-5

Vinceković, M., Pustak, A., Tuek-Boi, L., Liu, F., Ungar, G., Bujan, M., … Filipovi-Vinceković, N. (2010). Structural and thermal study of mesomorphic dodecylammonium carrageenates. *Journal of Colloid and Interface Science*, *341*(1), 117–123. https://doi.org/10.1016/j.jcis.2009.09.021

Vinceković, M., Katona, J., Bujan, M., & Sovilj, V. (2011). Interactions between dodecylammonium chloride and carrageenans in the semidilute regime. *Colloids and Surfaces A: Physicochemical and Engineering Aspects*, *384*(1–3), 739–748. https://doi.org/10.1016/j.colsurfa.2011.05.056

Wang, Q., Li, L., Liu, E., Xu, Y., & Liu, J. (2006). Effects of SDS on the sol-gel transition of methylcellulose in water. *Polymer*, *47*(4), 1372–1378. https://doi.org/10.1016/j.polymer.2005.12.049

Warner, E. L., Norton, I. T., & Mills, T. B. (2019). Comparing the viscoelastic properties of gelatine and different concentrations of kappa-carrageenan mixtures for additive manufacturing applications. *Journal of Food*

Engineering, *246*, 58–66. https://doi.org/10.1016/j.jfoodeng.2018.10.033

Yang, J., & Pal, R. (2020). Investigation of surfactant-polymer interactions using rheology and surface tension measurements. *Polymers*, *12*(10), 1–20. https://doi.org/10.3390/polym12102302

Yin, T., Qin, M., Yang, Y., Zheng, P., Fan, D., & Shen, W. (2014). The interactions of ι-carrageenan with cationic surfactants in aqueous solutions. *Soft Matter*, *10*(23), 4126–4136. https://doi.org/10.1039/c4sm00322e

Zuleger, S., & Lippold, B. C. (2001). Polymer particle erosion controlling drug release. I. Factors influencing drug release and characterization of the release mechanism. *International Journal of Pharmaceutics*, *217*(1–2), 139–152. https://doi.org/10.1016/S0378-5173(01)00596-8

3.8 Appendix

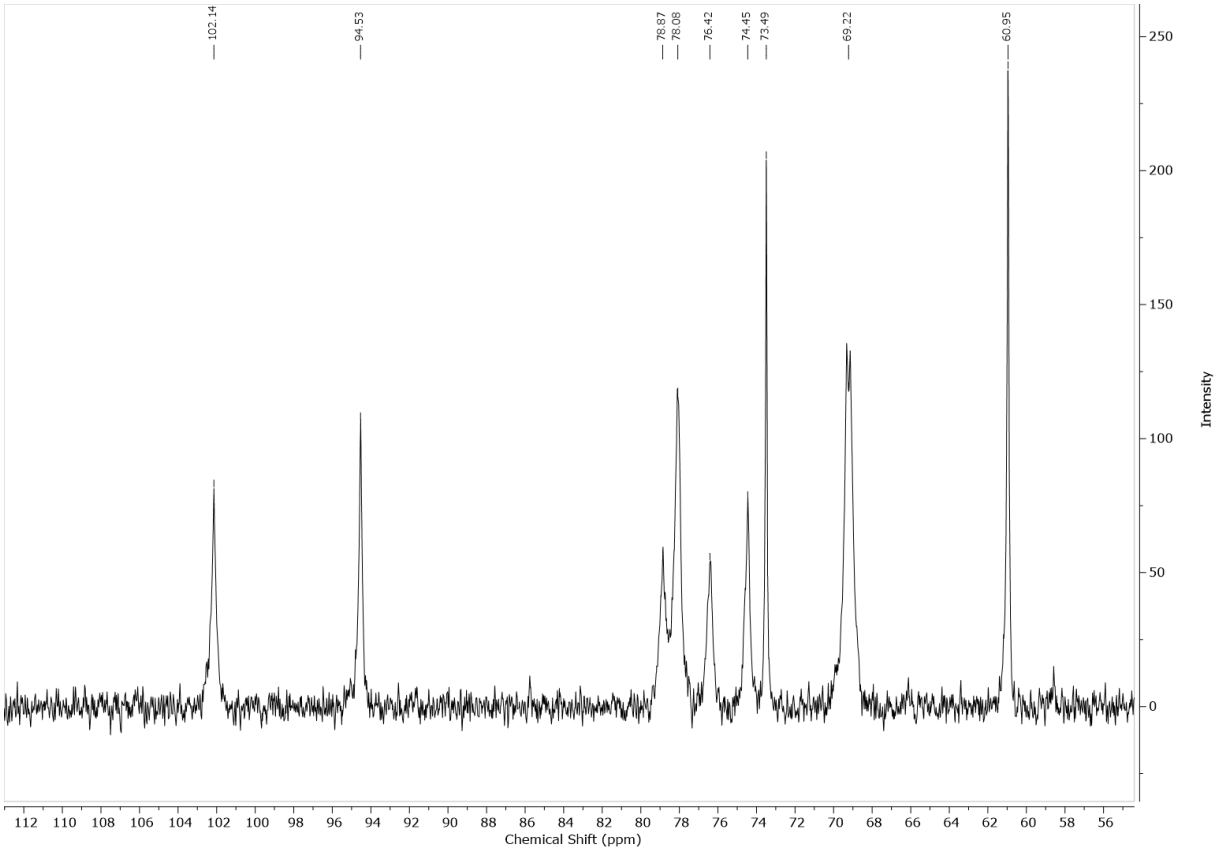

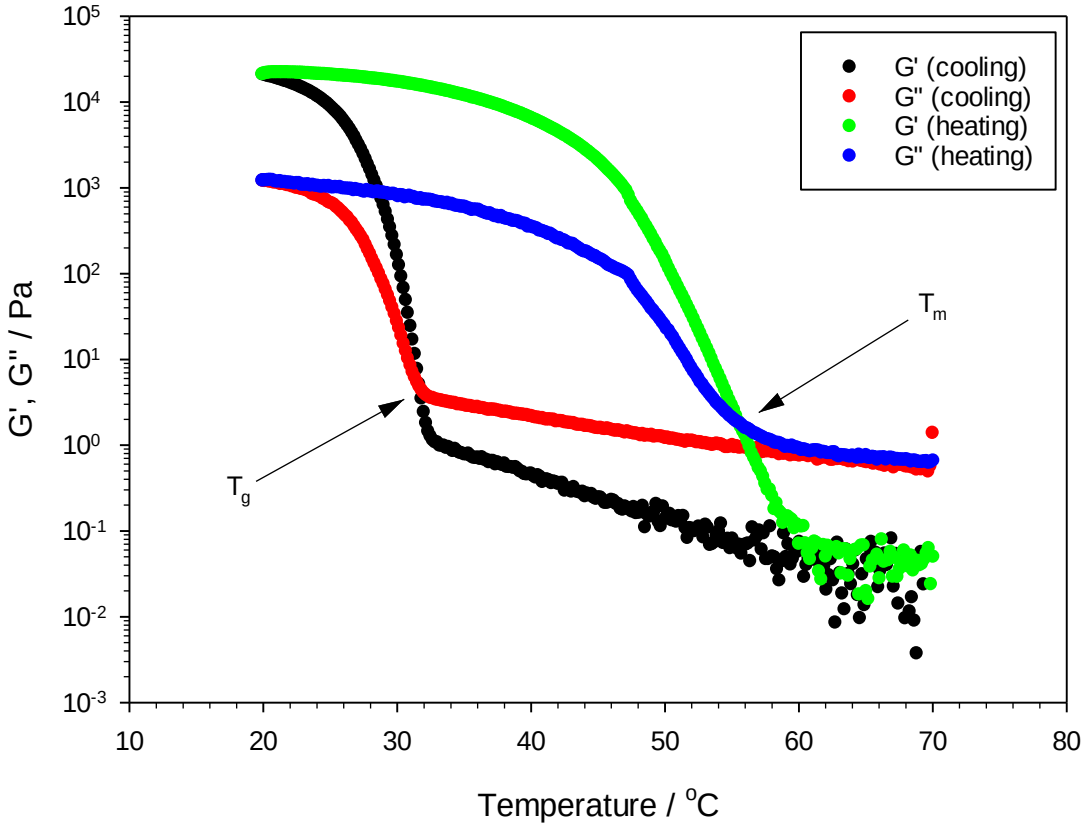

Figure 3.10 - Example of how temperature sweep data is used to determine the gelling temperature (T_g) and melting temperature (T_m) of a sample by the crossover of the elastic modulus (G') and the viscous modulus (G"). This example is taken from a sample of 2% w/w Genugel® with 1% w/w Tween 20.

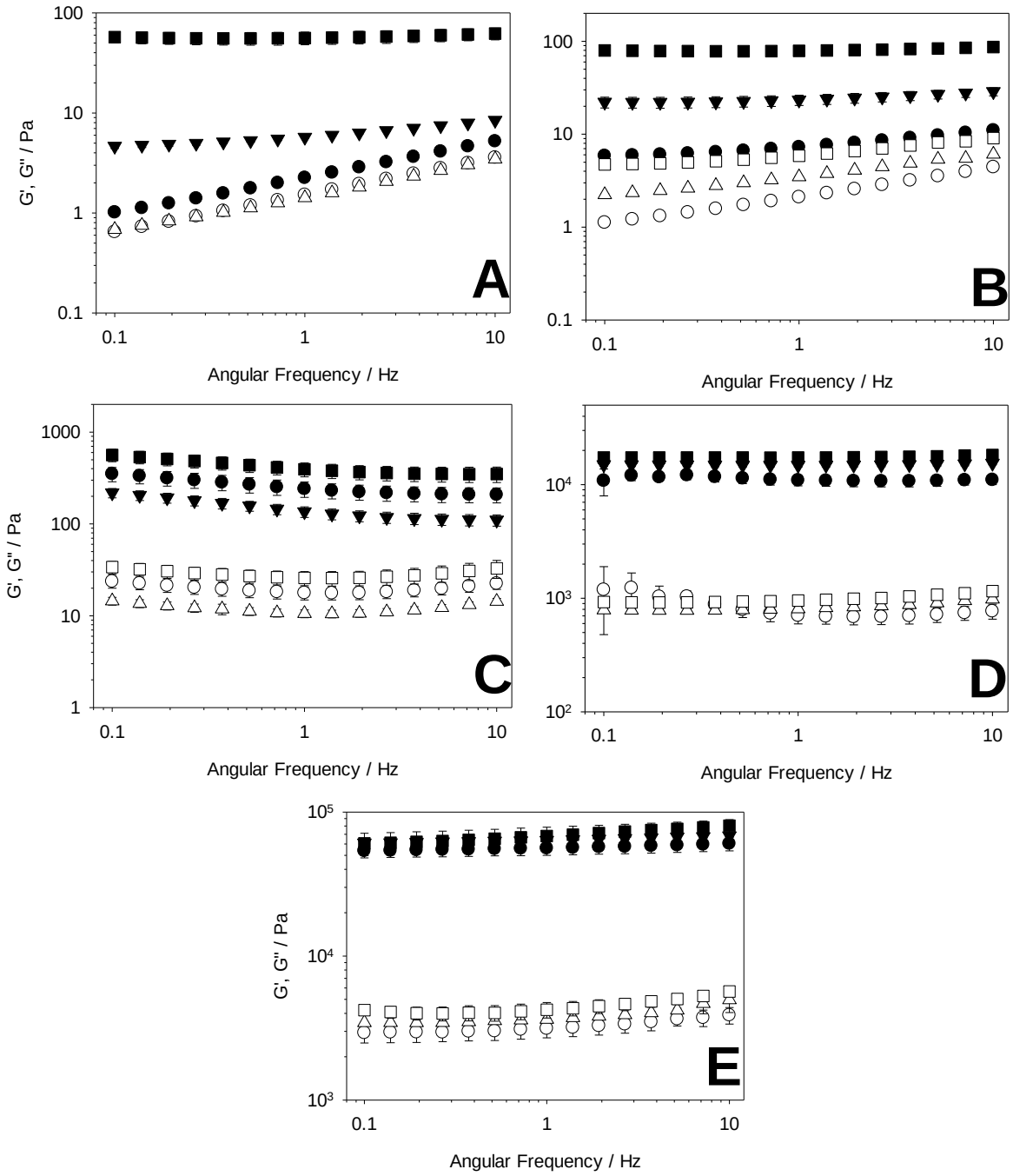

Figure 3.11 - Frequency sweep data for Genugel and surfactant solutions. (A) – 0.6% Genugel with Tween 20, (B) –0.6% Genugel with Dehypon LS 36 (C) – 1% Genugel with Tween 20, (D) – 2% Genugel with Tween 20, and (E) – 3% Genugel with Tween 20. Filled black symbols indicates values of G', and filled white symbols indicates values for G". Different concentrations of surfactant are denoted by the symbol shape – ● - 0.1% surfactant, ▼ - 2% surfactant, ■ - 4% surfactant.

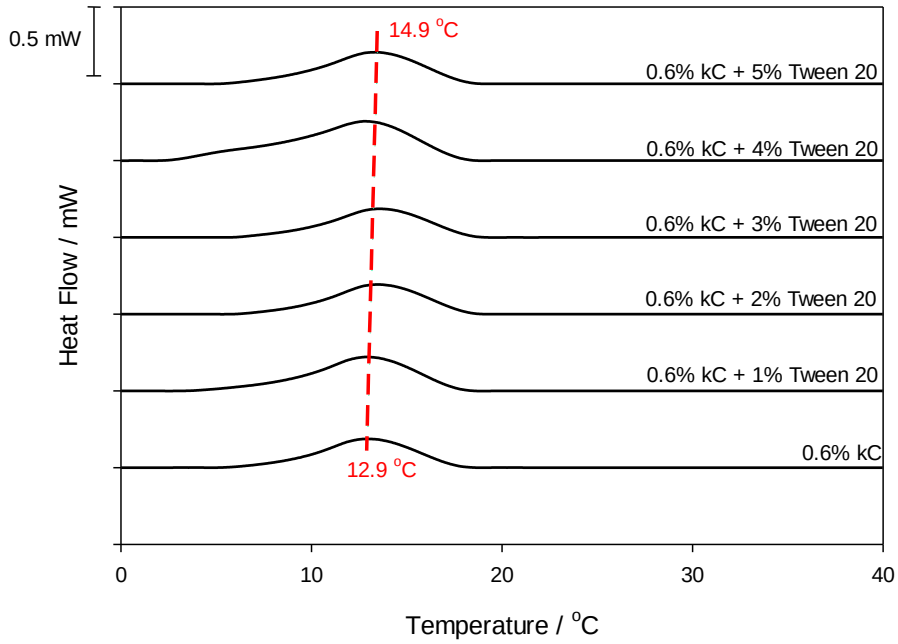

Figure 3.12 - Thermal profiles obtained by μDSC for upon cooling 0.6% w/w carrageenan in the presence of Tween 20.

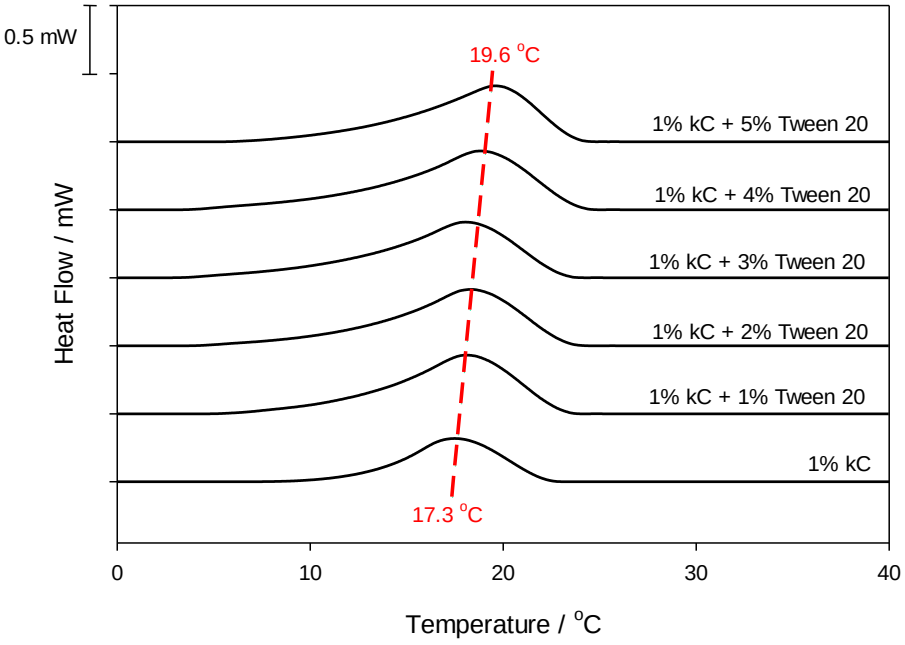

Figure 3.13 - Thermal profiles obtained by μDSC for upon cooling 1% w/w carrageenan in the presence of Tween 20/

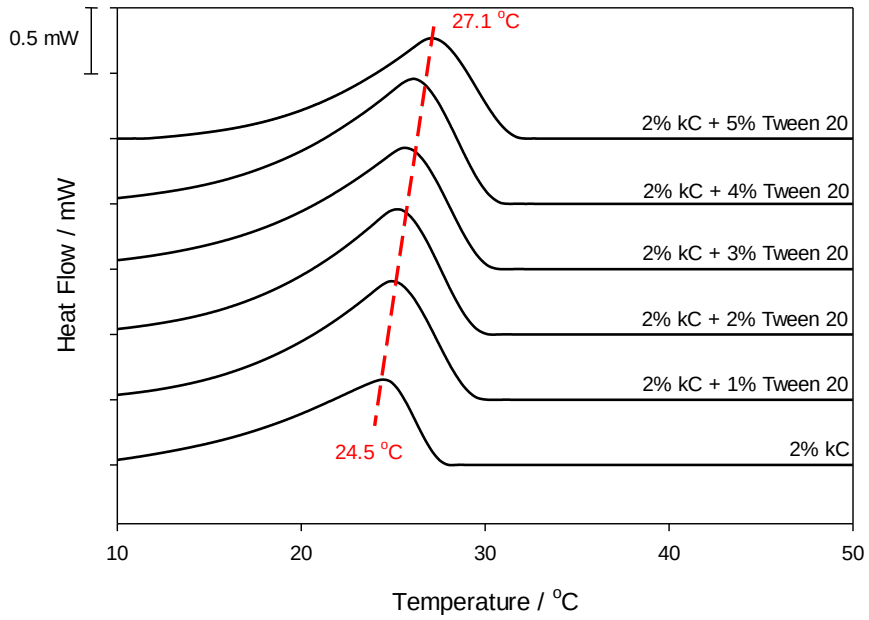

Figure 3.14 - Thermal profiles obtained by μDSC for upon cooling 2% w/w carrageenan in the presence of Tween 20.

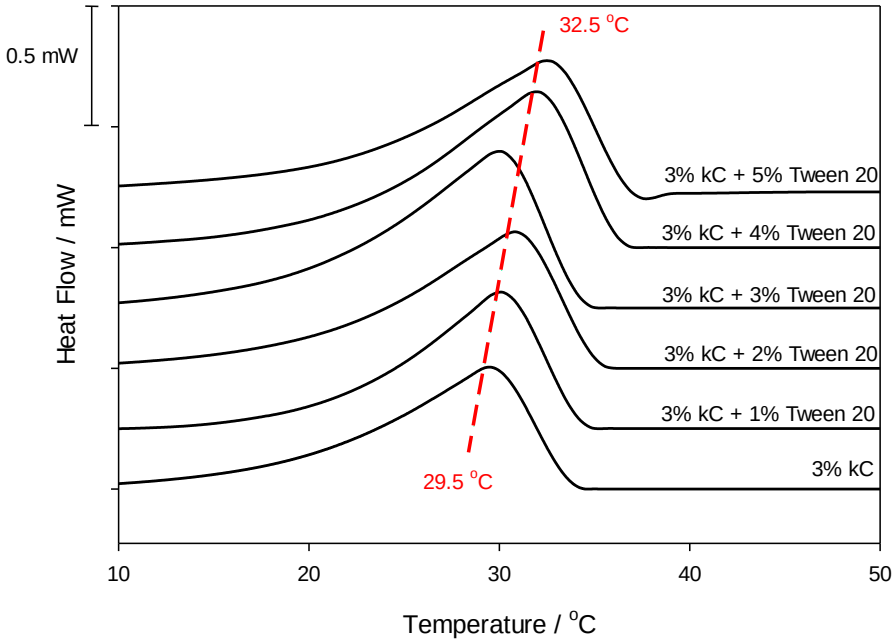

Figure 3.15 - Thermal profiles obtained by μDSC for upon cooling 3% w/w carrageenan in the presence of Tween 20.

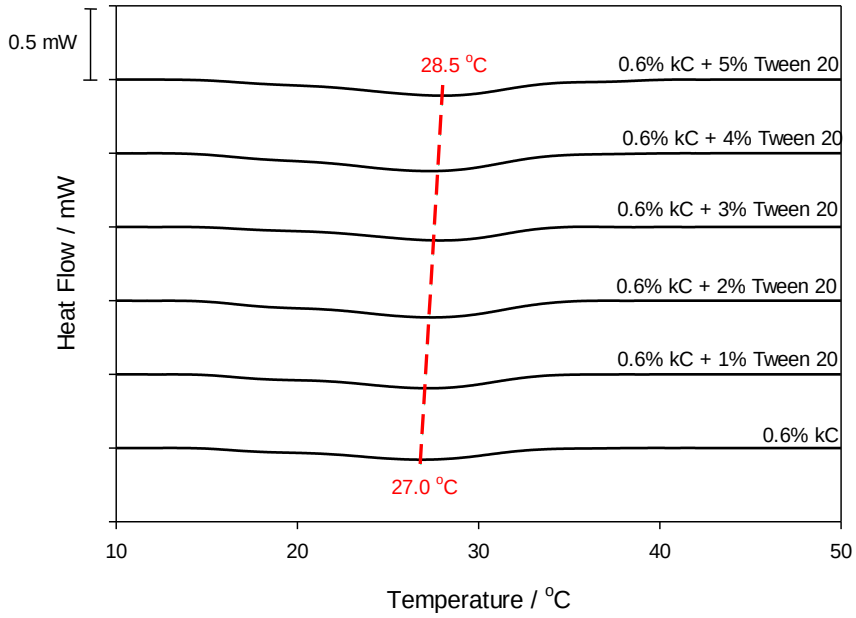

Figure 3.16 - Thermal profiles obtained by μDSC for upon heating 0.6% w/w carrageenan in the presence of Tween 20.

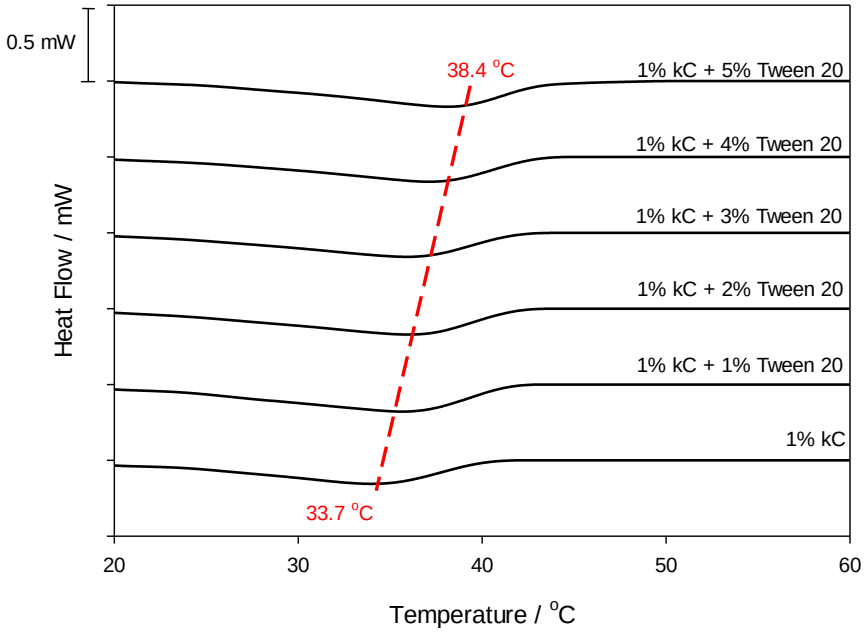

Figure 3.17 - Thermal profiles obtained by μDSC for upon heating 1% w/w carrageenan in the presence of Tween 20.

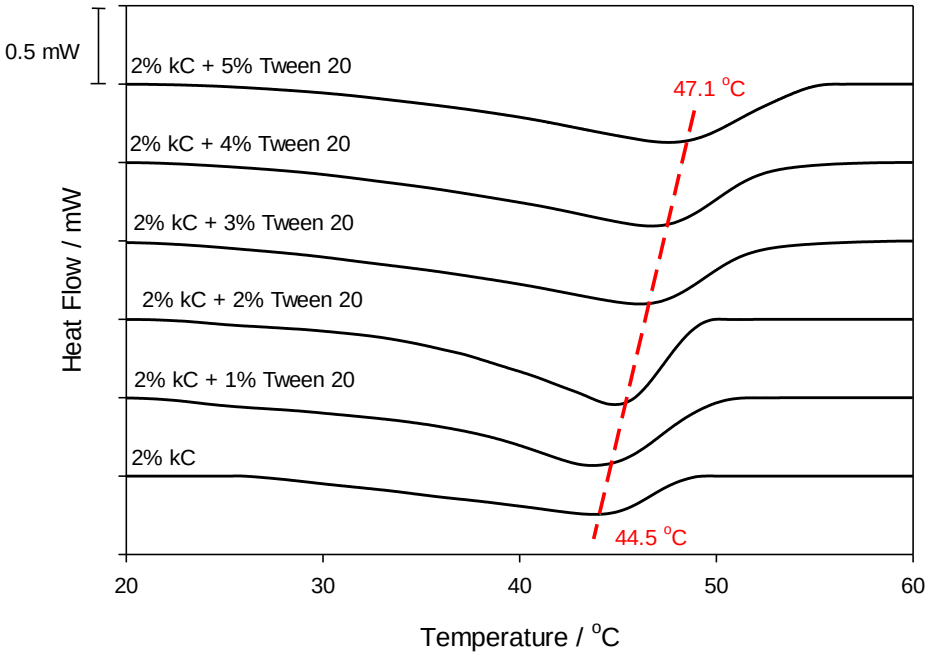

Figure 3.18 - Thermal profiles obtained by μDSC for upon heating 2% w/w carrageenan in the presence of Tween 20.

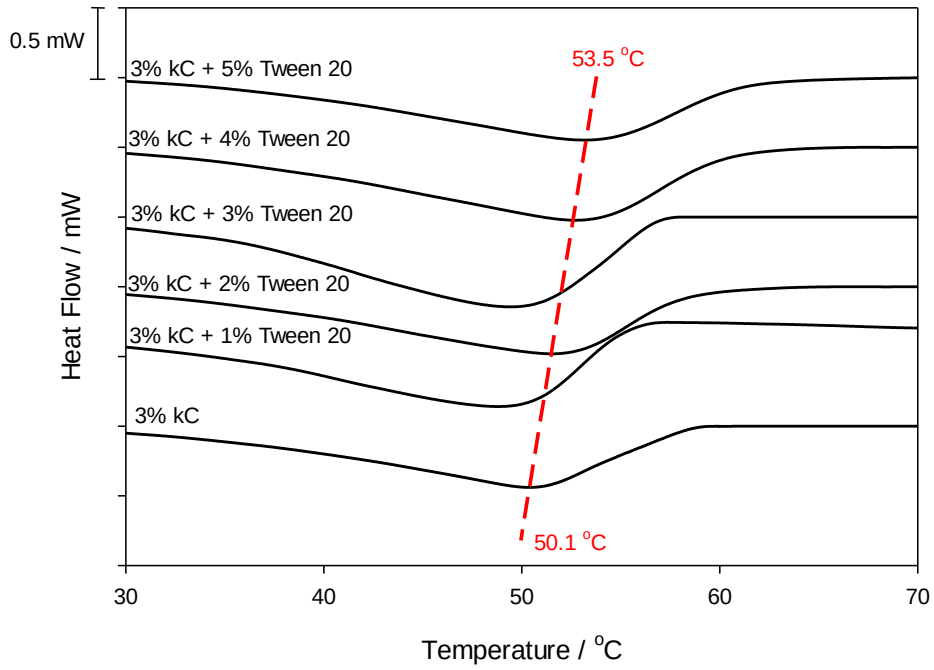

Figure 3.19 - Thermal profiles obtained by μDSC for upon heating 3% w/w carrageenan in the presence of Tween 20.

Table 3.3 – Comparing gelling and melting temperatures of carrageenan gels obtained with rheology. The formulations consist of carrageenan in water, carrageenan with 5 g reduced water content, and carrageenan with 5 g of water replaced with 5 g of Tween 20. Values given are mean averages from three measurements with the standard deviation.

Carrageenan concentration / % w/w	**Carrageenan-only**		**5 g reduced water**		**Carrageenan-5% Tween 20**	
	T_g / °C	**T_m / °C**	**T_g / °C**	**T_m / °C**	**T_g / °C**	**T_m / °C**
0.6	10.27 ± 0.51	31.77 ± 0.05	12.73 ± 0.35	29.97 ± 3.65	14.28 ± 0.28	34.77 ±1.99
1	20.22 ± 0.09	43.31 ± 0.36	21.67 ± 0.67	43.37 ± 0.72	22.12 ± 1.67	44.89 ± 1.19
2	28.93 ± 0.15	51.73 ± 0.49	30.30 ± 0.61	53.17 ± 0.59	31.90 ± 0.69	54.30 ± 0.40
3	35.10 ± 1.23	56.82 ± 1.95	38.53 ± 0.91	60.17 ± 0.55	42.99 ± 1.91	66.52 ± 1.22

4

Formulation and additive manufacturing of polysaccharide-surfactant hybrid gels as gelatine analogues in food and detergency applications

Originally published in*:

Fenton, T., Gholamipour-Shirazi, A., Daffner, K., Mills, T., & Pelan, E. (2021). Formulation and additive manufacturing of polysaccharide-surfactant hybrid gels as gelatine analogues in food applications. Food Hydrocolloids, 106881. https://doi.org/10.1016/j.foodhyd.2021.106881

*Printing of the gels was carried out by Dr Azarmidokht Gholamipour-Shirazi

4.1 Abstract

A vegetarian alternative to gelatine, for use in food applications was proposed as a synergistic combination of 0–2 wt% low acyl gellan gum (LAG) and 0–2 wt% tamarind seed xyloglucan (TSX). The mechanical, thermal and temperature-mediated release properties of the gels were examined using rheology and conductivity. The influence of the addition of a food grade emulsifier, Tween® 20, was also investigated. It was found that both the total concentration of biopolymers and the ratio of polymer blends influenced thermal (gelling and melting temperatures) and mechanical (storage modulus and phase angle) properties, however the total polymer concentration was the major factor. The addition of Tween® 20 led to small increases gelling and melting temperatures, elastic modulus and a small reduction phase angle in most of the LAG/TSX samples. Using rheological data the LAG/TSX samples were predicted to be printable using extrusion-based additive manufacturing, which was then performed on a custom-made printer. The rheological and release data suggested that 0.5 wt% LAG/1.5 wt% TSX/1 wt% Tween® 20 was the most similar to a tested sample of 5 wt% porcine gelatine in terms of viscoelastic moduli, gelling & melting temperatures and release profile, and could therefore be developed as a printable gelatine replacement. No difference was found between the release properties of moulded versus printed gels.

4.2 Introduction

Across many industries, notably the food and pharmaceutical industries, there is a need for the development of vegetarian gels that provide 'melt-in-the-mouth' behaviour (Shinya Ikeda & Talashek, 2007), as an alternative to porcine gelatine-based formulations. This due to concerns over gelatine's animal-based origins. Additionally, the junction zones in gelatine continually re-arrange to become gradually more thermally stable, hence the gel strength and melting temperature of gelatine is a direct function of its age (Ledward, 2000). Gelatine alternatives must be firm at room temperature yet must soften significantly at body temperature (37 °C) to provide the correct mouthfeel and release properties. In such edible formulations it is often advantageous to include an emulsifier to allow for the stable inclusion of oil-based flavourings and additives (Kralova & Sjöblom, 2009). Initial characterisation of a gel-surfactant system would pave the way for future gel-oil-surfactant formulations for the food industries and beyond.

Gellan gum is an extracellular polysaccharide secreted by *Sphingomonas elodea* (syn. *Pseudomanos elodea*) micro-organisms (Moorhouse, Colegrove, Sandford, Baird, & Kang, 1981). Its primary structure consists of a linear repetition of four saccharide derivatives: →3)-ß-D-Glcp-(1→4)-ß-D-GlcpA-(1→4)-ß-D-Glcp-(1→4)-α-L-Rhap-(1→ (Jansson et al., 1983). In its native high acyl form, the polymer has two acyl substituents present on the 3-linked glucose (Kuo, Mort, & Dell, 1986), however these can be removed through heating under alkaline conditions to yield the deacylated (low acyl) form (Chilvers & Morris, 1987). Both gellans undergo

gelation in the presence of sufficient gelling cations through the formation and subsequent aggregation of double helices, achieved by hydration at an elevated temperature followed by cooling (Grasdalen & Smidsrød, 1987). The degree of acyl substitution determines the resultant gel properties: high acyl gellan (HAG) gum typically forms thermoreversible, soft, elastic gels whereas low acyl gellan (LAG) gum generally forms non-thermoreversible, hard, brittle gels (H. Lee, Fisher, Kallos, & Hunter, 2011). Divalent cations are much more effective at promoting gelation in gellan compared to monovalent cations (Grasdalen & Smidsrød, 1987).

Tamarind seed xyloglucan (TSX) is a non-ionic, branched polysaccharide which is extracted from the seed of the tamarind tree *Tamarindus indica* (Kaur, Yadav, Ahuja, & Dilbaghi, 2012; Nayak, Pal, & Santra, 2014). TSX has a backbone of (1→4)ß-D-glucans substituted with side chains of α-D-xylopyranose which are linked (1→6) to glucose molecules (Kaur et al., 2012). In water, TSX swells and causes a rise in viscosity which sees it used mainly as a thickener and stabiliser in the food industry (Nayak et al., 2014), however, it does not form a gel on its own.

A synergistic combination of two biopolymers describes a case whereby a mixture of polymers shows different properties than what is possible from any of the individual substituent polymers. The origin of this synergistic effect is due to the formation of either a phase-separated or a coupled network, depending on whether direct binding takes place or not between the two polymers. In either case a

synergistic effect is often indicated by the viscosity of a mixture being greater than the sums of the viscosities of its substituents (Nishinari et al., 2006). Morris (1995) noted that many synergistic interactions arise from mixtures of a polysaccharide that undergoes a coil-helix transition, such as carrageenan, xanthan gum and gellan gum, mixed with another polysaccharide with a ß(1→4) linked cellulosic backbone, such as locust bean gum, konjac glucomannan or tamarind seed xyloglucan (Nishinari et al., 2006). Work by Grisel *et al.* (2015), who investigated the synergistic interactions between xanthan and galactomannans, suggested that the mechanism of synergy between the two polymers is dependent on the degree of compatibility between the two molecular structures: in the attractive scenario, unsubstituted areas on the galactomannan can interact with linear, non-helical regions on the xanthan which allows the formation of hybrid junction zones, whereas if the structures are geometrically incompatible, then such junction zones cannot form, and instead the synergy results from a repulsive, phase-separated microstructure.

In an unmodified state, both HAG and LAG have a melting temperature that far exceeds the target for a gelatine replacement (T_m > 70 °C). The synergistic combination of LAG with TSX has been briefly reported in the literature previously (Nayak et al., 2014; Nishinari et al., 2006; Nitta et al., 2003), however its use as a potential gelatine replacement has not been exploited to the authors' knowledge. Ikeda *et al.* (2004) attempted to elucidate the nature of the interaction between TSX and LAG using rheology and atomic force microscopy (AFM). It was found

that by mixing two non-gelled mixtures of LAG and TSX, a gel network was formed, however it could not be definitively stated if this synergism was the result of phase separation or coupling between the polymers. Nitta *et al.*, (2003) also reported synergy between LAG and TSX as detected by rheology and differential scanning calorimetry, but once again, mechanistically the nature of the interaction was not defined.

Surfactants are used widely in edible formulations, primarily as an emulsifier to allow the stable inclusion of hydrophobic additives, such as fats, flavourings and colourings, to water-based formulations (Kralova & Sjöblom, 2009). Polysorbate 20, or Tween® 20, is a non-ionic surfactant widely used as an additive in foodstuffs to stabilise oil-in-water emulsions (Genot, Kabri, & Meynier, 2013). Generally, non-ionic surfactants are preferred in edible formulations due to their low toxicity compared to their charged counterparts (Fasolin et al., 2013). It has generally been reported that charged biopolymers, such as gellan, and polysorbates do not associate (Fasolin et al., 2013) even up to concentrations of 10% w/v, except for chitosan-polysorbate 80 which formed structures on a nanometre and micrometre scale at extremely low (below 0.01% w/v) and extremely high (above 50% w/v) surfactant concentrations (Picone & Cunha, 2013). However, new studies have indicated that non-ionic surfactant micelles can contribute to electrostatic shielding of gelling biopolymers through weak hydrophobic interactions (Yang & Pal, 2020).

Additive manufacturing (3D printing) has recently found its way in food applications (Lipton, Cutler, Nigl, Cohen, & Lipson, 2015; Sun, Peng, Yan, H Fuh, & Soon Hong, 2015; Fan; Yang, Zhang, & Bhandari, 2017). Among the current 3D printing methods for food applications (Chia & Wu, 2015; Guo & Leu, 2013), extrusion is a prevailing technique because it is easy to develop and it has the broadest set of 'inks' (Guvendiren et al., 2016; Tan, Toh, Wong, & Lin, 2018) which can be tailored to match certain rheological requirements (Daffner et al., 2021; Godoi, Prakash, & Bhandari, 2016). Among all the available extrusion techniques, cold extrusion 3D food printing has emerged as the technology which enables the manufacture of food in different compositions, textures, tastes or shapes, and offers huge potential for personalised food products beyond what is achievable with conventional moulding. However, the high cost of production compared to existing manufacturing techniques is a barrier to commercialisation of 3D printing (Godoi et al., 2016). Warner, Norton and Mills (2019) reported that due to the slow gelation time of gelatine, 3D printing of gelatine-based formulations, without a gelation accelerant, results in distortion of printed shapes after printing. Hence, the development of a printable gelatine analogue would be advantageous.

This study aimed to explore LAG and TSX, firstly as a gelatine replacement, and secondly as an 'ink' to manufacture 3D printed gelled structures. The influence of a common food-grade emulsifier, Tween® 20, was also investigated. Rheology gave information on the thermal and mechanical properties of the gels through temperature and frequency sweeps. The release performance of the gels was

measured with respect to temperature in water using conductivity – made possible due to the efflux of cations upon gel erosion. The release profiles from both quiescent and 3D printed gels were compared.

4.3 Experimental

4.3.1 Materials

Kelcogel® F (batch 8F0778A), a commercially available low acyl gellan gum was kindly gifted by CP Kelco (USA). Tamarind seed xyloglucan (batch UG660FJ) was purchased from Tokyo Chemical Industry (UK). Gelatine from porcine skin (batch BCBH5042V, 240 - 270 g bloom, type A) was purchased from Sigma Aldrich (Germany). Tween® 20 was purchased from Merck (Germany). All materials were used as received without further purification or modifications. The ion content of Kelcogel® F and tamarind seed xyloglucan was determined by Inductively Coupled Plasma-Optical Emission Spectroscopy (PerkinElmer Optima 8000) as shown in Table 4.1.

Table 4.1 - Ion content for polysaccharide samples. Values given are mean averages from at least three successive measurements and the associated standard deviation. (* = negative values for ion contents were generated as the concentration was below the detectable limits).

	Ion content ($10^5 \times$ % w/w)			
	Na^+	K^+	Mg^{2+}	Ca^{2+}
Kelcogel® F	31.31 ± 0.08	229.9 ±1.8	2.906 ± 0.473	6.908 ± 0.847
TSX	2.427 ± 0.064	3.283 ± 0.072	-0.472 ± 0.020*	-0.847 ± 0.028*

4.3.2 Methods

4.3.2.1 Preparation of gel solutions

Polymer powders were weighed (wet basis) and were slowly added to a vessel of deionized water (Milli-Q, Millipore®) at 80 °C under agitation from a magnetic stirrer bar at a moderate speed to avoid clumping. The flask was covered to prevent evaporation and was kept isothermal under agitation for several hours until no powder clumps remained, and the solution was homogeneous. If required, Tween® 20 was then added dropwise and stirred for 10 minutes under gentle agitation to minimise foaming. Solutions were then stored overnight at room temperature (20 °C) until testing, at which time they were re-heated to 80 °C under gentle agitation. The total concentrations of biopolymers tested were 1 – 3 wt%, and surfactant concentrations were 0 – 1 wt%.

4.3.2.2 Rheological measurements

A MCR 302 rheometer (Anton Paar, Austria) equipped with a PP50-TG parallel plate geometry (D = 50.0 mm) and a P-PTD200/62/TG lower plate geometry (D = 62.0 mm) was used to characterise the rheology of the samples. In all measurements, samples were loaded in liquid form at 80 °C and trimmed to a gap of 1 mm, with the geometry pre-heated to 60 °C to avoid pre-gelation ($\delta > 45°$). A thin layer of silicone oil was immediately added to the outer edge of the samples to prevent evaporation and a Peltier hood (H-PTD-200) was lowered. For the amplitude and frequency sweep measurements the temperature of the geometry was reduced to 20 °C and held isothermally for 5 minutes before proceeding.

4.3.2.2.1 Amplitude sweep to determine the linear viscoelastic region (LVR)

An amplitude sweep was performed from 0.01 to 100% strain, at a frequency of 6.28 rad s^{-1} (1 Hz) and a temperature of 20 °C. The linear viscoelastic region was determined as the range of strain values which showed no significant degradation (± 1%) in the value of the storage modulus (G').

4.3.2.2.2 Temperature sweep to determine the gelling and melting temperatures

A temperature sweeps was performed from 60 °C to 10 °C and back to 60 °C for each sample, in triplicate. The applied strain was 1% as this was found to be within the LVR of the samples and all sweeps were performed at a frequency of 6.28 rad s^{-1} (1 Hz). The rate of temperature change was 1 °C per minute. Gelling and

melting temperatures were determined by the crossover of the elastic (G') and viscous (G'') modulus.

4.3.2.2.3 Frequency sweep to determine the mechanical spectra and printability

A frequency sweep was performed in triplicate, with the frequency varying between 62.8 rad s^{-1} to 0.628 rad s^{-1} (10 Hz to 0.1 Hz), at a strain of 1%. The measurements were performed at 20 °C.

4.3.2.3 3D Printing

A custom-built food 3D printing system was used in this study to conduct extrusion-based printing. 3D digital design of the object was generated with Cura 15.04.6 (Ultimaker B.V., Netherlands). A 10 mL syringe and a 22G needle (inner diameter 0.413 mm) were used for all samples. The syringe was filled with liquid samples (80 °C). All samples were printed at a flow level of 60% (Derossi et al., 2018). The cubes (15 mm × 15 mm × 15 mm) were printed for printability assessment. All objects were printed at a printing bed temperature of 50 °C.

4.3.2.4 Release Measurements

A SevenEasy conductivity meter (Mettler Toledo, USA) was used to monitor conductivity. Gel cubes (dimensions 15 mm × 15 mm × 15 mm) were formed in a custom 3D-printed mould by pouring liquid samples (50 °C) into the mould recess, covering with plastic film and were then stored at room temperature overnight in

an air-tight container before measurement. The bottom portion and sides of the mould were wrapped in Parafilm® M tape to prevent sample leakage through the slightly porous plastic. A 1 litre beaker was filled with 900 mL of distilled water and a custom 3D printed lid was placed on top of the beaker. The lid contained holes, through which a conductivity probe and a temperature probe were inserted, and a net which extended down into the beaker for placement of the gel cubes. The beaker was placed on a stirrer hotplate and the water was kept isothermal at either 20, 30 or 40 °C. The water was agitated gently at a constant rate of 100 rpm with a 70 mm pivoted PTFE stirrer bar. Conductivity was logged via Mettler Toledo LabX Direct-pH software, which recorded the measured conductivity once per second until it was manually stopped. The endpoint of the release measurement was determined once the conductivity value was steady (± 0.01 mS cm^{-1}) for 5 minutes.

4.3.2.5 Statistical Analysis

Data was analysed by calculating the Pearson correlation coefficient (ρ): the further the value of ρ from 0 indicates a strong positive or negative correlation between the two variables, depending on if the value of ρ is positive or negative respectively. Data was fitted using the linear regression analysis and data populations were compared using two-sample T-tests: both in the Analysis Toolpak for Microsoft Excel. A linear fit was assumed statistically accurate if $R^2 \geq 0.90$ and populations were considered statistically different if P(one-tail) ≤ 0.05. Non-linear

regression was performed using the curve fitting tool in SigmaPlot 14.5, and a fit was assumed accurate if $R^2 \geq 0.90$.

4.4 Results

4.4.1 Rheology

4.4.1.1 Temperature sweeps to determine the gelling and melting temperatures

The values of the gelling (T_g) and melting (T_m) temperatures of LAG/TSX gels were obtained as a function of total polymer concentration (at a constant polymer ratio) and a function of polymer ratio (at a constant total polymer concentration). The addition of 1 wt% Tween® 20 on the value of the gelling and melting temperatures was also investigated. These data are shown in Figure 4.1.

In general, it was found that the values of the gelling and melting temperatures increased with total biopolymer concentration ($\rho = 0.99$ and 0.90 respectively): at 1 wt% these values were ca. 24 °C and ca. 27 °C, increasing up to ca. 34 °C and ca. 39 °C at 2.5 wt% respectively. At a total biopolymer concentration of 3 wt%, there was no crossover of the viscoelastic moduli detected in the heating step of the temperature sweep i.e. the gel samples did not melt in the experimental temperature range. The increase in gelling temperature values with the total biopolymer concentration had a good linear fit ($R^2 = 0.99$), however this was untrue for melting temperatures ($R^2 = 0.81$), likely due to the discontinuous rise in T_m at 2.5 wt% total polymer concentration. The introduction of Tween® 20 led to

statistically significant increases in the gelling temperatures (ca. 2 °C), and the melting temperatures (ca. 5 °C) as indicated by P(one-tail) = 0.005 and 0.03 respectively. The increase in gelling temperature upon addition of surfactant was independent of total biopolymer concentration (ρ = -0.24) yet the melting temperature was found to be dependent (ρ = 0.92), hence indicating that the surfactant had a greater influence on the melting temperature of more concentration formulations.

In the second set of data shown in Figure 4.1, the total biopolymer concentration was kept constant at 2 wt% and the polymer blend was varied: this concentration was chosen as it was a sensible value based on the previous data set. At 0% LAG content, i.e. 100% TSX content, no gelling or melting was detected, and at and beyond 75% LAG content, no melting was detected, hence there are no data at these points. Increasing the LAG content from 25% to 50% only lead to a very small increase in the values of the gelling temperature (ca. 1 °C), and the melting temperature remained constant, indicating very similar gel microstructures. However, as the LAG content was then increased to 75% and 100%, the gelling temperatures increased dramatically (ca. 10 °C per additional 25% LAG) and the melting temperatures increased to beyond the experimental maximum temperature (60 °C), indicating a significant microstructural change

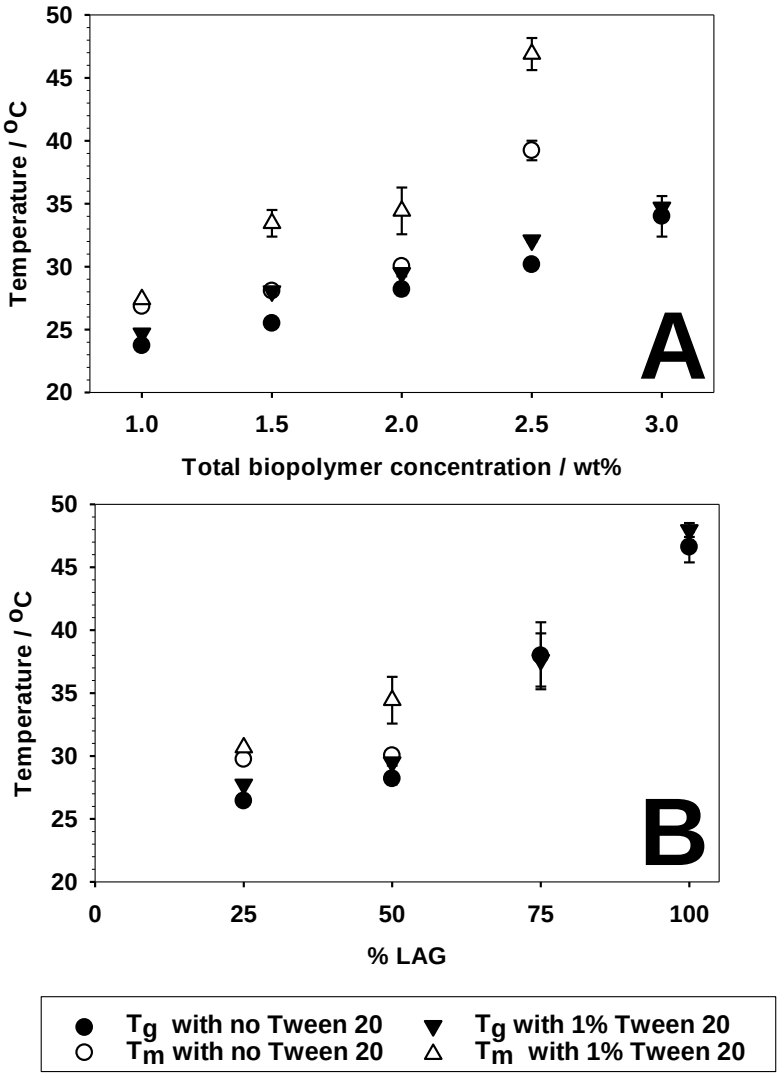

Figure 4.1 - Gelling and melting temperature data for LAG/TSX samples. In figure A, the ratio of LAG:TSX was kept at 1:1 and the total concentration of biopolymer was changed. In figure B, the total biopolymer concentration was kept constant at 2 wt% and the ratio of LAG:TSX was varied. Values given are mean averages from three measurements and error bars represent standard deviation.

Over the range of polymer blends tested, there was a strong positive correlation between the gelling temperatures and the percentage of LAG ($\rho = 0.97$) however there were too few (only two) data points to perform statistical analysis for the

melting temperatures. The addition of 1 wt% Tween® 20 to these samples, produced no statistical change in the phase transition temperatures of the LAG/TSX gels at a constant biopolymer concentration [P(one-tail) = 0.49].

In summary, it was found that only the total concentration of biopolymers was sensitive to the addition of Tween® 20 with greater shifts in gelling and melting temperatures seen at higher total polymer concentrations. In contrast, small increases in gelling and melting temperatures were seen across all the blends tested, regardless of the polymer ratio.

For comparison, samples of 5 wt% gelatine with and without 1 wt% Tween® 20 were made, and the measured gelling and melting temperatures were ca. 21.5 °C and 30.3 °C in each case, regardless of the presence of surfactant. This data can be used to determine which, if any, of the LAG/TSX samples would be potentially suitable as a gelatine replacement. Osorio *et al.* (2007) obtained gelling and melting temperatures for gelatine using the crossover of the viscous and elastic moduli, and these values are approximately 18 – 28 °C and 32 – 37 °C respectively, with thermal hysteresis values in the order of ca. 10 °C: this agrees well with the measured values in this study.

4.4.1.2 Frequency sweeps to determine the mechanical spectra

Frequency sweeps were conducted to determine two important rheological parameters: the phase angle (δ) and storage modulus (G'), and their dependence on the measurement frequency. This was performed for the LAG/TSX gels with or without the addition of 1 wt% Tween® 20, and the results are shown in Figure 4.2. A larger error bar indicates that the sample was more frequency-dependent, and hence more liquid-like.

As the total concentration of biopolymer was increased – again, at a fixed blend of 50:50 LAG:TSX – a steady decrease in the phase angle was seen ($\rho = -0.95$), dropping from ca. 20° at a concentration of 1 wt% to ca. 7° at a concentration of 3 wt%. The standard deviation in the phase angle significantly decreased as the total biopolymer concentration was increased ($\rho = -0.91$), so the samples became less frequency-dependent. Conversely, the value of the storage modulus (G') increased exponentially ($\rho = 0.93$, $R^2 = 0.98$) as the total biopolymer concentration was increased, from ca. 30 Pa to ca. 1000 Pa. All of these data suggested that increasing the total concentration of biopolymer increased gel strength and made the gel more solid-like.

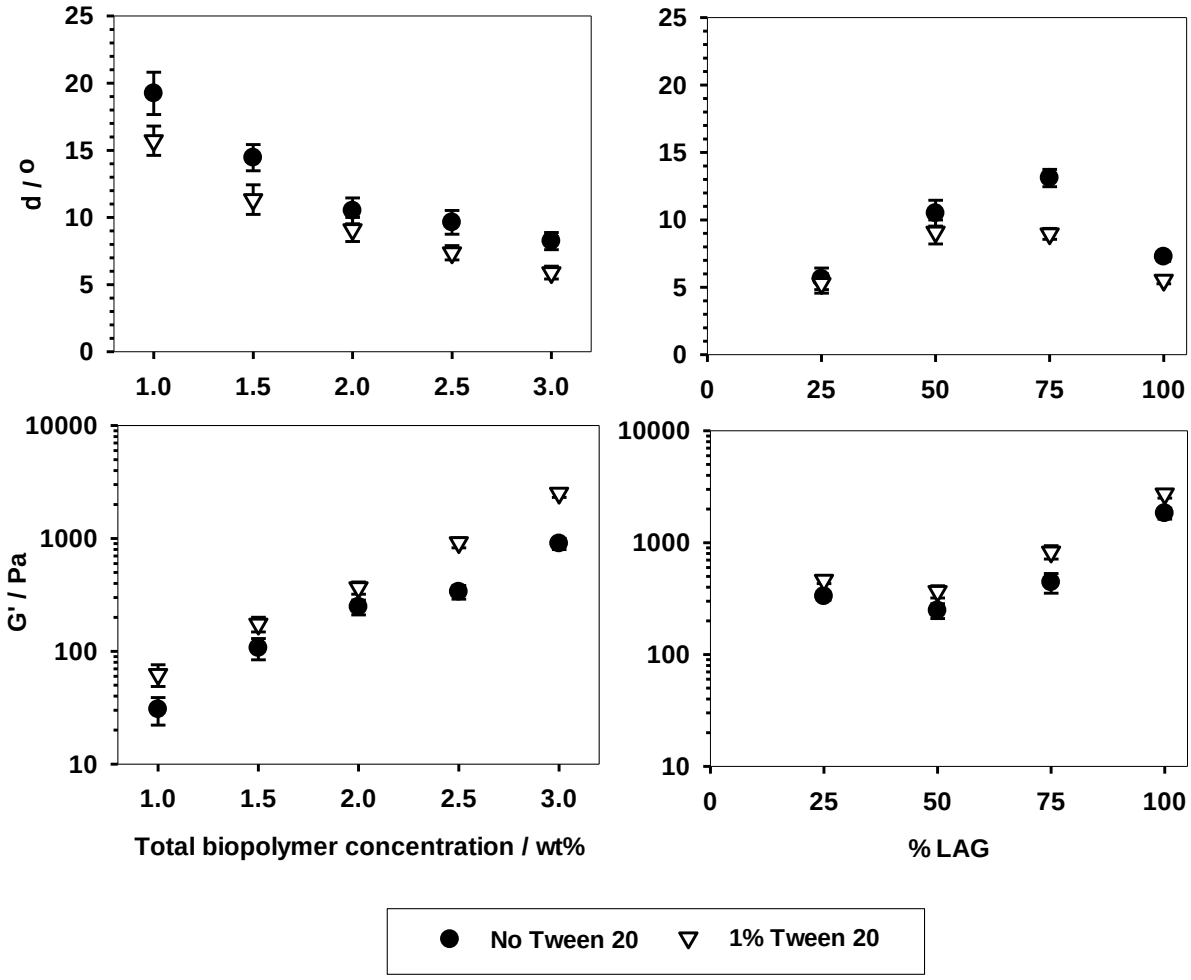

Figure 4.2 - Frequency sweep data for LAG/TSX samples, plotting phase angle (δ) or elastic modulus (G') against formulation parameters. Values given are mean averages from all data points in the three frequency sweeps, and error bars represent standard deviation.

At a fixed biopolymer concentration of 2 wt%, the phase angle showed a steady increase from ca. 5° to ca. 13° from 25 to 75% LAG content, followed by a decrease as the blend reached 100% LAG back to ca. 7°, hence indicating that the gel was least solid-like at 75% LAG content. This was accompanied by an initial decrease in the value of the storage modulus of 300 Pa to 250 Pa from 25% to 50% LAG

content, followed by another exponential increase to ca. 2000 Pa up to 100% LAG, hence indicating a minimum in gel strength was measured at 50% LAG. A negative second-order polynomial trendline showed good agreement for both the phase angle (R^2 = 0.94) and the storage modulus (R^2 = 0.98) with respect to percentage LAG content.

The frequency dependence was low (SD ≤ 1°) in all blends tested, yet it was still found to correlate in a strong negative relationship with the percentage of LAG (ρ = -0.97), indicating that the higher the percentage of LAG in a blend, the less frequency dependent, and more solid-like, the gel was. In the constant blend experiments, the addition of 1 wt% Tween® 20 led to statistically significant decreases (P(one-tail) = 0.0014) in measured phase angles, in the order of 1 - 5°, compared to samples without surfactant. There was some indication that the storage modulus increased upon addition of Tween® 20 however these were found to be not statistically significant (P(one-tail) = 0.098). The size of the reduction in phase angle upon addition of Tween® 20 was found to be mostly independent of the total biopolymer concentration ($\rho = -0.64$) in this case.

In the constant total polymer concentration experiments, the addition of Tween® 20 showed the largest decreases to the phase angle of LAG/TSX gels with the highest phase angle (ρ = 0.87): i.e., the largest change was seen for the 75% LAG, 25% TSX sample which had the largest starting phase angle. Furthermore, the

magnitude of the increase in the storage modulus upon addition of Tween® 20 was found to be strongly dependent on both the percentage of LAG in the blend (ρ = 0.91) and the initial storage modulus (ρ = 0.97): the two are related. Hence, once again it was seen that the addition of surfactant had the greatest influence on the weaker, low thermal hysteresis gels compared to the stronger, high thermal hysteresis gels.

For comparison, frequency sweeps with formulations consisting of 5% gelatine with and without 1 wt% Tween® 20 were performed. It was found that the storage moduli were 360 ± 40 Pa and 445 ± 48 Pa, and the phase angles were 1.20 ± 0.43° and 1.17 ± 0.44° for the sample without and with Tween® 20 respectively. This provided a target storage modulus and phase angle for a gelatine replacement.

4.4.2 3D Printing

4.4.2.1 Rheology to predict printability

The printability of a range of LAG/TSX and gelatine gels was predicted using rheological data obtained from frequency sweeps. Phase angles (δ) and the relaxation exponents (m) can be used to predict the suitability of a material to being manufactured using a 3D printing process (Gholamipour-Shirazi et al., 2019). One can obtain the relaxation component by noting the dependence of the elastic modulus (G') on angular frequency (ω) in a power-law relationship as shown in Equation 4.1 (Kavanagh & Ross-Murphy, 1998), using frequency sweep data.

Previous work by Gholamipour-Shirazi, Norton and Mills (2019) showed that if 3°< δ < 15° and 0.03 < m < 0.13, the formulation was printable. The summary of printability results for LAG/TSX and LAG/TSX/Tween® 20 gels are shown in Table 4.2 - Table 4.6. Formulations were stated to be 'feasibly printable' if the required rheological parameters were partially in the required range, and 'printable' if the parameters were fully in the required range, including any standard deviation. As can be seen, $R^2 \geq 0.95$ in all LAG/TSX samples, with and without surfactant, indicating a good fit to the power-law equation.

$$G'(\omega) \approx k_1 \omega^m \quad (4.1)$$

Table 4.2 – Table of rheological parameters used to determine printability based on the formula given in Equation 4.1. All samples consisted of a 50:50 blend of LAG:TSX whilst the total polymer concentration was varied. Values given are mean averages from three frequency sweeps with standard deviation. († = mean values are in the required range however printability is uncertain due to calculated error).

Biopolymer concentration (wt %)	δ (°)	k_1 (Pa s rad^{-1})	m	R^2	Printable?
1	19.24 ± 1.57	20.75 ± 0.87	0.190 ± 0.002	0.9990	No
1.5	14.45 ± 0.98	79.93 ± 2.96	0.14 ± 0.04	0.9992	No
2	10.50 ± 0.96	203.6 ±10.3	0.10 ± 0.05	0.9970	Yes†
2.5	9.42 ± 0.81	359.4 ± 16.2	0.09 ± 0.05	0.9964	Yes†
3	8.24 ± 0.64	811.1 ± 31.6	0.07 ± 0.04	0.9965	Yes

Table 4.3 – Table of rheological parameters used to determine printability based on the formula given in Equation 4.1. All samples consisted of 1 wt% Tween 20 with a 50:50 blend of LAG:TSX whilst the total polymer concentration was varied. Values given are mean averages from three frequency sweeps with standard deviation. († = mean values are in the required range however printability is uncertain due to calculated error).

Biopolymer concentration (wt %)	δ (°)	k_1 (Pa s rad^{-1})	m	R^2	Printable?
1	15.72 ± 1.09	51.91 ± 5.25	0.14 ± 0.10	0.9947	No
1.5	11.33 ± 1.10	152.9 ± 8.8	0.10 ± 0.06	0.9974	Yes†
2	9.10 ± 0.90	326.2 ± 13.4	0.083 ± 0.041	0.9968	Yes
2.5	7.38 ± 0.53	838.2 ± 29.1	0.068 ± 0.035	0.9967	Yes
3	5.90 ± 0.48	2334 ± 61	0.055 ± 0.03	0.9962	Yes

Table 4.4 – Table of rheological parameters used to determine printability based on the formula given in Equation 1. All were formulated at 2 wt% total gelling biopolymer concentration whilst ratio of LAG:TSX was varied. Values given are mean averages from three frequency sweeps with standard deviation. († = mean values are in the required range however printability is uncertain due to calculated error).

% LAG	δ (°)	k_1 (Pa s rad^{-1})	m	R^2	Printable?
100	7.26 ± 0.34	1578 ± 4	0.078 ± 0.002	0.9992	Yes
75	13.11 ± 0.64	336.8 ± 7.2	0.14 ± 0.02	0.9994	No
50	10.50 ± 0.96	203.6 ±10.3	0.10 ± 0.05	0.9970	Yes†
25	5.63 ± 0.80	302.7 ± 12.6	0.049 ± 0.042	0.9913	Yes

Table 4.5 – Table of rheological parameters used to determine printability based on the formula given in Equation 1. All were formulated with 1 wt% Tween 20 at 2 wt% total gelling biopolymer concentration whilst the ratio of LAG:TSX was varied. Values given are mean averages from three frequency sweeps with standard deviation.

% LAG	δ (°)	k_1 (Pa s rad^{-1})	m	R^2	Printable?
100	5.53 ± 0.27	2455 ± 6	0.057 ± 0.002	0.9972	Yes
75	8.96 ± 0.40	701.1 ± 9.1	0.092 ± 0.013	0.9992	Yes
50	9.10 ± 0.90	326.2 ± 13.4	0.083 ± 0.041	0.9968	Yes
25	5.28 ± 0.71	443.1 ± 16.6	0.043 ± 0.037	0.9900	Yes

Table 4.6 - Table of rheological parameters used to determine printability based on the formula given in Equation 1. All were formulated with 5 wt% gelatine whilst the concentration of Tween 20 was varied. Values given are mean averages from three frequency sweeps with standard deviation.

Concentration Tween 20 (wt %)	δ (°)	k_1 (Pa s rad^{-1})	m	R^2	Printable?
0	1.20 ± 0.43	518.6 ± 106.6	-0.040 ± 0.21	0.8730	No
1	1.17 ± 0.44	633.0 ± 124.6	-0.039 ± 0.20	0.8847	No

Upon addition of 1 wt% Tween 20 to the samples ascribed in Table 4.2 (data in Table 4.3) the phase angle and the relaxation exponent decreased (P(one-tail) = 0.01), hence the samples became more printable. Without surfactant, formulations at 2 - 2.5 wt% total biopolymer concentration were feasibly printable and 3 wt%

was predicted to be printable. Whereas upon addition of 1 wt% surfactant, 1.5 wt% samples were now feasibly printable, and printable at 2 wt% and beyond.

The ratio of biopolymers in the blend was also investigated to see if it influenced printability Table 4.4. It was discussed previously that the phase angle had a parabolic relationship with the percentage of LAG (at a constant total concentration of gelling biopolymers). In this case the parabolic behaviour can be seen to carry over, with 75% LAG being the only blend not deemed printable due to its high mean phase angle. As previously, the addition of 1 wt% Tween 20 was investigated Table 4.5. Apart from the 25% LAG blend, both the phase angle relaxation exponent showed significant changes upon addition of Tween 20 (P(one-tail) = 0.04), and all samples became printable.

For comparison, a sample of 5 wt% gelatine with and without 1 wt% Tween 20 was investigated in an identical manner Table 4.6. It was found that the formulations were not printable since the phase angle and relaxation component were too small for the printing requirements.

4.4.2.2 3D printing of samples

Following the printability predictions, three LAG/TSX samples of varying formulation were tested for real-world printability. The samples tested were 0.5 wt% LAG/1.5 wt% TSX, 1.25 wt% LAG/1.25 wt% TSX, and – 1 wt% LAG/1 wt% TSX. Concentrations were chosen to represent a range of printability values within the permitted values for printability (Gholamipour-Shirazi et al., 2019). When comparing the predicted printability of the samples to the printed samples, shown in Figure 4.3, the images suggest that the rheological rules outlined by Gholamipour-Shirazi, Norton and Mills (2019) were generally a good indicator of printability.

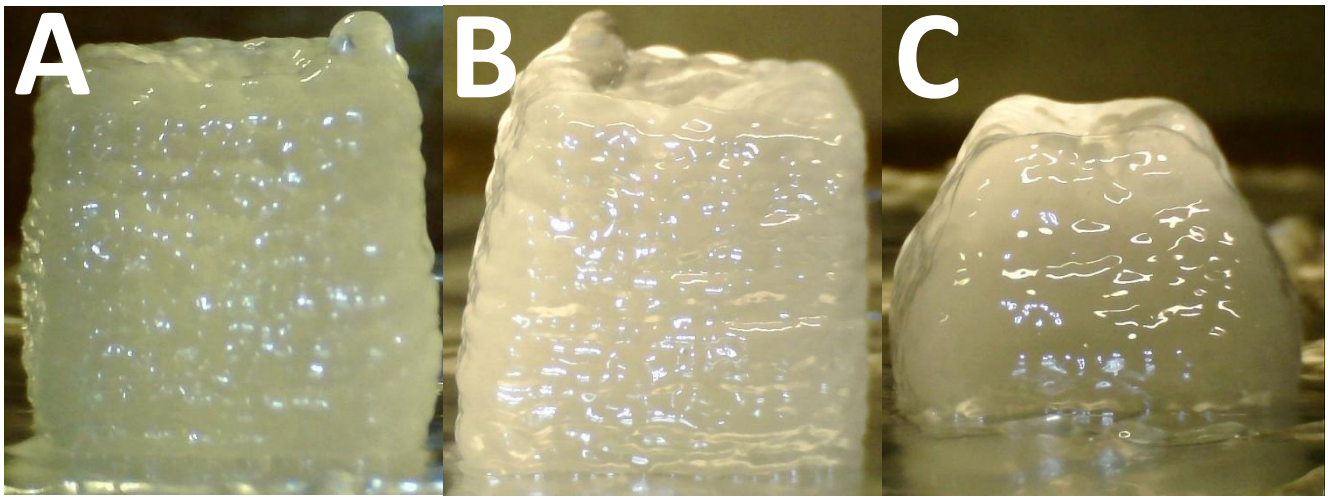

All samples were predicted to be printable, based on the value of the phase angle and the release exponent, however samples B and C could only be predicted to be feasibly printed because of the error in the measurements extended outside the printable parameters. In each sample successful printing was achieved, with

varying degrees of accuracy. Samples A and B were printed with good accuracy and the finished gel resembled a cube geometry. Sample C did form a self-supporting gel, however it is clear that the gel sagged post-printing made evident by the narrowing of the cube nearer the top.

4.4.3 Measuring temperature-mediated release from moulded and printed gels

Following from the rheological measurements and 3D printing experiments, two LAG/TSX/Tween® 20 blends were chosen to represent potential gelatine replacements in release studies: these samples were 0.5 wt% LAG/1.5 wt% TSX/1 wt% Tween® 20 and 1 wt% LAG/1 wt% TSX/1 wt% Tween® 20. These concentrations were chosen because the measured melting temperatures were ca. 31 °C and 36 °C: at each extremity for the theoretical melting requirements of a gelatine replacement (greater than ambient temperature but below body temperature), and the storage moduli were very similar (within 100 Pa) of the measured storage modulus of 5 wt% gelatine with 1 wt% Tween® 20, hence the gel strength was similar. Additionally, based on the rheology of samples in section 4.4.1, both samples were predicted to be printable and so the influence of moulding versus printing the samples on the release behaviour could be investigated. To this end, a sample of 0.5wt% LAG/1.5 wt% TSX/1 wt% Tween 20 was printed and compared to a moulded sample: all other samples in the release studies were moulded. The release profiles of the gels were measured in water at 20, 30 and 40 °C using conductivity, and the results are shown in Figure 4.4.

The 5 °C difference in melting temperatures between the two LAG/TSX blends led to significant differences in the release profiles. At 20 °C, the release time for both the gels was similarly slow (several hours), however, at 30 °C the 0.5 wt% LAG/1.5 wt% TSX/1 wt% Tween® 20 gel showed rapid melting behaviour, reaching a maximum conductivity value in under ten minutes, with 40 °C taking less than three minutes. Conversely, the 1 wt% LAG/1 wt% TSX/1 wt% Tween® 20 took over an hour to reach maximum conductivity at 30 °C, and under ten minutes at 40 °C.

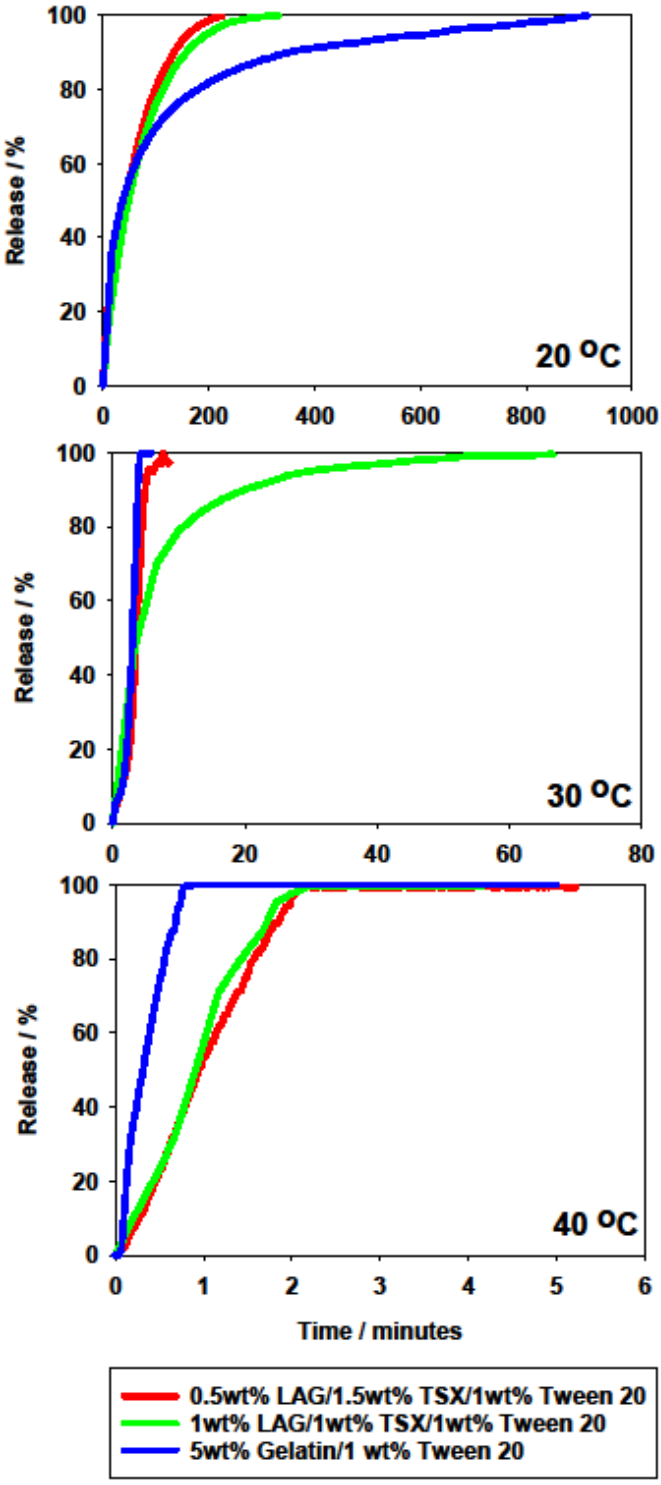

Figure 4.4 – Release data obtained from conductivity measurements of LAG/TSX/Tween and Gelatine/Tween Gels.

As a reference the release of 5 wt% gelatine with 1 wt% Tween® 20 was analysed in the same manner: release at 20 °C took nearly sixteen hours, yet at 30 °C and 40 °C maximum conductivity was achieved in approximately five minutes and one minute respectively.

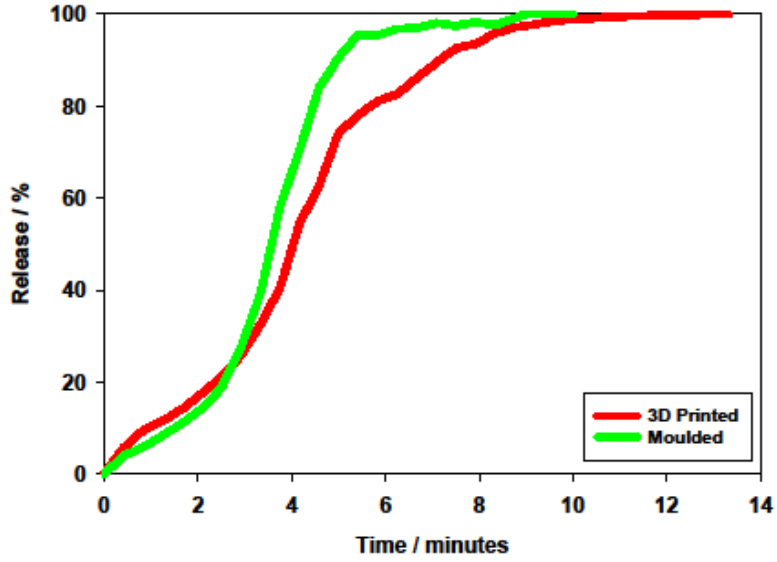

Figure 4.5 - A comparison of release data from a 3D printed and a moulded sample of 0.5wt% LAG/1.5wt% TSX/1wt% Tween® 20.

Furthermore, a comparison between gel samples manufactured using 3D printing and moulding was performed to see if the release profiles were similar, as shown in Figure 4.5. To this end, a sample of 0.5wt% LAG/1.5wt% TSX/1wt% Tween® 20 was prepared, printed and tested for release at 30 °C. The initial findings suggest that there was no statistical difference between the release profiles for the moulded gel and the printed gel. Further investigation between moulded and 3D printed

samples was intended, however complications due to COVID-19 made further production of 3D printed samples unattainable for the foreseeable future.

4.5 Discussion

The rheological data showed a statistically significant relationship that as the total biopolymer concentration was increased this led to a greater gelling temperature, melting temperature, storage modulus and a lower phase angle. This is a common occurrence for many gelling biopolymers that gel with a cation-driven helical-aggregation mechanism, such as kappa-carrageenan or gellan. At a higher polymer concentration – and therefore gelling cation concentration – greater aggregation of helices can take place, owing to better screening of repulsive charges on adjacent helices. This leads to more thermally stable aggregates that can form at higher temperatures and consequently need a higher temperature to overcome, explaining the greater gelling and melting temperatures. The increased helical aggregation also explained the greater storage modulus and lower phase angle as gel strength and solid-like character of the gels increases in such circumstances. Similar rheological trends in gellan with polymer and cation concentration have been reported by previous authors (H. Lee et al., 2011; Picone & Cunha, 2011).

The blend ratio, however, showed a more variable influence on the rheological properties of the gels. The gelling temperature showed a strong positive correlation with LAG content: this is expected due to the high gelling temperatures of LAG,

and as the blend of LAG increased, the more LAG aggregates can form. Hence it is predicted that the gelling temperatures are controlled by the LAG content. In contrast, the storage modulus and phase angle had parabolic relationship with the LAG content, with a maximum in phase angle achieved at 75% LAG and a minimum in storage modulus at 50% LAG. If the morphology of the LAG/TSX was phase separated, one would expect a gradual decrease in phase angle and an increase in storage modulus as the LAG content was increased, since TSX does not form a gel network on its own – such as the trends observed in the gelling temperature. Therefore, the strong mechanical properties at 25% LAG content suggest the existence of some coupled polymer network. Nevertheless, the purpose of this paper is not to unravel the mechanism of LAG and TSX interactions, however these observations invoke some interesting questions.

In the constant blend experiments, the introduction of Tween® 20 to the LAG/TSX gel mixture led to an increase in gelling temperature, melting temperature and storage modulus, and a reduction in the phase angle and frequency dependence across the tested samples. Whereas in the constant total biopolymer concentration experiments, only the frequency dependence and the magnitude of the increase in the storage modulus showed change upon the addition of Tween® 20. Pragmatically, this means that the total biopolymer concentration is the primary factor in determining the rheological properties of the gels, and the blend of LAG and TSX is secondary to this.

The alteration in rheological properties upon the addition of Tween® 20 is unlikely to simply be due to an increase in the effective concentration of the gelling biopolymers: an increase in polymer concentration by 1% would not explain the magnitude observed change in rheological behaviour. Volume exclusion effects could theoretically increase the effective polymer concentrations, however this is unlikely to be responsible for the shift in properties due because Tween® 20 micelles occupy a very similar volume to the equivalent mass of water that they replace, i.e. in micellar form, the density of Tween® 20 is very similar to that of water. Previous work concerning formulations of an anionic polymer with a non-ionic surfactant showed a similar increase in the gelling and melting temperature compared to the data reported here, and this was attributed to electrostatic shielding of the charged polymer helices by the surfactant micelles which enhanced helical aggregation (Fenton, Kanyuck, et al., 2021; Yang & Pal, 2020). Fortunately, the magnitude of the increase in gelling, and more importantly, the melting temperatures was such that the LAG/TSX system could still be viable as a gelatine replacement.

The rheological data was also used to evaluate the printability of the polymer solutions. Generally, the samples found to be most printable were those whose total gelling biopolymer concentration was at least 2 wt%, or 1.5 wt% if 1 wt% Tween 20 was added. Printability was predicted to improve as biopolymer concentration was increased up to 3 wt%. Furthermore, printability was influenced by the LAG:TSX blend, with the 75% LAG blend being the least printable of all

samples tested, and the 25% LAG blend the most printable. The addition of 1 wt% Tween® 20 improved the printability parameters of almost all samples tested, by decreasing the phase angle and the relaxation exponent and in no case did the printability parameters become less favourable. This is likely because there was a small microstructural change upon the addition of Tween® 20, as discussed previously, and this simply led to samples which were more rheologically suited for a printing process. When examining the data for 5 wt% gelatine, it is clear that the samples were unprintable, hence the novelty of this formulation can be extended beyond providing similar mechanical and melting behaviours from a renewable, vegan formulation to being processible using additive manufacturing.

The significant difference in real-world printability between samples B & C is contrasted by their apparent similarities in both their measured phase angles and relaxation exponents, with differences of ca. 1° and 0.01 respectively, with both samples showing feasible printability. This suggests that the rules set out by Gholamipour-Shirazi, Norton and Mills (2019) successfully predicted if a sample was *at all* printable, but for samples that have printability parameters that are close to printability limits, the variability in rheological measurements make it difficult to successfully predict printability. Additionally, there may be another factor affecting the accuracy of the printed shape such as gelling temperature or gelation time. According to the measured values in section 3.1, sample B had a gelling temperature of ca. 2 °C higher than sample C: whether such a small difference in gelling temperature would lead to a marked difference in printability

is debatable. If so, reducing the extrusion temperature or the bed temperature may improve the printability of samples with a lower gelling temperature.

The measured release profiles are useful for indicating if the gel formulations could be suitable gelatine replacements, by seeing if they mimic the same melt-in-the-mouth behaviour that gelatine shows. From the release profiles obtained for the 5 wt% gelatine gel, it is clear that the requirement must be quick melting at 30 °C (under 10 minutes) and even quicker melting at 40 °C (1-2 minutes). Similar melting behaviour has been reported previously for gelatine (Mills et al., 2011). At 20 °C, the release profiles for both of the moulded LAG/TSX gels were similarly slow – ca. 2-3 hours – and the release at this temperature for the LAG/TSX gels was driven mainly by diffusion of counter-ions out of the gel and subsequent erosion of the weakened gel layer. Slight differences between different LAG/TSX blends arise at this temperature due to slightly different gel porosities and counter-ion concentrations within the gel, even though both gels have a melting temperature well above 20 °C. Gelatine, on the other hand, took significantly longer to show 100% release at 20 °C and that because the chemical nature of the gel network is markedly different: in the case of LAG/TSX, it relies on the existence of counter-ions to 'glue' the helices together in an aggregated network, and hence if these counter ions diffuse out of the gel in to water then the gel network collapses and is simply eroded from the outside, inwards, as diffusion of ions from the surface of the gel is much faster compared to diffusion from the bulk gel. As the gel is eroded, this speeds up further diffusion of counter-ions from the gel by increasing

the porosity of the gel and reducing the diffusion distance between counter-ions and the water. However, in the case of gelatine the movement of counter ions from the gel is pure-diffusion since there is no erosion, resulting in much slower diffusion (Mills et al., 2011). This mechanism of erosion in LAG/TSX versus pure diffusion in gelatine is further evidenced by the fact that at the end of the release experiments at 20 °C, there was no solid material left in the LAG/TSX experiments, whereas for gelatine there was no observable change in the physical dimensions of the gel compared to the start of the experiment. This diffusion-erosion mechanism is shown graphically in Figure 4.6. The results suggest that the 0.5 wt% LAG/1.5 wt% TSX polymer blend has a much more similar melting behaviour to gelatine compared to 1 wt% LAG/1 wt% TSX, because at 30 °C release was comparatively much slower in the latter blend, than the former, which was much closer to those results obtained for gelatine.

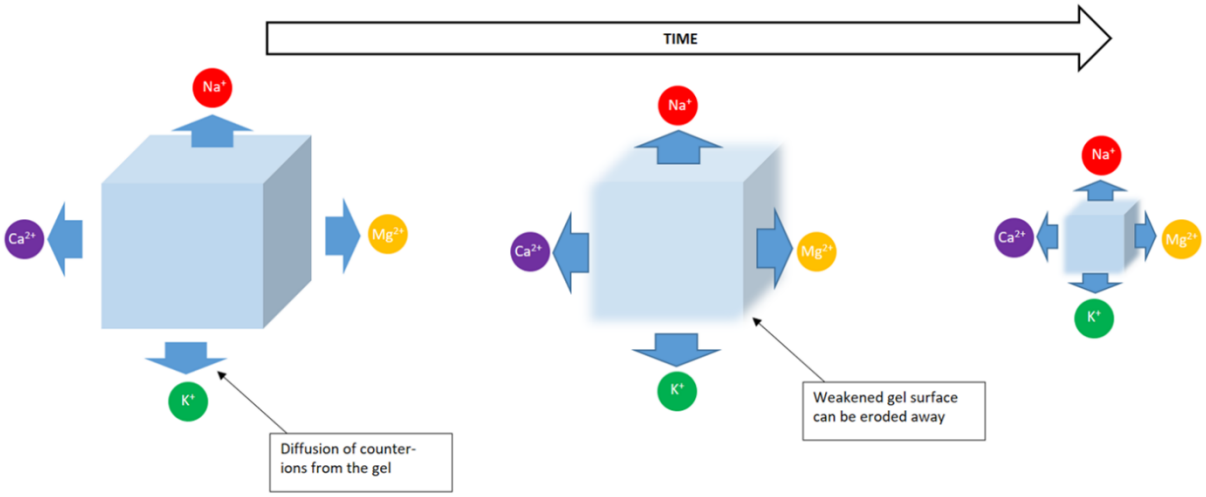

When comparing the release curves for a moulded sample compared to the 3D printed sample, the profiles are indistinguishable from one another, indicating that the 3D printing process did not significantly alter the structure of the final gel, and either technique could be used to manufacture gel samples. However, the authors recognise that further data in this area would be advantageous.

4.6 Conclusions

Overall these data have shown that the formulation engineering approach of a vegetarian gelatine replacement using low acyl gellan and tamarind seed xyloglucan is possible. The most similar blend tested was 0.5 wt% LAG/1.5 wt% TSX, which showed very similar gel strength and melting behaviour to 5 wt% gelatine. Furthermore, it was shown that LAG/TSX gels can be manufactured using 3D printing, whereas this is not possible for gelatine gels. The introduction of Tween® 20 to the LAG/TSX formulations had no detrimental effect on the printability of the LAG/TSX samples, and in many cases improved printability. Additionally, there was a small increase in the measured gelling and melting point temperatures which could influence efficacy in some applications if melting is required. The origin of these phenomena is currently unknown due to poor understanding of the mechanism of LAG/TSX interactions and how the formation of the hybrid gel network forms and exactly what influence the surfactant has on the junction zones of the LAG/TSX system. Further work could involve more clearly elucidating the nature of this interaction with advanced imaging

techniques such as scanning electron microscopy (SEM). The LAG/TSX system represents an exciting avenue for further research in to gelatine replacements.

4.7 References

Chilvers, G. R., & Morris, V. J. (1987). Coacervation of gelatine-gellan gum mixtures and their use in microencapsulation. *Carbohydrate Polymers*, *7*(2), 111–120. https://doi.org/10.1016/0144-8617(87)90053-1

Daffner, K., Vadodaria, S., Ong, L., Nöbel, S., Gras, S., Norton, I., & Mills, T. (2021). Design and characterization of casein–whey protein suspensions via the pH–temperature-route for application in extrusion-based 3D-Printing. *Food Hydrocolloids*, *112*. https://doi.org/10.1016/j.foodhyd.2020.105850

Fasolin, L. H., Picone, C. S. F., Santana, R. C., & Cunha, R. L. (2013). Production of hybrid gels from polysorbate and gellan gum. *Food Research International*, *54*(1), 501–507. https://doi.org/10.1016/j.foodres.2013.07.026

Fenton, T., Kanyuck, K., Mills, T., & Pelan, E. (2021). Formulation and characterisation of kappa-carrageenan gels with non-ionic surfactant for melting-triggered controlled release. *Carbohydrate Polymer Technologies and Applications*, *2*, 100060. https://doi.org/10.1016/j.carpta.2021.100060

Genot, C., Kabri, T. H., & Meynier, A. (2013). Stabilization of omega-3 oils and enriched foods using emulsifiers. In *Food Enrichment with Omega-3 Fatty Acids* (pp. 150–193). Elsevier Inc. https://doi.org/10.1533/9780857098863.2.150

Gholamipour-Shirazi, A., Norton, I. T., & Mills, T. (2019). Designing hydrocolloid based food-ink formulations for extrusion 3D printing. *Food Hydrocolloids*, *95*, 161–167. https://doi.org/10.1016/J.FOODHYD.2019.04.011

Godoi, F. C., Prakash, S., & Bhandari, B. R. (2016). 3d printing technologies applied for food design: Status and prospects. *Journal of Food Engineering*. https://doi.org/10.1016/j.jfoodeng.2016.01.025

Grasdalen, H., & Smidsrød, O. (1987). Gelation of gellan gum. *Carbohydrate Polymers*, *7*(5), 371–393. https://doi.org/10.1016/0144-8617(87)90004-X

Grisel, M., Aguni, Y., Renou, F., & Malhiac, C. (2015). Impact of fine structure of galactomannans on their interactions with xanthan: Two co-existing mechanisms to explain the synergy. *Food Hydrocolloids*, *51*, 449–458. https://doi.org/10.1016/j.foodhyd.2015.05.041

Ikeda, S., Nitta, Y., Kim, B. S., Temsiripong, T., Pongsawatmanit, R., & Nishinari, K. (2004). Single-phase mixed gels of xyloglucan and gellan. *Food*

Hydrocolloids, *18*(4), 669–675. https://doi.org/10.1016/j.foodhyd.2003.11.005

Ikeda, S. and Talashek, T. A. (2007) *Low acyl gellan gels with reduced thermal hysteresis and syneresis*. United States Patent and Trademark Office Patent no. US 2009/0123628 A1. Available at: https://patents.google.com/patent/US20090123628A1/en (Accessed: 1 February 2021).

Jansson, P. E., Lindberg, B., & Sandford, P. A. (1983). Structural studies of gellan gum, an extracellular polysaccharide elaborated by Pseudomonas elodea. *Carbohydrate Research*, *124*(1), 135–139. https://doi.org/10.1016/0008-6215(83)88361-X

Kaur, H., Yadav, S., Ahuja, M., & Dilbaghi, N. (2012). Synthesis, characterization and evaluation of thiolated tamarind seed polysaccharide as a mucoadhesive polymer. *Carbohydrate Polymers*, *90*(4), 1543–1549. https://doi.org/10.1016/j.carbpol.2012.07.028

Kavanagh, G. M., & Ross-Murphy, S. B. (1998). Rheological characterisation of polymer gels. *Progress in Polymer Science*, *23*(3), 533–562. https://doi.org/10.1016/S0079-6700(97)00047-6

Kralova, I., & Sjöblom, J. (2009, October). Surfactants used in food industry: A review. *Journal of Dispersion Science and Technology*. https://doi.org/10.1080/01932690902735561

Kuo, M. S., Mort, A. J., & Dell, A. (1986). Identification and location of l-glycerate, an unusual acyl substituent in gellan gum. *Carbohydrate Research*, *156*, 173–187. https://doi.org/10.1016/S0008-6215(00)90109-5

Ledward, D. A. (2000). Gelatine. In G. O. Phillips & P. A. Williams (Eds.), *Handbook of Hydrocolloids* (2nd ed., pp. 67–86). Cambridge, UK: Woodhead Publishing Limited.

Lee, H., Fisher, S., Kallos, M. S., & Hunter, C. J. (2011). Optimizing gelling parameters of gellan gum for fibrocartilage tissue engineering. *Journal of Biomedical Materials Research - Part B Applied Biomaterials*, *98 B*(2), 238–245. https://doi.org/10.1002/jbm.b.31845

Mills, T., Spyropoulos, F., Norton, I. T., & Bakalis, S. (2011). Development of an in-vitro mouth model to quantify salt release from gels. *Food Hydrocolloids*, *25*(1), 107–113. https://doi.org/10.1016/j.foodhyd.2010.06.001

Moorhouse, R., Colegrove, G. T., Sandford, P. A., Baird, J. K., & Kang, K. S. (1981). PS-60: A New Gel-Forming Polysaccharide. In *ACS Symposium Series, Vol. 150* (pp. 111–124). American Chemical Society. https://doi.org/10.1021/bk-1981-0150.ch009

Morris, V. J. (1995). Synergistic Interactions with Galactomannans and Glucomannans. In S. E. Harding, S. E. Hill, & J. R. Mitchell (Eds.), *Biopolymer Mixtures* (pp. 289–314). Nottingham: Nottingham (United Kingdom)

University Press.

Nayak, A. K., Pal, D., & Santra, K. (2014). Tamarind seed polysaccharide-gellan mucoadhesive beads for controlled release of metformin HCl. *Carbohydrate Polymers*, *103*(1), 154–163. https://doi.org/10.1016/j.carbpol.2013.12.031

Nishinari, K., Kim, B. S., Fang, Y., Nitta, Y., & Takemasa, M. (2006). Rheological and related study of gelation of xyloglucan in the presence of small molecules and other polysaccharides. *Cellulose*, *13*(4), 365–374. https://doi.org/10.1007/s10570-005-9041-0

Nitta, Y., Kim, B. S., Nishinari, K., Shirakawa, M., Yamatoya, K., Oomoto, T., & Asai, I. (2003). Synergistic gel formation of xyloglucan/gellan mixtures as studied by rheology, DSC, and circular dichroism. *Biomacromolecules*, *4*(6), 1654–1660. https://doi.org/10.1021/bm034103w

Osorio, F. A., Bilbao, E., Bustos, R., & Alvarez, F. (2007). Effects of concentration, bloom degree, and pH on gelatine melting and gelling temperatures using small amplitude oscillatory rheology. *International Journal of Food Properties*, *10*(4), 841–851. https://doi.org/10.1080/10942910601128895

Picone, C. S. F., & Cunha, R. L. (2011). Influence of pH on formation and properties of gellan gels. *Carbohydrate Polymers*, *84*(1), 662–668. https://doi.org/10.1016/j.carbpol.2010.12.045

Picone, C. S. F., & Cunha, R. L. (2013). Formation of nano and microstructures by polysorbate-chitosan association. *Colloids and Surfaces A: Physicochemical and Engineering Aspects*, *418*, 29–38. https://doi.org/10.1016/j.colsurfa.2012.11.019

Warner, E. L., Norton, I. T., & Mills, T. B. (2019). Comparing the viscoelastic properties of gelatine and different concentrations of kappa-carrageenan mixtures for additive manufacturing applications. *Journal of Food Engineering*, *246*, 58–66. https://doi.org/10.1016/j.jfoodeng.2018.10.033

Yang, J., & Pal, R. (2020). Investigation of surfactant-polymer interactions using rheology and surface tension measurements. *Polymers*, *12*(10), 1–20. https://doi.org/10.3390/polym12102302

5

Encapsulation of α-amylase in polysaccharide gels for controlled release in detergency applications

5.1 Abstract

Automatic dishwashing detergent (ADD) formulations have seldom changed in several decades and offer only rudimentary control over the order and timing of ingredient addition, and often harsh ingredients, such as bleach, can deactivate more sensitive ones, such as enzymes, leading to a loss in cleaning performance. It was investigated whether α-amylase, a key ADD ingredient could be successfully encapsulated into a biopolymer gel, with release triggered once a temperature of 35 – 40 °C is reached. For this purpose, gels based on kappa carrageenan (kC) and low acyl gellan with tamarind seed xyloglucan (LAG/TSX) were tested for their release properties, using spectrophotometry, and structural characteristics, using rheology and texture analysis. It was found that the 0.5% LAG/0.5% TSX and 0.5% LAG/1.5% TSX gels showed the best performance by retaining the α-amylase inside the gel at temperatures below the target temperature but exhibited burst type release when the target temperature was reached. In many cases the addition of α-amylase to the gel altered the rheological properties of the gels by changing the phase angle and storage modulus, however there was no correlation between neither the rheology, nor the textural analysis results with the release profiles. This is purported to be because kC was prone to erosion when placed in the aqueous release medium due to diffusion of counter ions from the gel into the bulk, which prematurely release α-amylase. It is therefore concludable that all the gel formulations were sufficiently resistant to the shear experienced during the release testing to avoid premature break-up.

5.2 Introduction

Biopolymer gels have been used to encapsulate a variety of active ingredients for the purpose of controlled release including flavourings & nutrients (Burey et al., 2008) and pharmaceutical drugs (Kumari, Yadav, & Yadav, 2010) amongst others. The purpose of the encapsulation is to either protect the active ingredient from external conditions, or to alter the release profile of the ingredient such that it is more effaceable, or both. Modification of the release profile could involve extending the time the ingredient takes to fully release compared to a non-encapsulated ingredient, or to delay any release until specific conditions are met, such as time, temperature, or pH. The release mechanism is either governed by diffusion of encapsulated molecules through the gel matrix into the bulk phase or is triggered by the rapid breakdown of a gel network in response to external stimuli.

Biopolymer gels make ideal controlled release vehicles due to their availability, ease of manufacture and having a structure that is strongly dependant on external conditions such as temperature and pH. Gelling polysaccharides originate from plants or other organisms, such as algae, hence resulting in high biocompatibility compared to synthetic polymers (Pal et al., 2009), which cannot be broken down *in vivo*. The gel microstructure can easily be tuned to suit the specific application through choice of biopolymer and the formulation characteristics. Properties such as the melting temperature, mechanical strength and network pore size can be tweaked by altering the formulation. It has been identified in previous published work that there are two formulations which show promising release temperature-

mediated behaviour between 35 and 40 °C, triggered by melting: kappa carrageenan (kC) and low acyl gellan gum (LAG) with tamarind seed xyloglucan (TSX) (Fenton, Gholamipour-Shirazi, et al., 2021; Fenton, Kanyuck, et al., 2021). Further detail on the origin, structure and properties of those polymers can be found in those publications, along with the successful formulations which formed the basis for those used in this study.

Starch is a high molecular weight [10^4 – 10^9 g mol^{-1} (Van Soest, Benes, De Wit, & Vliegenthart, 1996)] carbohydrate that is composed of two polysaccharides: amylose and amylopectin, with the former being mostly linear (α-1,4-glycosidic bonds) and the latter having a high degree of branching (α-1,6-glycosidic bonds). The formation of helical structures in amylose and regularity in the branching of amylopectin causes starch to be semi-crystalline in nature (Kumar et al., 2016). Starches are extractable from a variety of cereal, legume or tuberous sources, such as potato, corn, wheat and rice, with the ratio of amylose to amylopectin varying with its botanical origins, and therefore its resultant properties (Cano, Jiménez, Cháfer, Gónzalez, & Chiralt, 2014; Martens, Gerrits, Bruininx, & Schols, 2018). Starch granules are typically insoluble in water however at elevated temperatures (ca. 70 °C) gelatinisation of starch in water occurs irreversibly through granular swelling and dissociation of the starch double helices (Perry & Donald, 2002), which leads to a rapid and significant increase in viscosity. Therefore gelatinised starch is a very common ingredient in food products as a thickening agent (Ai & Jane, 2015).

α-amylase is an enzyme that breaks down starches in to oligosaccharides through hydrolysis of the α-1,4-glycosidic bonds (Tester et al., 2006). Maltogenic amylase, as used in this study, produces maltose from amylose and amylopectin (Christophersen, Otzen, Norman, Christensen, & Schäfer, 1998; Li et al., 2021). Maltose is a disaccharide and can be further hydrolysed to glucose if maltase enzyme is present. Enzymatic hydrolysis is vital for any process where starch must be degraded due to starch's high resistance to temperature and pH. Additionally, the semi-crystalline nature of starch results in some degree of resistance to enzymatic hydrolysis: as a general rule, the more crystalline in nature, the more resistance starches show to enzymatic hydrolysis (Tester et al., 2006). Gelatinised starch is easier to hydrolyse enzymatically due to its lower crystallinity (Tester et al., 2006).

Commonly α-amylase is added to automatic dishwasher detergent (ADD) to degrade and remove starchy soils during the cleaning process (Olsen & Falholt, 1998). However, the protein-based structure of enzymes are sensitive to changes in temperature, pH, ion concentrations and to the presence of strong chemical oxidising and reducing agents. Hence the oxidising bleaches also found in ADD formulations have been shown to deactivate enzymes upon reacting with the protein structure (Tomlinson & Carnali, 2007), therefore it is advantageous to separate these species, both in storage and in the wash cycle. Current generations of ADD formulations seek to subvert this issue by placing the enzyme(s) and bleach in spatially separate compartments, however there is no mechanism in place to

stop the bleach and enzyme(s) reacting during the wash cycle. Separate encapsulation of the enzymes and bleach in biopolymer gels could potentially allow for precise release tailoring of each ingredient by adjustments to the microstructure of the biopolymer gel.

The aim of this work was to encapsulate amylase enzyme inside a biopolymer gel, composed of either kappa carrageenan (kC) or a combination of low acyl gellan (LAG) with tamarind seed xyloglucan (TSX). The influence of the amylase encapsulation on the structure of the gels was investigated using rheology and texture analysis. The activity of the amylase before and after encapsulation was determined by placing either an amylase solution or amylase-containing gels in a solution of gelatinised starch and monitoring the production of glucose using an assay based on Benedict's reagent: this is a solution which contains, amongst other species, Cu^{2+} ions which gives rise to a blue colour in water. The Cu^{2+} ions are reduced to Cu^{+} by reducing sugars, such as those produced by enzymatic hydrolysis of starch by amylase, which gives rise to a brick-red precipitate. Therefore, the higher the concentration of reducing sugars, the lower the concentration of Cu^{2+} ions, hence the blue colour disappears, which can be monitored using spectrophotometry.

5.3 Experimental

5.3.1 Materials

Kelcogel® F (low acyl gellan gum), and Genugel® CG-130 (kappa carrageenan) were kindly gifted by CP Kelco (USA). Tamarind seed xyloglucan was purchased from Tokyo Chemical Industry (UK). Maltogenic α-amylase, potato starch and sodium carbonate were purchased from Sigma Aldrich (USA). Copper (II) sulphate pentahydrate was purchased from VWR Chemicals. Trisodium citrate dihydrate and maltose monohydrate were purchased from Fisher Scientific. All water used was deionised using a reverse osmosis purification unit (Milli-Q, Millipore®). All materials were used as received without further purification or modifications.

5.3.2 Methods

5.3.2.1 Preparation of gel solutions

Biopolymer powders were weighed (% w/v basis) and were slowly added to a vessel of deionized water at 80 °C under agitation from a magnetic stirrer bar at a moderate speed to avoid clumping. The flask was covered to prevent evaporation and was kept isothermal at 80 °C under agitation for several hours until no powder clumps remained, and the solution was homogeneous. After the biopolymer was dispersed and hydrated, if required, amylase was then added by cooling the gel solution to 50 °C and slowly adding the enzyme under agitation, after which it was stirred for a further hour.

5.3.2.2 Preparation of gel cubes for release and texture analysis

Gel cubes with dimensions 25 mm × 25 mm × 8 mm were formed by pouring 5 g of liquid hot gel solution (50 °C) into each division of a silicone ice cube tray. Evaporation was prevented by covering immediately with plastic film and the cubes cooled to room temperature (20 °C) and were subsequently stored at fridge temperature overnight (2 °C). Before measurement, the gel cubes were allowed to equilibrate to room temperature for one hour.

5.3.2.3 Preparation of Benedict's reagent

Benedict's reagent was formulated based on a modified version of methods previously published (Benedict, 1909; Hernández-López et al., 2020). Copper (II) sulphate pentahydrate (2.73 g), trisodium citrate dihydrate (9.85 g) and sodium carbonate (5.00 g) were added to distilled water (100 mL) and stirred until fully dissolved. The reagent was stored in an air-tight container at room temperature (20 °C) until required.

5.3.2.4 Rheological measurements (oscillatory)

A MCR 302 rheometer (Anton Paar, Austria) equipped with a PP50-TG parallel plate geometry (D = 50 mm) and a P-PTD200/62/TG lower plate geometry (D = 62 mm) was used to characterise the rheology of the samples. In all measurements, samples were loaded in liquid form at 60 °C and trimmed to a gap of 1 mm, with the geometry pre-heated to 60 °C to avoid premature gelation. A thin layer of

silicone oil was immediately added to the outer edge of the samples to prevent evaporation and a Peltier hood (H-PTD-200) was lowered. During all rheological measurements, a constant normal force of 0 N was set, in order to allow the sample gap to increase or decrease in accordance with any volume changes during the measurement.

5.3.2.4.1 Amplitude sweep to determine the linear viscoelastic region (LVR)

Immediately following sample loading and trimming, the temperature of the geometry was lowered from 60 °C to 5 °C, held at 5 °C for 10 minutes and then increased to 20 °C and held at a fixed temperature for a further 10 minutes. An amplitude sweep was performed from 0.01 to 100% strain, at a frequency of 6.28 rad s^{-1} (1 Hz) and a temperature of 20 °C. The linear viscoelastic region was determined as the range of strain values which showed no significant degradation (± 1%) in the value of the storage modulus (G').

5.3.2.4.2 Temperature sweep to determine gelling and melting temperatures

Two temperature sweeps were performed initially from 60 °C to 5 °C, and then back to 60 °C for each sample, in triplicate, with a 5 minute hold at 5 °C between sweeps. The applied strain was 1% as this was found to be within the LVR of the samples and all sweeps were performed at a frequency of 6.28 rad s^{-1} (1 Hz). The exception to this was 2% low acyl gellan, which was instead measured at 0.1%

strain, due to a narrower LVR. The rate of temperature change was 1 °C per minute in all cases.

5.3.2.5 Rheological measurements (viscometry)

A MCR 302 rheometer (Anton Paar, Austria) equipped with a starch stirrer cell (ST24-2D/2V/2V-30/129) and cup geometry (C-CC27/T200/SS) was used to measure viscosity. 35 mL of 1% w/v gelatinised potato starch was added to the rheometer and its temperature was equilibrated at 40 °C. The starch was then sheared at a shear rate of 100 s^{-1} for 10 minutes at 40 °C, and the viscosity was recorded once per minute. After the initial shear step, 350 uL of 1% w/v amylase was added to the starch and a second viscometry measurement was immediately started. As previously, the shear rate was 100 s^{-1}, the temperature was 40 °C and the viscosity was recorded once per minute over a two hour period. This experiment was completed in triplicate, with a fresh sample in each case.

5.3.2.6 Release Measurements

5.3.2.6.1 Preparation of gelatinised starch release medium

A 1% w/v gelatinised potato starch solution was formed by dispersing a known mass of potato starch in a small volume of cold water (approximately a 1:10 ratio of starch to water) under gentle agitation to form a homogeneous dispersion. The requisite remaining mass of water was heated to 90 °C and the starch dispersion

was added to this under gentle stirring. The gelatinised starch solution was then cooled and stored at room temperature overnight until required.

5.3.2.6.2 Amylase activity assay using Benedict's reagent and UV/Vis spectrometry

A 500 g sample of the gelatinised starch solution was added to a 1 L beaker and was placed on a thermostatic hotplate in order to heat the starch to 60, 40 or 20 °C (no heat) under gentle agitation from a magnetic stirrer bar. A custom 3D printed lid was added to the beaker which contained two small holes for sampling and the placement of a temperature probe, and an extending net which went into the starch solution. Once the beaker had stabilised at the desired temperature (± 1 °C) the stirrer speed was set at 500 rpm and the gel cube was gently dropped into the release net. The sugar content of the starch solution at different time points was calculated using a modified version of the method outlined by Hernández-López et al. (2020). A mechanical pipette was used to take 500 µL samples of the starch solution at designated time points. This starch aliquot was added to 1 mL of Benedict's reagent in a 1.5 mL Eppendorf tube, mixed by inverting the tube several times and was submerged in a boiling water bath for 10 minutes. After cooling to room temperature (20 °C), the mixtures were centrifuged at 2400 g for 2 minutes. A 200 µL aliquot of the supernatant was diluted in 1 mL of distilled water, and the absorbance at 720 nm was measured using a Genova Bio UV/Vis spectrophotometer (Jenway, UK). The chosen time intervals to take aliquots from the starch solution were 5, 10, 20, 30, 40, 50, 60, 90 and 120 minutes after adding

the gel cube, alongside a sample of starch solution taken just before the gel cube was added (referred to as "0 minutes"). Each formulation was tested in triplicate.

5.3.2.6.3 Calibration curve for determining sugar equivalent concentrations

In order to convert absorbance values into concentration (maltose equivalents), a calibration curve was used. A stock solution of 100 mg / mL maltose was prepared by dissolving 1 g of maltose in 100 mL of water in a volumetric flask. This was subsequently diluted by varying quantities of water in order to obtain final maltose concentrations of 0 – 10 mg / mL with 1 mg / mL intervals. The samples were processed with Benedict's reagent in an identical manner to the starch aliquots (5.3.2.6.2), and each the absorbance of concentration was measured in triplicate. Absorbance values were plotted against maltose concentration and a linear regression model was used to analyse the data.

5.3.2.7 Texture Analysis

A TA-XT plus texture analyser (Stable Micro Systems, UK) was used to examine the mechanical properties of moulded gels. A 40 mm cylindrical aluminium geometry was used at a constant speed of 1 mm / s, and the trigger force used was 0.1 N. Gel cubes of dimensions 25 mm x 25 mm x 8 mm were prepared as previously described, and the peak force was measured over 5 mm of sample deformation. Each sample was measured five times.

5.4 Results

5.4.1 Calibration curve for determining maltose concentrations

A calibration curve is used for converting the absorbance values measured with UV/Vis spectrometry in to the equivalent concentration of maltose. By formulating known concentrations of maltose in tandem with the previously ascribed method for determining sugar concentration with Benedict's reagent, a relationship between absorbance and maltose concentration can be derived: this is shown in Figure 5.1.

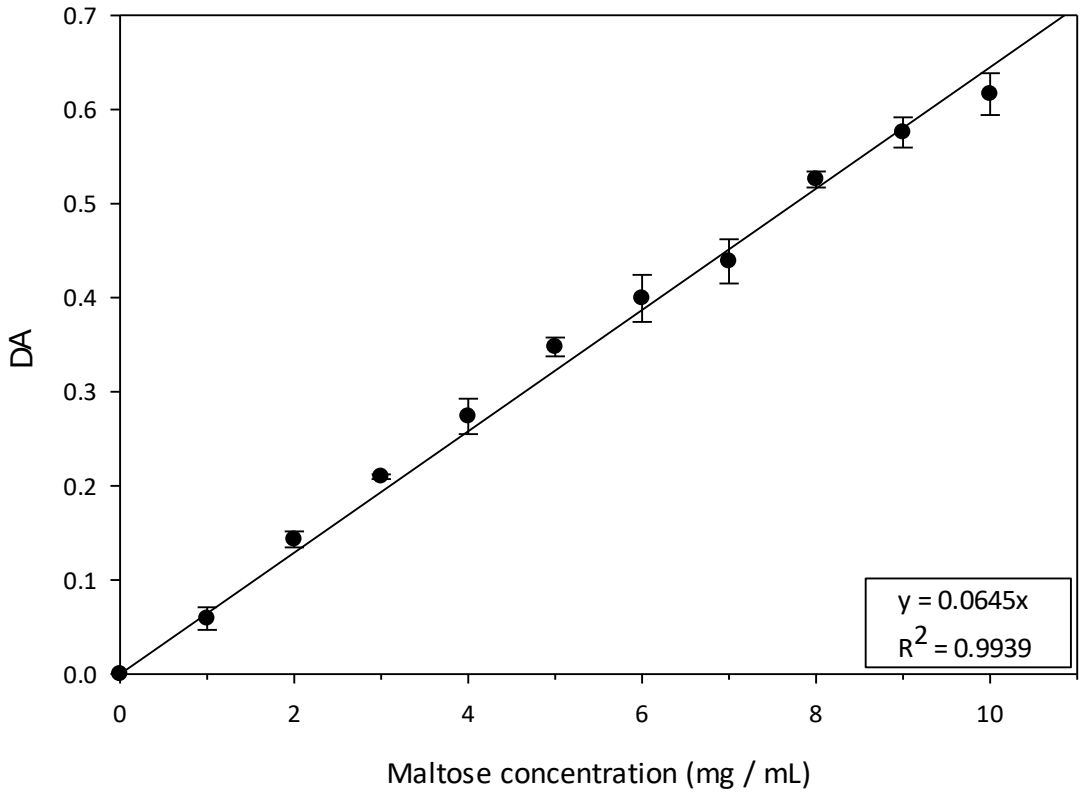

Figure 5.1 - Calibration curve for calculation maltose concentrations from the change in absorbance values (ΔA) obtained using UV/Vis spectroscopy. A linear trendline was fitted to the data, and the associated equation and least-squares value are shown in the bottom-right of the figure.

Due to the fact that the maltose concentration was directly proportional to the disappearance, rather than the appearance of the coloured compound (copper sulphate), there were slight differences between the starting absorbance values, i.e. the absorbance when no maltose was present. Hence, in order to normalise the absorbance data, the change in absorbance (ΔA), was calculated by subtracting the absorbance at a time 't' (A_t) from the initial absorbance (A_0) and additionally the intercept of the trendline was set to 0.

As can be seen from the calibration curve, a linear relationship between the concentration of maltose and the absorbance change was observed. This agrees with previous findings by Hernández-López et al. (2020), who have reported a similarly linear relationship between absorbance and concentration of maltose. Establishing linearity between these two variables is vital in order to correctly analyse data where the concentration of maltose is not initially known, and the absorbance must be converted. Due to the fact that the concentration of starch used in the release experiments was 1% w/v, or 10 mg / mL, provided that mass must be conserved this means that the maximum maltose concentration was 10 mg / mL, hence the entire possible range of maltose concentrations was analysed. All of the absorbance values were $0 < A < 1$, which according to the Beer-Lambert law, ensures that absorbance was directly proportional to concentration.

5.4.2 Comparing amylase activity to concentration

In order to correctly analyse the release profiles from gel-encapsulated amylase, it firstly must be understood what rates of hydrolysis are shown for unencapsulated amylase. Following this, it can then be estimated how much of the enzyme has been released from the gel, and therefore the release mechanisms can be discussed. To this end, different concentrations of amylase were prepared and added to a stirred vessel of 1% w/v gelatinised potato starch, and the change in maltose concentration was measured using UV/Vis spectroscopy. These results are shown in Figure 5.2 and a two-sample T Test was performed to indicate the similarities between different amylase concentrations, and this is shown Table 5.1.

Table 5.1 - Statistical examination of the data presented in Figure 5.2 using a two-sample T test, assuming unequal variances. Each enzyme activity curve at a given temperature was compared to the data at the same temperature with 1% Amylase (the experimental concentration used in later testing). P-value indicates the probability that the data sets are statistically equal. A P-value of 0.05 or less is required to ensure that data sets are significantly different.

Amylase Concentration (% w/v)	**T-Test P-value vs. activity at 1% w/v amylase**		
	20 °C	**40 °C**	**60 °C**
0.1	0.0038	0.011	0.0039
0.5	0.19	0.63	0.24
0.75	0.87	0.87	0.51
2	0.94	0.40	0.86

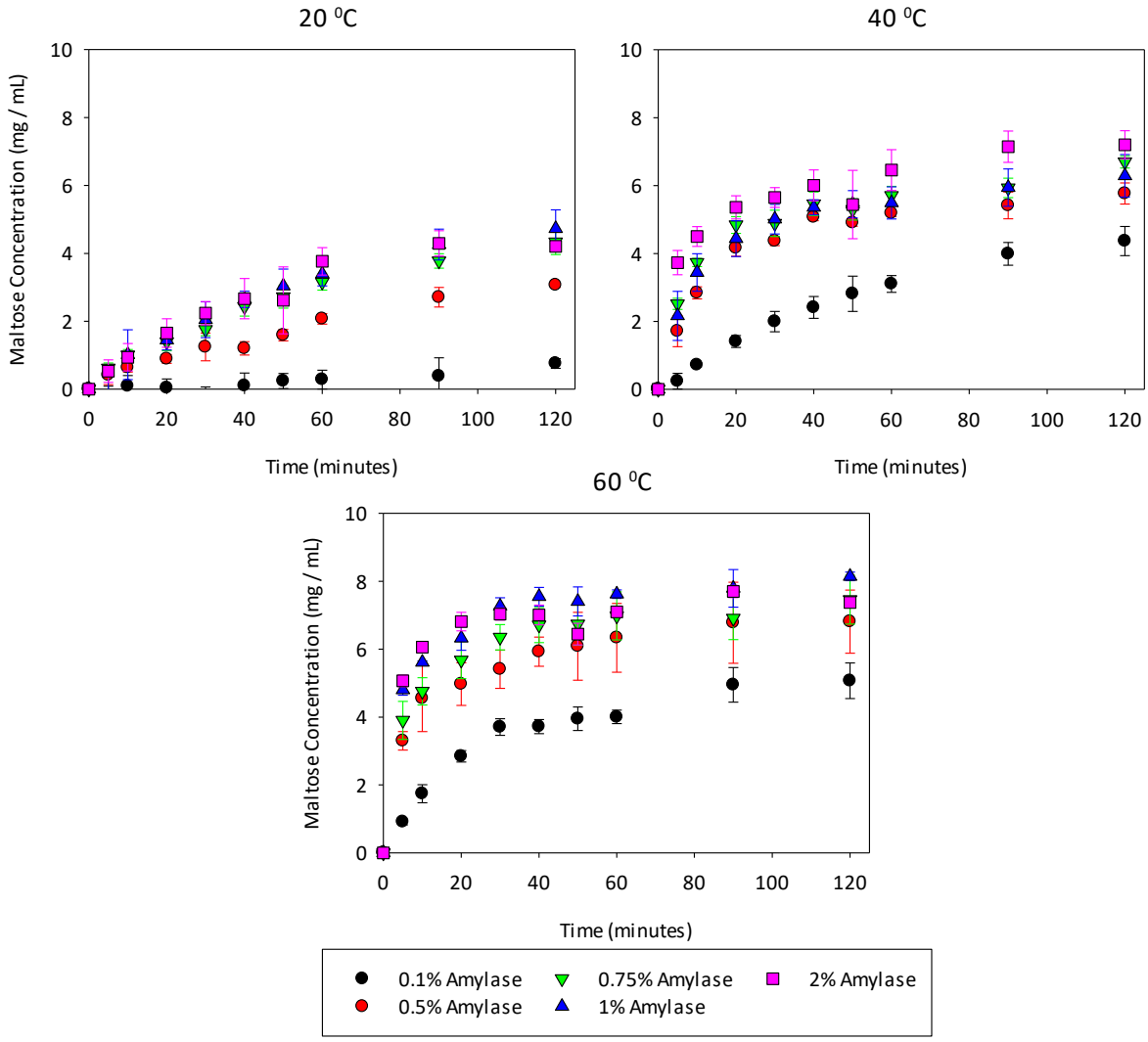

Figure 5.2 - Comparing the relative activities of different concentrations of amylase solutions at temperatures of 20, 40 and 60 °C.

As can be seen from the data in Figure 5.2 and Table 5.1, the hydrolysis profiles resulting from 0.5, 0.75 and 2% w/v amylase concentrations were statistically indistinguishable from 1% w/v amylase, across all three measured temperatures. Hence there was relatively poor sensitivity in the release data when more than 50% of the amylase had been released, as no difference in the release profile would be measured. Comparing 1% w/v to 0.1% w/v amylase, there was a significant

difference ($P \leq 0.05$) in release profiles across all measured temperatures, and this can be seen in Figure 5.2 by the much slower rate of hydrolysis for 0.1% w/v amylase. Attempts were made to adjust various experimental variables such as the volume of gelatinised starch in the release vessel, the concentration of copper sulphate in Benedict's reagent and the subsequent aliquot dilution ratios, however there was no setup where the sensitivity was suitable at amylase concentrations near 0.1% w/v, and 0.5 – 0.75% w/v (data not given). For example, when the volume of starch in the release vessel was increased from 0.5 L to 2 L, this allowed more slightly more separation between 0.5, 0.75 and 1% w/v amylase, however the hydrolysis from 0.1% w/v amylase was reduced to the level that it became undetectable.

5.4.3 Release and activity of amylase from gel formulations

Eight different biopolymers gels were formulated to contain 1% w/v concentration amylase and the activity of amylase was measured over a period of 2 hours. These experiments were performed at temperatures of 20, 40 and 60 °C with a three kC and five LAG/TSX formulations. For use in a detergency application, it would be advantageous to have fully retarded release at 20 °C, but complete release to have occurred between 40 and 60 °C within minutes of exposure to that temperature. The results of the release experiments are shown graphically in Figure 5.3, and data for 1% amylase with no gel is also plotted for reference.

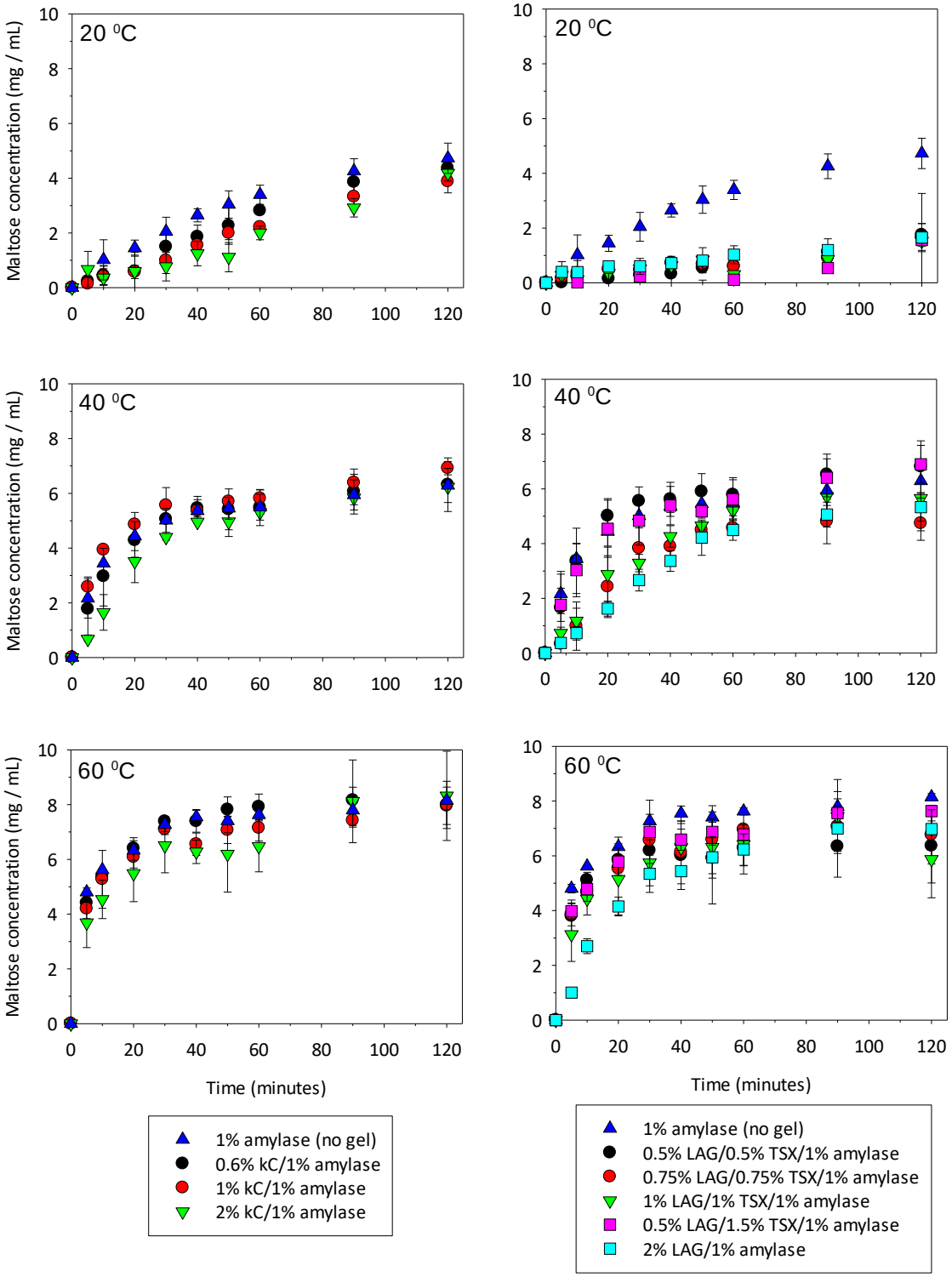

Figure 5.3 - Enzyme activities resulting from hydrocolloid gel encapsulated amylase being placed in a gelatinised starch solution to yield maltose, which was detected using a UV/Vis assay and converted to concentration using a previously produced calibration curve.

Firstly examining the kappa carrageenan gels, at 20 °C the unencapsulated amylase showed the highest activity, followed by 0.6%, 1% and 2% kappa carrageenan in order of decreasing activity. The fact that enzyme activity was seen in all the gels means that amylase was able to escape from the gel, either by diffusion or by erosion. Because the release was slower than unencapsulated enzyme, this indicates that the release of enzyme was retarded to some degree, but not completely. At 40 °C and 60 °C the unencapsulated amylase, 0.6%, 1% and 2% carrageenan gels all showed very similar release profiles, which indicates that the carrageenan was disintegrating rapidly.

For the LAG/TSX gels, markedly different release profiles were observed at 20 °C: none of the gels showed similar activity to the unencapsulated enzyme, as was seen in the kappa carrageenan gels. There was a slight measurable increase in maltose concentration over the two-hour experimental period, and this seemed to be relatively consistent regardless of LAG/TSX formulation. At 40 °C, the 0.5% LAG/0.5% TSX, 0.5% LAG/1.5% TSX and unencapsulated amylase all showed very similar release profiles, indicating the breakdown of the gel formulations was rapid at this temperature. The remaining gel formulations showed measurably slower rates of maltose production, with 2% LAG showing the lowest enzyme activity, indicating that the release of amylase was partially retarded.

At 60 °C, the unencapsulated amylase and all gel formulations showed very similar amylase activities, apart from 2% LAG which displayed measurably lower amylase activity compared to the other formulations. Overall, these release data indicate that the LAG/TSX gels could be more suited to a dishwashing application as much less amylase was able to escape from the gels at lower temperatures.

5.4.4 Oscillatory rheology of biopolymer-amylase gels

5.4.4.1 Determination of gelling and melting temperatures

The gelling (T_g) and melting (T_m) temperatures of the biopolymer gels can be determined by noting the temperature at which the storage modulus (G') and the loss modulus (G'') become equal. This was performed for all gel formulations, with and without the addition of 1% amylase, and the results are shown in Table 5.2.

For the gelling and melting temperatures of the gels without amylase, the values measured agree closely with those published in previous studies (Fenton, Gholamipour-Shirazi, et al., 2021; Fenton, Kanyuck, et al., 2021). For the kC gels, the addition of amylase seemed to have very little measurable impact on the values of both the gelling and melting temperature.

Table 5.2 - Gelling (T_g) and melting (T_m) temperatures of different formulations of kappa carrageenan (kC) and low acyl gellan (LAG)/tamarind seed xyloglucan (TSX) gels, with and without the addition of 1% w/v amylase. Values given are mean averages from three measurements, and the standard deviation was calculated from these and is given as the error.

Formulation	**No amylase**		**With 1% w/v amylase**	
	T_g (°C)	**T_m (°C)**	**T_g (°C)**	**T_m (°C)**
0.6% kC	17.4 ± 0.4	36.4 ± 0.7	16.6 ± 1.1	33.3 ± 1.4
1% kC	21.6 ± 0.2	43.7 ± 0.3	23.9 ± 1.4	43.4 ± 1.9
2% kC	28.1 ± 0.3	51.5 ± 0.2	29.9 ± 0.7	50.5 ± 0.3
0.5% LAG / 0.5% TSX	23.5 ± 0.2	26.6 ± 0.1	32.3 ± 0.4	> 60
0.75% LAG / 0.75% TSX	26.1 ± 0.2	29.4 ± 1.5	34.7 ± 0.8	> 60
1% LAG / 1% TSX	28.3 ± 0.2	30.6 ± 0.3	36.2 ± 0.4	> 60
0.5% LAG / 1.5% TSX	26.6 ± 0.1	29.8 ± 0.1	31.9 ± 0.5	> 60
2% LAG	> 60	> 60	> 60	> 60

In contrast, for the LAG/TSX gels, every formulation showed significant increases in both the gelling and the melting temperatures upon addition of amylase, with the latter showing the largest increases: no LAG/TSX formulation showed evidence of melting below 60 °C upon addition of 1% amylase, whereas without amylase the melting temperatures were relatively low at ca. 30 °C. For 2% LAG, both the gelling and melting temperatures were above 60 °C regardless of the addition of amylase, hence showing the requirement to blend with LAG with an additional species.

In all cases the gel formulations with amylase were opaque and turbid in appearance, and when formulating amylase in water for the release experiments, sedimentation of the amylase happened almost instantly, hence suggesting that at the conditions used in this study the amylase was not fully soluble. As an exception, the LAG/TSX gels were naturally opaque in appearance hence it could not be determined visually if the amylase was soluble. The pH of all the amylase-containing formulations was measured as ca. pH 6 for amylase in water, ca. pH 7 for kC/amylase and ca. pH 5-6 for LAG/TSX/amylase. The isoelectric point for this amylase was not stated by the manufacturer, and was not measured as part of this work. One would expect the solubility of amylase to be strongly dependent on its surface charge, which in turns depends on its ionic environment (pH, concentration of salts) and its isoelectric point. The reported isoelectric points of amylases vary greatly, hence it is not possible to estimate the isoelectric point of this amylase based on previous reported literature.

5.4.4.2 Relationship between phase angle and temperature

In an attempt to replicate the conditions inside a modern dishwasher, the stirrer speed during the release experiments was set to 500 rpm, resulting in a significant shear force on the tablet, such as what would be experienced during a wash cycle. To estimate the release mechanism of amylase from the gels the phase angle of each gel at 20, 40 and 60 °C can be examined. If $\delta > 45°$ then it is likely that release occurred due to melting since liquids have very little resistance to shear, however if $\delta < 45°$ but the release was still rapid, then it is likely that the tablets disintegrated, rather than melted, since break-up happened very quickly whilst the gel was still solid-like. Establishing under what conditions rapid release occurs is vital to formulating controlled release gels. As such, phase angle data from the temperature sweep measurements is shown in Table 5.3 for the different gel formulations at temperatures of 20, 40 and 60 °C.

For ease of comparison, the gel formulations which showed similar amylase activity rates to the unencapsulated amylase are shaded in green. It was measured that all gels which had $\delta > 45°$ showed rapid release behaviour, hence when melting took place then the amylase could be released rapidly, as would be expected. However, there were several formulations, particularly for the LAG/TSX samples, which had $\delta < 45°$ yet still showed rapid release behaviour: for example, at 60°C, 1% LAG / 1% TSX had $\delta = 10°$, yet still showed rapid release behaviour. Rapid release was only seen for LAG/TSX gels when $\delta > 10°$, whereas in kC rapid release was detected when $\delta = 3°$.

Table 5.3 - Phase angle (δ) data of different formulations of kappa carrageenan (kC) and low acyl gellan (LAG)/tamarind seed xyloglucan (TSX) gels, with and without the addition of 1% w/v amylase at temperatures of 20, 40 and 60°C. Values given are mean averages from three measurements, and the standard deviation was calculated from these and is given as the error. Cells shaded in green are samples which displayed rapid release behaviour during the release tests.

Formulation	**No amylase**			**With 1% w/v amylase**		
	$\delta_{20°}$ (°)	**$\delta_{40°}$ (°)**	**$\delta_{60°}$ (°)**	**$\delta_{20°}$ (°)**	**$\delta_{40°}$ (°)**	**$\delta_{60°}$ (°)**
0.6% kC	18.5 ± 2.3	90.0 ± 0.0	90.0 ± 0.0	1.8 ± 1.0	88.5 ± 2.6	89.9 ± 0.1
1% kC	2.3 ± 0.1	11.7 ± 1.1	87.6 ± 3.6	2.0 ± 0.1	8.5 ± 5.3	90.0 ± 0.0
2% kC	2.5 ± 0.0	3.3 ± 0.1	83.6 ± 2.7	2.6 ± 0.0	2.9 ± 0.2	87.1 ± 3.5
0.5% LAG / 0.5% TSX	15.5 ± 0.3	83.4 ± 11.5	86.9 ± 2.8	6.6 ± 0.5	11.8 ± 6.9	30.2 ± 3.2
0.75% LAG / 0.75% TSX	11.0 ± 0.4	67.2 ± 17.1	80.9 ± 8.4	5.2 ± 0.1	6.5 ± 0.6	17.3 ± 5.0
1% LAG / 1% TSX	8.5 ± 0.2	64.6 ± 2.0	83.8 ± 0.9	4.3 ± 0.2	6.2 ± 0.5	10.1 ± 0.9
0.5% LAG / 1.5% TSX	3.9 ± 0.0	77.4 ± 0.5	81.4 ± 1.1	5.8 ± 0.1	20.1 ± 2.2	46.9 ± 10.9
2% LAG	4.6 ± 2.4	2.8 ± 0.9	2.9 ± 0.5	2.0 ± 0.3	1.8 ± 0.4	2.3 ± 0.6

These data indicate that the phase angle was not a useful parameter for predicting release behaviour in either gel system under the experimental release conditions.

5.4.4.3 Relationship between storage modulus and temperature

It is clear from the release profiles and the rheological data that some of the gels, notably the LAG/TSX gels showed rapid release indicative of melting, however the rheological data suggests that melting hadn't taken place as $\delta < 45°$. Therefore, it is possible that some of the gels underwent temperature-induced weakening, which allowed rapid disintegration of the gel at elevated temperatures, without exhibiting a measurable phase change. The fact that the stirrer speed was set to a relatively high speed caused shear on the gel, which may have exploited the temperature-induced weakening. The breakdown of gel structure could be indicated by a drop in storage modulus, therefore the values of the storage modulus of the gels at different temperatures can be analysed in a similar manner to that of the phase angle. These data are shown in Table 5.4.

The addition of amylase to the kC gels caused a significant increase in G', with the greatest increases seen at lower kC concentrations: at 20 °C, the G' of 0.6% kC increased approximately ten-fold, 1% kC increased approximately three-fold and 2% kC approximately doubled. There was a measurable increase in storage modulus in all kC gels at temperatures where $\delta < 45°$.

Table 5.4 - Storage modulus (G') data of different formulations of kappa carrageenan (kC) and low acyl gellan (LAG)/tamarind seed xyloglucan (TSX) gels, with and without the addition of 1% w/v amylase at temperatures of 20, 40 and 60°C. Values given are mean averages from three measurements, and the standard deviation (SD) was calculated from these and is given as the error. Cells shaded in green are samples which displayed rapid release behaviour during the release tests.

Formulation	**No amylase**			**With 1% w/v amylase**		
	$G'_{20°}$ (Pa)	**$G'_{40°}$ (Pa)**	**$G'_{60°}$ (Pa)**	**$G'_{20°}$ (Pa)**	**$G'_{40°}$ (Pa)**	**$G'_{60°}$ (Pa)**
0.6% kC	21.7 ± 9.3	0.06 ± 0.01	0.02 ± 0.02	288 ± 78	0.004 ± 0.007	0.0002 ± 0.0003
1% kC	1090 ± 150	10.2 ± 2.5	0.02 ± 0.03	3190 ± 560	21.7 ± 31.3	0.000013 ± 0.000001
2% kC	17950 ± 960	2840 ± 200	0.22 ± 0.10	32900 ± 3500	4930 ± 1350	0.10 ± 0.13
0.5% LAG / 0.5% TSX	40.6 ± 2.8	0.08 ± 0.06	0.02 ± 0.00	314 ± 22.8	68.2 ± 4.6	5.3 ± 2.1
0.75% LAG / 0.75% TSX	137.6 ± 5.2	0.78 ± 0.77	0.14 ± 0.14	999 ± 111	248 ± 42	30.9 ± 7.0
1% LAG / 1% TSX	394 ± 18	3.1 ± 0.5	0.23 ± 0.04	2930 ± 180	880 ± 98	196 ± 14
0.5% LAG / 1.5% TSX	413 ± 9	1.29 ± 0.06	0.48 ± 0.06	812 ± 54	70.3 ± 15.2	6.4 ± 2.9
2% LAG	3730 ± 400	1680 ± 240	556 ± 86	24600 ± 7200	16100 ± 5900	7420 ± 500

After the gels were heated above their melting temperature ($\delta > 45°$), there was no measurable difference between the storage moduli of gels with and without amylase, which would be expected as the gel structure breaks down upon melting. In the LAG/TSX gels, there was also a significant increase in storage modulus upon addition of amylase: all gels apart from 0.5% LAG/1.5% TSX showed an increase of approximately 7-10X upon addition of amylase at 20 °C. The 0.5% LAG/1.5% TSX sample, however, only showed a doubling in storage modulus upon addition of amylase.

Comparing the values of the storage modulus to the phase angle and release behaviour, in kC it appears that even gels with a relatively large storage modulus can show rapid release behaviour: for 2% kC at 40 °C, the storage modulus was measured at approximately 4930 Pa and the phase angle was approximately 3°, yet it can be seen in the release profile that the production of maltose was very similar to the other formulations. In contrast, for the LAG/TSX gels, it seems that rapid release was only achieved when the storage modulus was below 200 Pa. This observation is analogous to the previous observation that rapid release was only observed when $\delta > 10°$. Both of these findings indicate that rheological measurements are accurate at predicting the release behaviour of LAG/TSX gels, suggesting a release mechanism based on physical disintegration, whereas in the kC gels no such definitive correlations could be found.

5.4.5 Texture analysis of cast gels

Texture analysis is an excellent way of rapidly quantifying the bulk strength of a gel and serves as a complimentary technique to the rheological measurements. The samples were placed underneath a geometry, and the force required to push the geometry through a pre-determined distance into the sample was measured. Hence, texture analysis was performed on all the amylase-containing gels, and the results are shown in Figure 5.4. In all cases, a single peak in the force vs distance trace was observed and the force at this peak was recorded. Each sample was measured five times, and the average peak force and standard deviation was calculated from these.

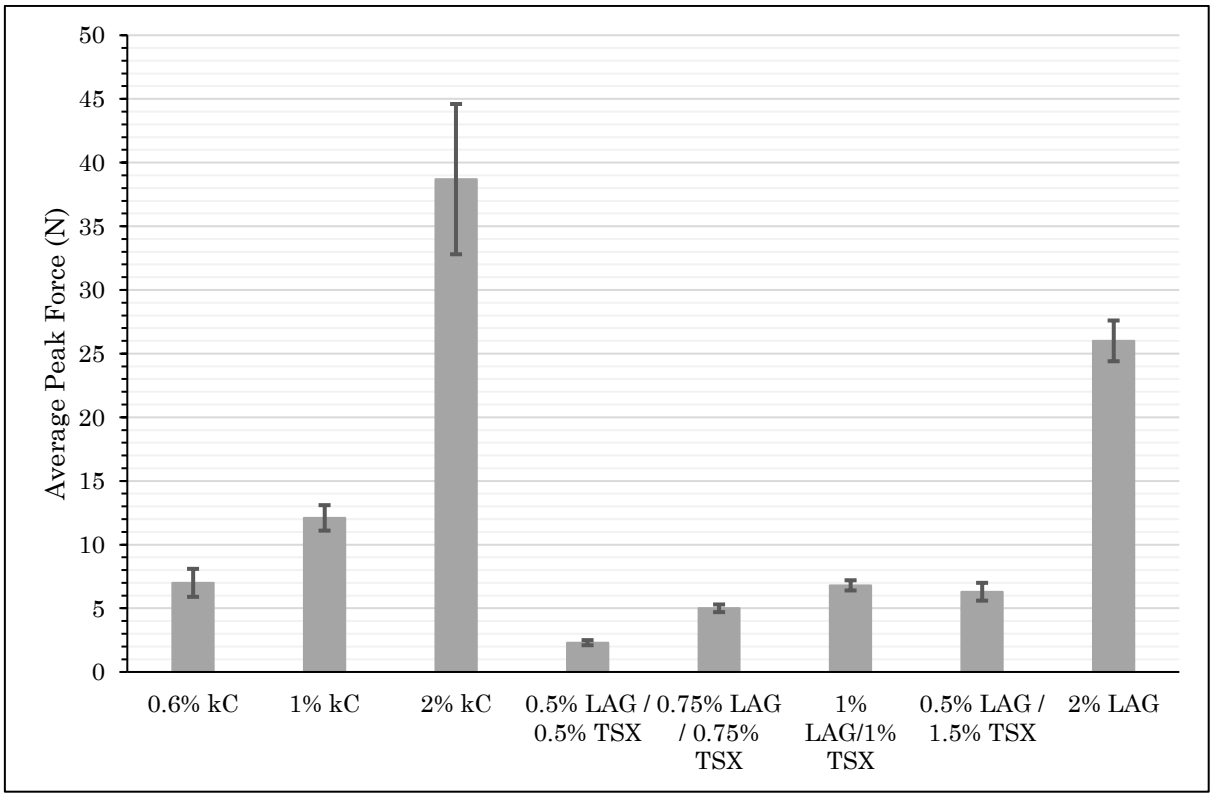

Figure 5.4 - Texture analysis data for gels containing 1% amylase. Displayed values are averages from 5 measurements and error bars show the standard deviation.

For the kC gels, an increase in average peak force was measured as the kC concentration was increased, indicating a firmer gel. This is also indicated by the rheological data through the increase in storage modulus. The same trends are also seen in the LAG/TSX data, with increases and decreases in storage modulus mirroring that of the increases and decreases in the peak force from the textural analysis data. The disadvantage of texture analysis is that it is very difficult to provide temperature control beyond ambient temperature, therefore the texture analysis measurements could not be performed at elevated temperatures in the same way that the rheological measurements were.

5.5 Discussion

The objectives of the work were two-fold: to formulate gel(s) able to release amylase selectively and rapidly at 40 °C, but that contain the amylase at 20 °C, and to understand the effect that amylase has on the structure of the gel(s). Two different hydrocolloid gel formulations were investigated: kappa carrageenan and a mixture of low acyl gellan gum and tamarind seed xyloglucan.

The first step to determining suitable gel formulations was to establish a method for measuring amylase activity. The assay, based on Benedict's reagent, showed enough resolution to tell apart gel formulations that were slowly leaching amylase versus gels which were rapidly melting and releasing all the amylase very quickly. The stipulation for this set of release experiments is that the rapid release of

enzyme due to melting or disintegration must be differentiable from slow enzyme release due to diffusion. Previous work by Kamlow, Vadodaria, Gholamipour-Shirazi, Spyropoulos, & Mills (2021) showed that release of encapsulated active ingredient due to pure diffusion, and diffusion-relaxation from kC occured on the timescale of several hours. In contrast, melting-mediated release from both kC and LAG/TSX gels has previously been shown to reach a maximum in the space of several minutes (Fenton, Gholamipour-Shirazi, et al., 2021; Fenton, Kanyuck, et al., 2021). As can be seen from the release profiles in Figure 5.3, the enzyme works very quickly to hydrolyse the starch after initial release, showing no lag-time even at 20 °C, and a rapid increase in maltose concentration is seen at the first data point (5 minutes). The disadvantage of this experimental setup, and measuring the release of enzymes in general, is that it was difficult to calculate the exact percentage of enzyme release at a given time point. This is because the concentration of maltose at a given time was not simply related to the concentration of amylase at that time, but instead it was related to the amylase concentration profile from the start of the experiment until that time. Performing an alternative assay to calculate the concentration of amylase, rather than the concentration of maltose, would have been possible, however it would not yield any information about whether the activity of the amylase enzyme has been retained after encapsulation and storage. Future studies could include performing a maltose assay and a protein assay in tandem.

The relationship between temperature and the activity of amylase was also interesting in this case: many enzymes are denatured at temperatures of 60 °C, however in this case the activity of amylase appeared to be just as high, if not higher at 60 °C compared to 40 °C. The activity at 20 °C was significantly slower than at 40 and 60 °C, indicating sub-optimal temperatures for the enzyme to operate in.

Once the method for measuring amylase activity was established, amylase was encapsulated inside the gel formulations and the release of enzyme from the gels could be measured. It was found that the kC gels showed limited ability to retain amylase at temperatures below their melting temperature, however the low acyl gellan/tamarind seed xyloglucan gels were much more effective at retaining amylase until the required temperature. Previous studies examining the release of non-ionic surfactant from kappa carrageenan gels have also shown that encapsulated materials are able to "leak" from the gel at temperatures well below the melting temperature (Fenton, Kanyuck, et al., 2021). The mechanism of this leaking was taken to be erosion, resulting from the diffusion of counter-ions from the gel causing the breakdown of the carrageenan gel structure, which relies on counter-ions such as potassium to form the gel structure. This erosion mechanism may explain why the kappa carrageenan gels "leaked" enzyme at temperatures below their melting temperature. Performing measurements such as mercury porosimetry in order to quantify the pore size of these carrageenan gels could have proved a useful addition to examine the mechanism of "leakage".

The rheological data can be compared to the release profiles in order to examine if rheology could be used to understand the release mechanism, and hence predict suitable formulations. It was found that the phase angle was a poor predictor of release behaviour for both kC and LAG/TSX gels, as some gels showed rapid release behaviour without melting. In contrast, the storage modulus was a relatively good predictor of release behaviour for the LAG/TSX: it was estimated for LAG/TSX gels that the onset of rapid release was accompanied by a decrease in storage modulus to < 200 Pa. The action of stirring caused shear on the gel, which may explain why temperature-induced weakening of the LAG/TSX gels, without melting, was sufficient to cause gel disintegration and rapidly release amylase. For the kC gels, even gels with a relatively high storage modulus > 4000 Pa showed rapid release, and this is likely due to the erosion mechanism being essentially independent of the mechanical properties of the gel.

The introduction of amylase to the gels caused a significant shift in the measured rheological properties, with kC showing small reductions in phase angle and small increases in storage modulus (above T_m), but no measurable changes in T_g or T_m. Whereas the LAG/TSX gels appeared to be much more sensitive to the introduction of amylase to the formulation, showing large increases in T_g, T_m, storage modulus and significant reductions in the phase angle. The increases in the melting temperature were such that no melting was detected up to the maximum experimental temperature of 60 °C. However, despite the fact that the LAG/TSX gels did not "melt" after addition of amylase, there was sufficient gel weakening at

elevated temperatures to provide rapid gel disintegration and release of amylase. The structure of LAG/TSX gels is poorly understood, and therefore it is not clear why the addition of amylase caused such a significant shift in the mechanical and thermal properties of the gels, and current research suggests that the structure of the LAG/TSX system is either phase separated or the two polymers are directly bonding (Fenton, Gholamipour-Shirazi, et al., 2021). If the morphology of the LAG/TSX gels was phase-separated, then the addition of amylase could theoretically increase the degree of phase separation and therefore one might expect weakening, rather than strengthening of the gel system. Conversely, for a coupled polymer system, the amylase may be interfering with the ability of the LAG and TSX to couple, hence the gel properties may shift towards that of pure LAG gels. This would result in an increase in storage modulus, gelling temperature and melting temperature and a decrease in phase angle, as shown by the measured rheological values. If amylase was disrupting the coupling between LAG and TSX, it may explain why the 0.5% LAG/1.5% TSX formulation showed smaller magnitude of rheological changes upon addition of amylase, as there was a higher ratio of TSX:LAG therefore it would be more resistant to the introduction of another species to disrupt the structure.

In the texture analysis results it is interesting that some of the LAG/TSX gels appeared to be the mechanically weakest of all gels measured, including all concentrations of kC, yet they were able to retains the α-amylase more effectively at temperatures below T_m compared to kC. Again, this is likely due to the fact that

the kC gels were seemingly more prone to disintegration in solution, which is a result of diffusion of counter ions from the gel rather than the bulk structural properties of the gel.

5.6 Conclusions

It has been shown that biopolymer gel encapsulation of α-amylase is possible, and low acyl gellan gum with tamarind seed xyloglucan was the most promising formulation for the purpose of temperature-mediated controlled release as it showed good retention of α-amylase prior to melting, but significant release upon melting. Future work could build the complexity of the single active ingredient formulation proposed in this work by combining other detergent active ingredients, such as non-ionic surfactant, in the same gel as the α-amylase. Additionally, it may be prudent to examine if there are changes in the gel structure or enzyme activity over time if the formulation were to be industrially adopted.

5.7 References

Ai, Y., & Jane, J. L. (2015). Gelatinization and rheological properties of starch. *Starch/Staerke*, *67*(3–4), 213–224. https://doi.org/10.1002/star.201400201

Benedict, S. R. (1909). A reagent for the detection of reducing sugars. *Journal of Biological Chemistry*, *5*(5), 485–487. https://doi.org/10.1016/S0021-9258(18)91645-5

Burey, P., Bhandari, B. R., Howes, T., & Gidley, M. J. (2008). Hydrocolloid gel particles: Formation, characterization, and application. *Critical Reviews in Food Science and Nutrition*, *48*(5), 361–377. https://doi.org/10.1080/10408390701347801

Cano, A., Jiménez, A., Cháfer, M., Gónzalez, C., & Chiralt, A. (2014). Effect of amylose:amylopectin ratio and rice bran addition on starch films properties. *Carbohydrate Polymers*, *111*, 543–555. https://doi.org/10.1016/j.carbpol.2014.04.075

Christophersen, C., Otzen, D. E., Norman, B. E., Christensen, S., & Schäfer, T. (1998). Enzymatic characterisation of novamyl®, a thermostable α-amylase. *Starch/Staerke*, *50*(1), 39–45. https://doi.org/10.1002/(SICI)1521-379X(199801)50:1<39::AID-STAR39>3.0.CO;2-S

Fenton, T., Gholamipour-Shirazi, A., Daffner, K., Mills, T., & Pelan, E. (2021). Formulation and additive manufacturing of polysaccharide-surfactant hybrid gels as gelatine analogues in food applications. *Food Hydrocolloids*, 106881. https://doi.org/10.1016/j.foodhyd.2021.106881

Fenton, T., Kanyuck, K., Mills, T., & Pelan, E. (2021). Formulation and characterisation of kappa-carrageenan gels with non-ionic surfactant for melting-triggered controlled release. *Carbohydrate Polymer Technologies and Applications*, *2*, 100060. https://doi.org/10.1016/j.carpta.2021.100060

Hernández-López, A., Sanchez Felix, D. A., Sierra, Z. Z., Bravo, I. G., Dinkova, T. D., & Avila-Alejandre, A. X. (2020). Quantification of reducing sugars based on the qualitative technique of Benedict. *ACS Omega*, *5*(50), 32403–32410. https://doi.org/10.1021/acsomega.0c04467

Kamlow, M. A., Vadodaria, S., Gholamipour-Shirazi, A., Spyropoulos, F., & Mills, T. (2021). 3D printing of edible hydrogels containing thiamine and their comparison to cast gels. *Food Hydrocolloids*, *116*, 106550. https://doi.org/10.1016/j.foodhyd.2020.106550

Kumar, R., Kumar, A., Sharma, N. K., Kaur, N., Chunduri, V., Chawla, M., … Garg, M. (2016). Soft and hard textured wheat differ in starch properties as indicated by trimodal distribution, morphology, thermal and crystalline properties. *PLoS ONE*, *11*(1), e0147622. https://doi.org/10.1371/journal.pone.0147622

Kumari, A., Yadav, S. K., & Yadav, S. C. (2010). Biodegradable polymeric nanoparticles based drug delivery systems. *Colloids and Surfaces B: Biointerfaces*, *75*(1), 1–18. https://doi.org/10.1016/j.colsurfb.2009.09.001

Li, J., Li, L., Zhu, J., & Ai, Y. (2021). Utilization of maltogenic α-amylase treatment to enhance the functional properties and reduce the digestibility of pulse starches. *Food Hydrocolloids*, *120*, 106932. https://doi.org/10.1016/j.foodhyd.2021.106932

Martens, B. M. J., Gerrits, W. J. J., Bruininx, E. M. A. M., & Schols, H. A. (2018). Amylopectin structure and crystallinity explains variation in digestion kinetics of starches across botanic sources in an in vitro pig model. *Journal of Animal Science and Biotechnology*, *9*(1), 1–13. https://doi.org/10.1186/s40104-018-0303-8

Olsen, H. S., & Falholt, P. (1998). The role of enzymes in modern detergency. *Journal of Surfactants and Detergents*, *1*(4), 555–567. https://doi.org/10.1007/s11743-998-0058-7

Pal, K., Paulson, A. T., & Rousseau, D. (2009). Biopolymers in Controlled-Release Delivery Systems. In *Modern Biopolymer Science* (pp. 519–557). Elsevier Inc. https://doi.org/10.1016/B978-0-12-374195-0.00016-1

Perry, P. A., & Donald, A. M. (2002). The effect of sugars on the gelatinisation of starch. *Carbohydrate Polymers*, *49*(2), 155–165. https://doi.org/10.1016/S0144-8617(01)00324-1

Tester, R. F., Qi, X., & Karkalas, J. (2006). Hydrolysis of native starches with amylases. *Animal Feed Science and Technology*, *130*(1–2), 39–54. https://doi.org/10.1016/j.anifeedsci.2006.01.016

Tomlinson, A., & Carnali, J. (2007). A Review of Key Ingredients Used in Past and Present Auto-Dishwashing Formulations and the Physico-Chemical Processes They Facilitate. In *Handbook for Cleaning / Decontamination of Surfaces* (Vol. 1, pp. 197–255). Elsevier Science B.V. https://doi.org/10.1016/B978-044451664-0/50006-1

Van Soest, J. J. G., Benes, K., De Wit, D., & Vliegenthart, J. F. G. (1996). The influence of starch molecular mass on the properties of extruded thermoplastic starch. *Polymer*, *37*(16), 3543–3552. https://doi.org/10.1016/0032-3861(96)00165-6

6

Thermoresponsive wax encapsulation of bleaching salts for detergency applications

6.1 Abstract

Encapsulation of small molecular weight molecules can be difficult due to the small pore size requirement, in order to prevent diffusion out of the capsule. Waxes make ideal thermoresponsive capsule materials by having a low porosity, high mechanical strength and well-defined melting and crystallisation temperatures. This work presents two different methods for the manufacturing of wax capsules, using a previously reported moulding method and a novel freeze dropped method. The waxes investigated were soy wax and paraffin wax, and the encapsulated material was sodium hypochlorite bleach solution. The aim was to manufacture capsules which showed little-to-no leakage during storage yet could provide burst-type release at 50 – 60 °C for use in detergency applications. A mass balance was used to determine the encapsulation efficiency, conductivity was used to monitor the storage stability of the wax capsules and the release behaviour and texture analysis was used to quantify the mechanical hardness of the capsules. It was found that both methods could produce capsules with very good storage stability (≤ 1% leakage over 7 days in DI water) however the best performing capsules were the paraffin wax capsules using the freeze dropped method: these showed the least leakage over 7 days, desirable release characteristics and high mechanical hardness.

6.2 Introduction

Automatic dishwashing detergent (ADD) formulations have seldom changed in the past several decades: formulations are either liquid pouches or compressed solids, and contain a mixture of detergency salts, bleaching agent, surfactants and other ingredients e.g. fragrances and colourings (Gambogi et al., 2009). A major innovation to ADD formulations was the introduction of enzymes: lipases, proteases and amylases to enzymatically digest food-based soils, allowing for more effective cleaning. However, the bleaches (sodium hypochlorite or sodium percarbonate), required to clean, sanitise and remove stains from crockery, can deactivate enzymes in storage and during the wash cycle, rendering them ineffective (Chun et al., 1990).

Encapsulation of ingredients is a common approach in many industries including food, pharmaceutical and personal care, for the purpose of altering functionality, improving shelf life or enhancing product safety. It is a simple process during which the active ingredient is 'trapped' within a matrix or inside a barrier material. Large molecular weight species have been successfully encapsulated within biopolymer gels such as carrageenan, gelatine or agar, whose aggregated gel microstructure acts as a 'molecular net' to contain and immobilise the active ingredient. However, the encapsulation of small molecular weight molecules such as salts, using biopolymer gels, can be ineffective due to the pore size in biopolymer gels being orders of magnitude larger than the these small molecular weight

molecules, allowing easy diffusion of the salts out the gel matrix and in to the bulk (Geonzon et al., 2019).

Waxes are organic molecules derived from animal, plant, petroleum or synthetic sources. Waxes differ from other lipids, such as fats and oils, by having two hydrocarbon chains – which are often saturated – joined by an ester linkage. Waxes can be effective for the encapsulation of small molecular weight species due to the dense microstructure formed upon crystallisation, which is much more resistant to diffusion compared to gels or fats (Mellema, Van Benthum, Boer, Von Harras, & Visser, 2006b). Furthermore, waxes go through a thermoreversible phase transition from a crystalline solid to liquid, hence burst-type controlled release can be easily and predictably achieved through melting of the wax at its melting point (Goertz, Demella, Thompson, White, & Raghavan, 2019b).

Goertz et al. (2019) have reported several methods for the production of wax capsules. One such method involved creating spherical paraffin wax capsules in the mm-range using a water-droplet method by where a cold (5 °C) aqueous solution was dropped into a container of molten paraffin wax kept just above its crystallisation temperature, hence, upon addition of the cold aqueous droplet to the wax, this caused the molten wax to crystallise around the cold water droplet forming a shell *in situ*. Also reported in the same work was a templating method by where a wax 'cup' was formed using a mould and stamp, allowing an active

ingredient to be added and subsequently sealed with an additional wax 'lid'. Using these methods, only paraffin wax was tested as a potential shell material, hence it would be prudent to examine if the reported techniques could be extended to other wax materials.

The aim of this work was to encapsulate liquid sodium hypochlorite solution (chlorine bleach) inside thermoresponsive wax capsules made of either paraffin wax or soy wax. The capsules must be able to retain the bleach during storage yet show burst-type release at temperatures of 50 to 60 °C (temperatures relevant for late-stage dishwashing). To this end, three different methods were tested to encapsulate the bleaches: the first two methods were the dropping or moulding methods reported by Goertz et al. (2019). The third method was a novel method, which involved rapidly freezing the active ingredient in liquid nitrogen and placing it in a melted wax solution held just above its melting temperature. The temperature difference between the frozen active ingredient and the wax would lead to rapid wax crystallisation around the active ingredient leading to a hard wax shell forming *in situ*. Differential scanning calorimetry (DSC) was used to determine the melting and crystallisation temperatures of the waxes. Texture analysis (TA) was used to examine the mechanical properties of the resultant wax capsules. The storage stability of the wax capsules was investigated by placing the bleach-containing wax capsules in either distilled water or a salt solution and monitoring the increase in conductivity over a 7-day period, in order to examine the influence of osmotic pressure on the rate of capsule leakage. The wax capsules

were placed in a simulated release environment (hot, stirred distilled water), and the conductivity of the water was used to monitor the release of bleach from the capsules.

6.3 Materials and Methods

6.3.1 Materials

Cargill NatureWax C-3 soy wax (SW) was obtained from Cargill, USA. Paraffin wax (PW) pellets were obtained from Sigma Aldrich, USA. Sodium hypochlorite solution (10 – 15% available chlorine) was obtained from Honeywell, USA. Sodium chloride was obtained from Fischer Scientific, UK. All water used was distilled using a reverse-osmosis Millipore unit. All materials were used as received with no further modifications.

6.3.2 Methods

6.3.2.1 Wax capsules using the cold dropping method (CD)

The sodium hypochlorite bleach solution was placed in the refrigerator at 5 °C overnight. Approximately 150 g of soy wax or paraffin wax was melted in a 250 mL beaker and held a temperature of 65 °C using a thermostatically controlled water bath. Using a pipette, individual drops of the cold sodium hypochlorite solution were made into the hot wax, the capsules were left to form for 10 – 15 seconds and then they were manually removed using a pair of tweezers.

6.3.2.2 Preparation of silicone moulds

To manufacture the moulds, negative casts were designed using Autodesk Tinkercad and printed with a Flashforge Dreamer 3D printer running FlashPrint v3.25.1, using polylactic acid (PLA) filament with the printing parameters listed in Table S7.1. SmoothOn Mold Star 20T, a commercially available silicone rubber was poured around the 3D printed casts, allowed to set for one hour at room temperature and removed. The moulds were designed to produce hollow capsules in the shape of half-spheres with an internal diameter of 22 mm, an external diameter of 30 mm and a shell thickness of 4 mm, giving an internal cavity of approximately 2.8 cm^3. An image of the negative 3D printed moulds are shown in Figure 6.1.

Figure 6.1 - Negative 3D printed moulds required for manufacturing capsules using the moulding method.

6.3.2.3 Wax capsules using the moulding (MM) method

The following method was adapted from Goertz et al. (2019). Silicone moulds and stamps prepared in section 6.3.2.2 were sprayed with Ambersil No-Sil mould release spray to prevent adhesion between the wax and mould. Soy or paraffin wax samples were heated until melted (ca. 80 °C), and ca. 3 g of wax was poured into each cavity of the mould before immediately placing the silicone stamp directly on top of the moulds and leaving to set at 5 °C for one hour. After setting, the stamps

were lifted away from the mould and 2.0 mL of sodium hypochlorite solution was loaded into the wax cavity using a pipette. Additional hot wax (ca. 80 °C) was poured on top of the hollow capsule until the capsule was fully sealed (determined visually by no gaps) and was cooled at 5 °C for one hour before allowing to come to room temperature and removal from the mould.

6.3.2.4 Wax capsules using the freeze dropping method (FD)

Sodium hypochlorite solution was diluted by half with distilled water, and 10 mL of this solution was pipetted into each module of a silicone ice cube tray (dimensions 28 mm x 28 mm x 18 mm) and frozen overnight at -23 °C. A beaker was filled approximately 80 % with soy or paraffin wax and melted in a thermostatically controlled water bath at 65 °C. The frozen bleach cubes were removed from the mould and were submerged in liquid nitrogen for 30 seconds until a uniform white appearance was achieved around the bleach cube. The cubes were removed from the liquid nitrogen and any excess liquid nitrogen on the cube was allowed to evaporate for 10 seconds before carefully lowering the cube into the hot wax bath. The cube was placed on a layer of greaseproof paper in the wax to prevent adhesion between the cube and the glass beaker. The cube was cured in the wax for 90 seconds, after which it was removed from the wax bath, turned upside down and returned to the wax for a further 90 seconds. After the second curing step, the cube was removed from the wax bath and allowed to cool at room temperature.

6.3.2.5 Determining thermal profiles using differential scanning calorimetry

A DSC 25 (TA Instruments, USA) differential scanning calorimeter (DSC) was used to determine the range of melting and crystallisation temperatures of the waxes. A small quantity of wax sample (5 ± 2 mg) was melted and loaded into a sample pan and sealed with a lid. The pan was loaded at 40 °C and heated to 100 °C where it was held at a constant temperature for 5 minutes to ensure the sample was fully melted. To record the thermal behaviour, the pan was then cooled to -20 °C for soy wax or 0 °C for paraffin wax, held isothermally for 5 minutes, before being re-heated to 100 °C. The heating or cooling rate was 10 °C per minute in all cases and an empty sample pan was used in the reference cell. TRIOS software v4.1.1.33073 (TA Instruments, USA) was used to determine the onset, endset and peak temperatures and phase transition enthalpy values. Each sample was measured in triplicate, with a fresh sample in each case.

6.3.2.6 Conductivity measurements for storage stability

Wax capsules previously prepared using either the moulding method (MM) or freeze dropping method (FD) were placed in a container of either distilled water or 15% w/v sodium chloride solution, and the conductivity was recorded using a Mettler Toledo SevenEasy conductivity meter. Conductivity measurements were repeated at intervals of 1, 2, 3, 4 and 7 days after preparation. Samples were stored in sealed containers at room temperature between measurements to prevent evaporation.

6.3.2.7 Conductivity measurements for release behaviour

Once the final conductivity measurement was made, each wax capsule was placed in a beaker of room temperature distilled water/sodium chloride solution with a magnetic stirrer bar. The beaker was then placed in a second larger beaker of water, held at 70 °C using a thermostatic hotplate stirrer. The conductivity probe was inserted into the sample container and the conductivity and temperature of the samples was logged via Mettler Toledo LabX Direct-pH software, which recorded values once per second until it was manually stopped at 65 °C. The stirrer was set to 200 rpm in order to gently agitate the contents of the beaker. Each formulation was tested in triplicate.

6.3.2.8 Hardness analysis of wax samples using TA

A TA.XT Plus Texture Analyser (Stable Micro Systems, UK) was used to characterise the mechanical strength of the wax capsules. Prepared samples were tested in compression mode using a 40 mm cylindrical aluminium plunger (contact area 1256.64 mm^2). Moulded samples were compressed by 7 mm and freeze dropped samples were compressed by 9 mm, both at a speed of 1 mm s^{-1}. Hardness was estimated using the peak force, and each measurement was made in at least triplicate. Capsules were made one day prior to testing were stored at room temperature overnight in sealed containers until testing.

6.4 Results and discussion

6.4.1 Differential scanning calorimetry

Recording the thermal behaviour of the wax used in the capsules is useful in order to determine the melting temperature range, and consequently the release temperature of the capsules. Additionally, it can be used to optimise capsule processing temperatures, and the enthalpy values can be used to understand the mechanical properties of the capsules – typically a higher enthalpy of crystallisation indicates more extensive wax crystallisation and hence a mechanically harder capsule. To this end, the thermal behaviour of paraffin wax and soy wax were measured using DSC and the results are tabulated in Table 6.1. Graphs of the thermograms for each wax are given in Figure 6.2 and Figure 6.3.

Melting of both waxes gave a melting thermogram with two endothermic peaks, and took place over a relatively wide temperature range of approximately 20 to 60 °C, and as can be seen from the DSC thermograms. The size of this range can vary depending on the wax sample: the melting of soy wax occurred over a ca. 30 °C range, whereas for paraffin wax the range was ca. 35 °C. This broadness in the range of melting temperatures was likely due to both of the waxes being composed of a mixture of organic molecules with different chain lengths, hence different melting points, rather than a single molecular type with a well-defined melting temperature.

Stating the melting temperature as a range of values with a span of 30 °C is not particularly useful when attempting to predict melting-mediated release mechanisms, as delivery of the active ingredient at a precise, predictable temperature was the primary objective. Hence one can use the values of T_{peak}, the temperature at which the heat flow was the highest, as a first approximation for a single melting point of the waxes. During heating, both paraffin wax and soy wax had 50 °C ≤ T_{peak} ≤ 60 °C, which was the criteria set out for an ADD formulation. Soy wax had a T_{peak} value approximately 5 °C lower than paraffin wax. Furthermore, the enthalpies of crystallisation and melting were approximately 2-3 times larger in paraffin wax compared to soy wax. Hence, it could be presumed that paraffin wax has a higher degree of crystallinity compared to soy wax: this can be inferred from the cooling thermogram, as any signal during the cooling step was due to wax crystallisation. This greater degree of crystallinity is an initial indicator that paraffin wax may be a harder material compared to soy wax, and therefore more resistant to breakage: this will be examined in greater detail in the texture analysis measurements.

Table 6.1 - DSC parameters obtained for soy wax and paraffin wax. T_{onset} and T_{endset} were calculated based on the intersection point between the baseline and the peak gradient. T_{peak} was the temperature at which the heat flow was at its maximum/minimum value depending on whether the wax was being cooled/heated respectively. Enthalpy values were obtained through integration of the thermogram and were normalised to the mass of sample. Mean average values from three measurements are given alongside the standard deviation (SD).

	Parameter	Soy Wax		Paraffin Wax	
		Average	SD	Average	SD
Cooling (crystallisation)	T_{onset} / °C	45.1	0.3	53.6	0.1
	T_{peak} / °C	15.7	0.1	50.7	0.4
	T_{endset} / °C	5.8	1.2	33.8	0.3
	ΔEnthalpy / J g^{-1}	72.5	4.3	178.0	25.4
Heating (melting)	T_{onset} / °C	19.1	0.5	24.9	2.0
	T_{peak} / °C	50.1	0.3	54.9	0.3
	T_{endset} / °C	52.7	1.0	58.5	0.7
	ΔEnthalpy / J g^{-1}	85.1	6.7	177.8	24.4

During the cooling thermograms of the waxes, T_{endset} is an important parameter as it will determine what temperatures the waxes must be cooled to in order to return to its maximum crystallinity. For soy wax this value was relatively low (ca. 5°C) compared to paraffin wax (ca. 34 °C), which from a practical standpoint means that soy wax must be cooled in a refrigerator to 'set' fully, however room temperature curing is sufficient for paraffin wax. The T_{peak} value during cooling for soy wax (ca. 15 °C) was much smaller than paraffin wax (ca. 50 °C), which further suggests that most of the crystallisation in soy wax occurs at temperatures below typical room temperatures.

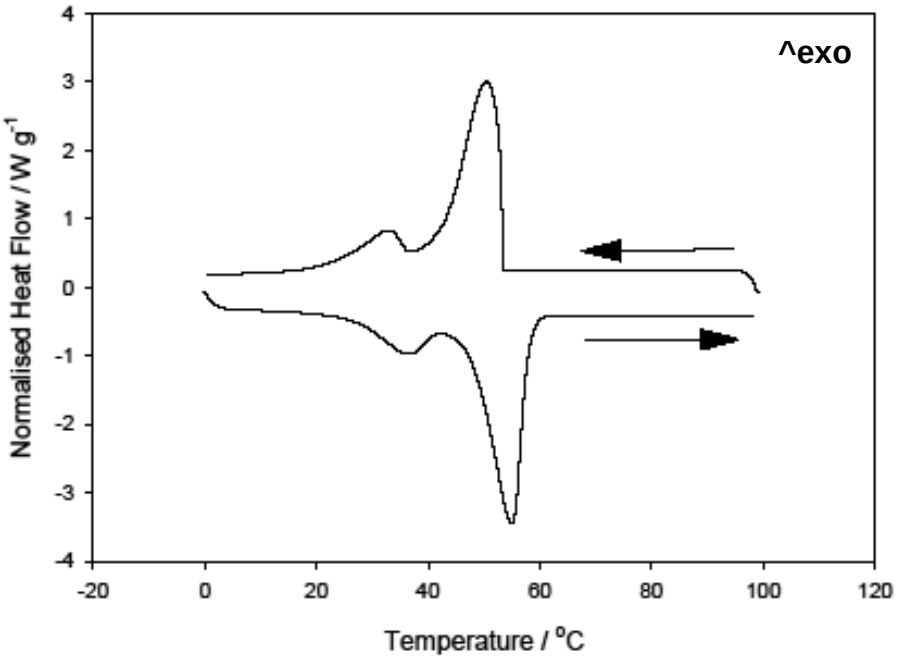

Figure 6.2 - DSC thermogram of paraffin wax. The direction of the arrows indicates cooling or heating.

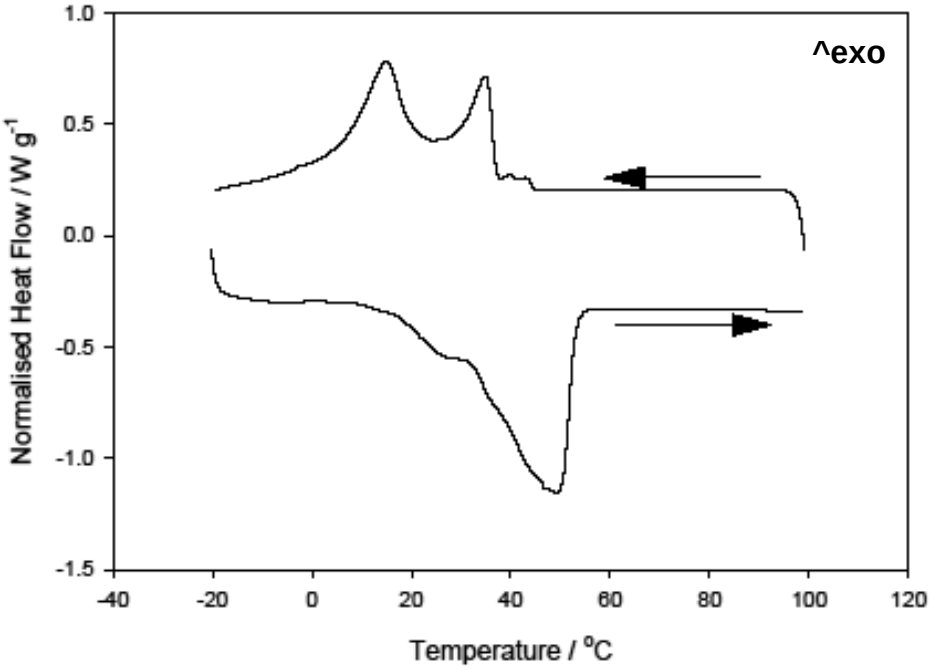

Figure 6.3 - DSC thermogram of soy wax. The direction of the arrows indicates cooling or heating.

From the DSC results, the optimum wax capsule manufacturing temperatures can be determined: once melted, the waxes must be kept slightly above T_{onset} (measured during the cooling step), to avoid premature wax crystallisation, and after capsule production the waxes must reach a minimum temperature of T_{endset} (measured during the cooling step) to ensure full wax recrystallisation. For soy wax these temperatures were 45.1 and 5.8 °C respectively, and for paraffin wax these temperatures were 53.6 and 33.8 °C.

6.4.2 Manufacturing of wax capsules – cold drop method (CD)

Manufacturing capsules using the cold drop method involved dropping cold aqueous droplets into a hot wax solution, held just above its T_{onset} temperature, determined during the cooling measurement of the waxes using DSC. Wax capsules formed with sodium hypochlorite solution and soy wax/paraffin wax using the cold drop method are shown in Figure 6.4.

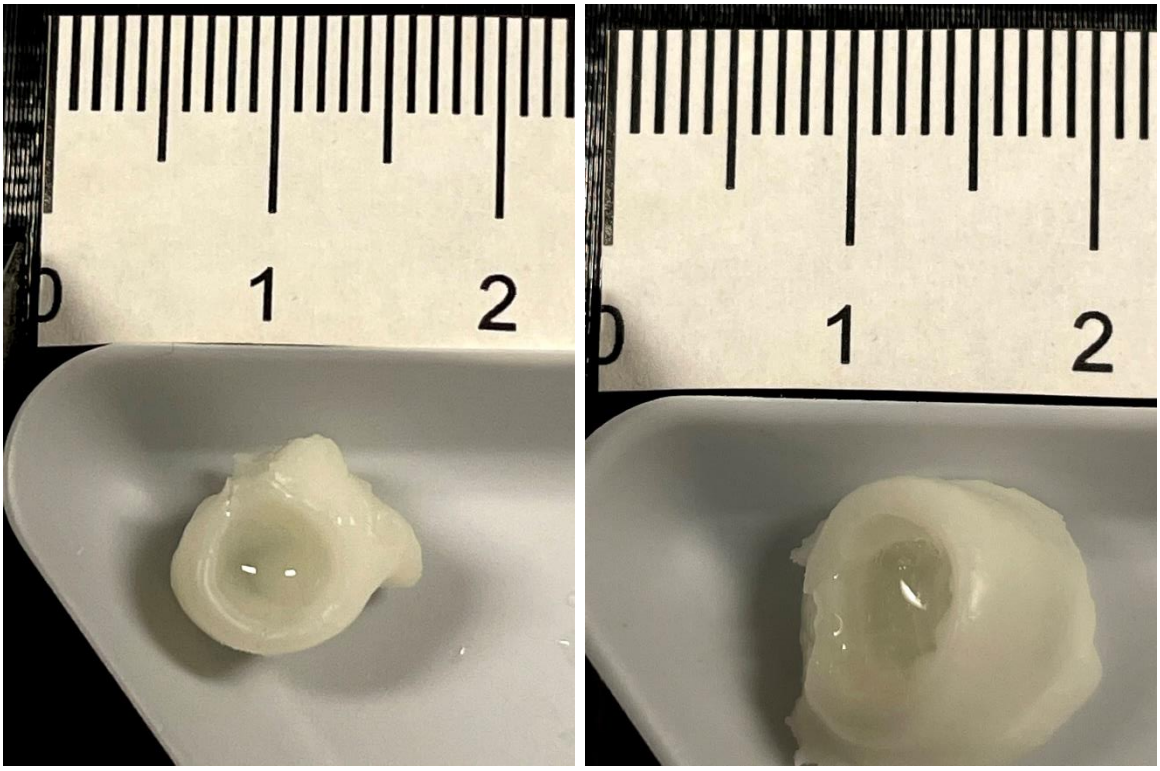

It was found that the cold drop method was not successful at manufacturing sealed wax capsules in this study – as shown by the large void in the top of each of the samples. It was found that the rate of sinking of the bleach droplet through the

wax solution was slower than that of pure water. This slow rate of sinking resulted in the sample failing to seal on the top, as it had cooled down too much to crystallise the wax by the time the whole droplet was submerged. The issue was apparent for both the soy wax and paraffin wax tests. It is interesting that the rate of sinking was slower in concentrated bleach solution compared to water, as the density is much higher in bleach solution (ca. 1.2 g / mL) compared to water (ca. 1.0 g / mL). It is possible that the surface tension was much lower in the bleach solution, hence creating a more 'wetted' droplet on the wax surface (with higher surface area) that experienced more drag when sinking through the melted wax. However, a more detailed investigation including additional trials and tensiometric measurements would be required to confirm this.

6.4.3 Manufacturing of wax capsules – moulding method and freeze dropping method

Manufacturing capsules using the moulding method involved forming a hollow 'shell', filling with bleach solution and then sealing with an additional 'lid'. The freeze dropping method required forming frozen cubes of bleach solution, which were super-cooled in liquid nitrogen before being submerged in hot wax solution where the shell was formed *in situ*. Examples of capsules made with both of these methods is shown in Figure 6.5.

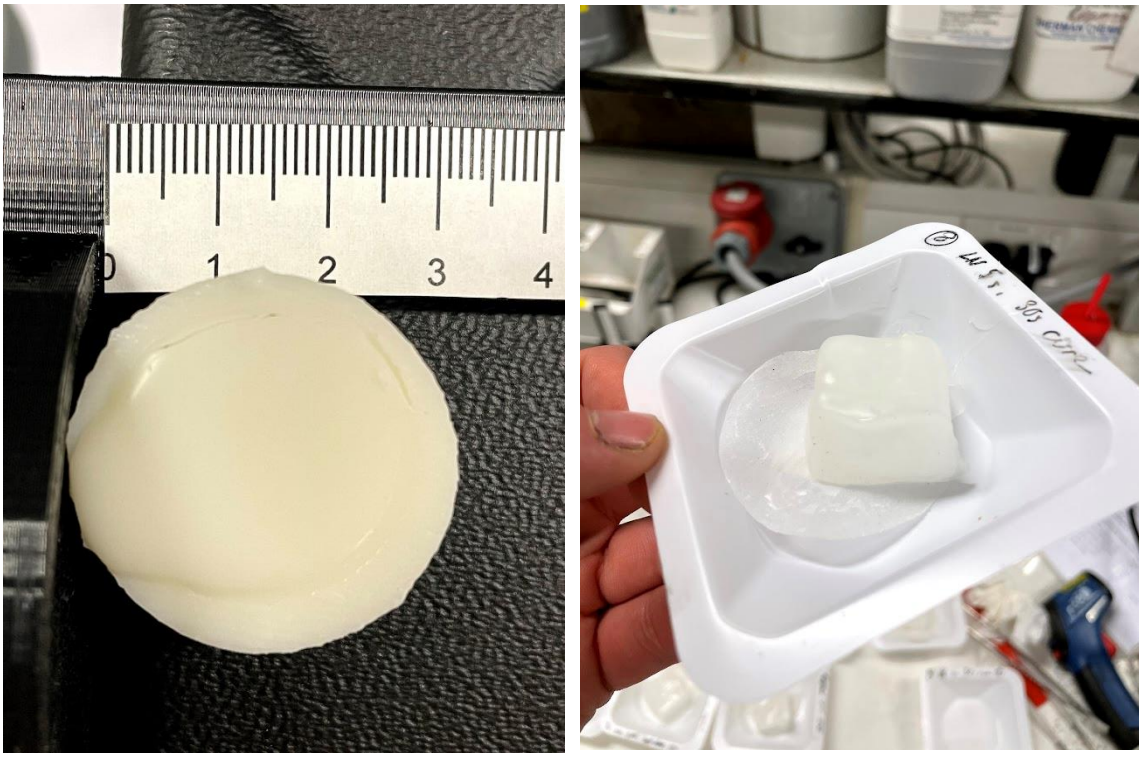

In practice, both methods were successful at manufacturing wax capsules. The moulding method produced sealed bleach-containing capsules with both soy wax and paraffin wax, however the freeze dropping method was only able to produce sealed capsules with paraffin wax. The soy wax capsules produced using the freeze dropping method had defects consisting of large voids in the underside of the wax shell, as the soy wax tended to adhere to the greaseproof paper during manufacturing, which made consistent production of soy wax capsules using this method unobtainable. An example of the defects produced by soy wax capsules using the freeze dropped method is shown in Figure 6.6.

Figure 6.6 - A defective soy wax capsule manufactured using the freeze dropped method. Scale is in centimetres.

The encapsulation efficiency [EE(%)], can be calculated the gravimetric ratio of encapsulated material to the mass of the entire capsule, and as shown Equation 6.1. These encapsulation efficiency results are shown in Table 6.2 for the capsules produced using the freeze dropped and moulding methods. The mass of encapsulated bleach was consistently 2.2 g for the MM capsules, and 10.9 g for the FD.

$$\mathrm{EE}(\%) = \frac{\text{mass of encapsulated bleach (g)}}{\text{total mass of final capsule (g)}} \times 100\% \qquad (6.1)$$

Table 6.2 - Encapsulation efficiency (EE) of wax capsules manufactured using the moulding or freeze dropping method. Mean values were calculated using Equation 1 from at six separate formulations and the standard deviation (SD) was calculated.

Manufacturing Method	**EE (%) ± SD**	
	Paraffin Wax	**Soy Wax**
Moulding Method (MM)	33.7 ± 1.8	30.5 ± 1.0
Freeze Dropping Method (FD)	48.2 ± 3.6	N/A

As can be seen from the EE(%) results, the freeze dropping method was more efficient than the moulding method, as less wax was used to carry out the encapsulation compared to the mass of encapsulated bleach. Goertz et al. (2019) did not report the encapsulation efficiency in their work, hence no direct comparison of efficiency can be made by other authors using the same encapsulation method. Olson (1989) patented the encapsulation of enzymes with a bleach deactivating substance at an encapsulation efficiency of 50 to 80 wt%, however this controlled-release mechanism relies on bleach being released *before* enzymes, which theoretically would be less effective than the converse ordering of release, as enzymes are sensitive to the high temperatures experienced towards the end of a wash cycle. Milanovic et al. (2010) developed a method for *in situ* encapsulation of vanillin, a hydrophobic food flavouring, using an emulsion method with carnauba wax, and was able to achieve an encapsulation efficiency of approximately 87%, however, as bleach is not soluble in melted wax (whereas

vanillin is), this technique would not be effective for bleach encapsulation. Mellema et al. (2006) reported on methods for wax encapsulation of water-soluble compounds using various techniques, and it was reported that at least 40% of the capsule must be wax in order to make the capsule rigid enough to withstand osmotic pressure, giving the capsules a maximum encapsulation efficiency of 60%.

6.4.4 Conductivity measurements

6.4.4.1 Storage stability

Conductivity was an ideal method for detecting any bleach leakage from the capsules, as sodium hypochlorite is a strong base (it fully dissociates in water into its constituent ions), causing an increase in the measured conductivity. Previous work by Mellema et al. (2006) has purported that leakage from wax capsules can occur due to a high osmotic pressure difference between encapsulated salt and an outer aqueous environment, which leads to crack formation in the wax structure. To this end, the storage stability of wax capsules in both distilled water and 15% w/v sodium chloride solution was tested – the former storage test leading to a high osmotic pressure difference, and the latter resulting in a lower osmotic pressure difference, due to the high concentration of sodium ions. If there was a significant difference between storing capsules in each medium, this suggests that osmotic pressure was at least partially responsible for salt leakage. The conductivity of the storage was logged over a period of 7 days and the results are shown in Figure 6.7, Figure 6.8, Figure 6.9, and Figure 6.10. After 7 days in storage, the capsules and the storage solution were heated so that the capsules melted and all the

encapsulated bleach was released. This was necessary to determine how much bleach was left in the capsule, and also served the purpose of examining the release behaviour of the capsules. The release data is discussed in section 6.4.4.2. The percentage of capsule leakage CL (%) was calculated using Equation 6.2. Calculation of capsule leakage relies on measuring the conductivity at a given time (σ_t) knowing the final conductivity after the release test (σ_{final}).

$$\text{CL}\ (\%) = \frac{\sigma_t}{\sigma_{final}} \times 100\% \qquad (6.2)$$

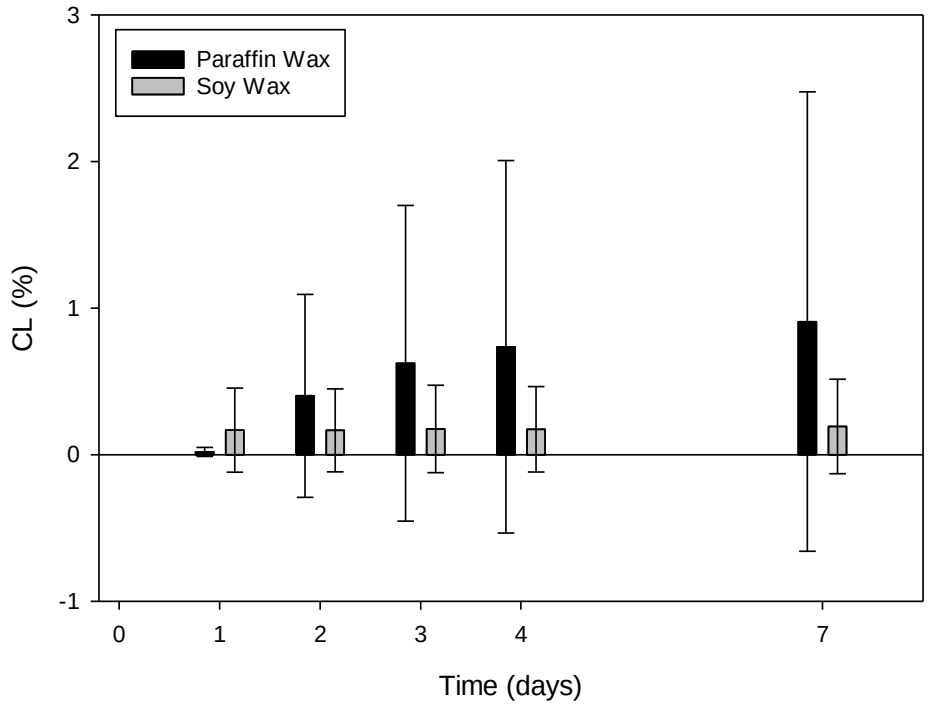

Figure 6.7 - Storage stability of paraffin wax and soy wax capsules containing sodium hypochlorite bleach, manufactured using the moulding method and stored in distilled water over the space of 7 days. Data is mean average from three measurements and error bars are standard deviation.

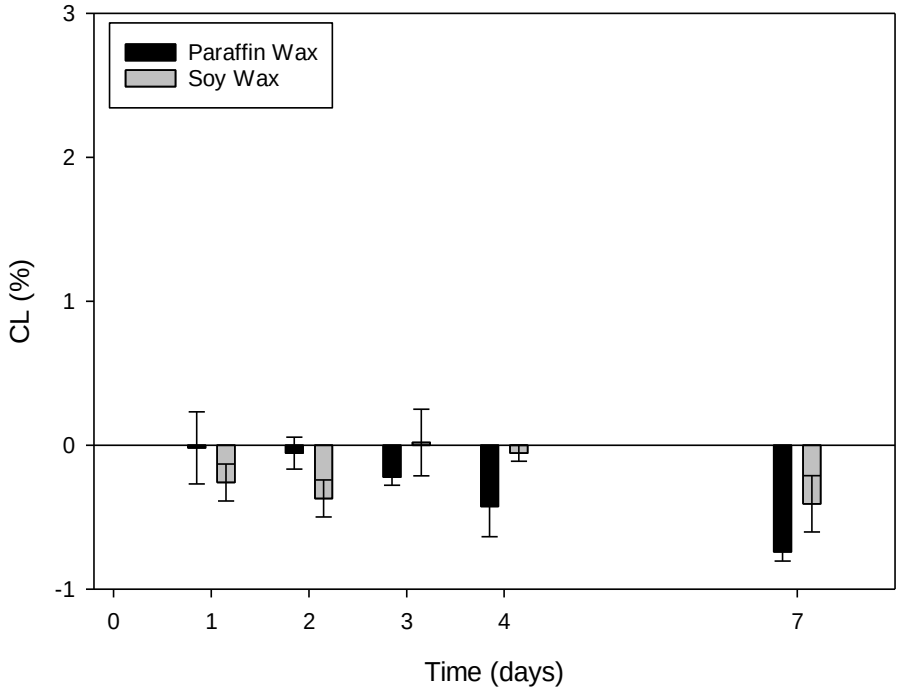

Figure 6.8 - Storage stability of paraffin wax and soy wax capsules containing sodium hypochlorite bleach, manufactured using the moulding method and stored in 15% NaCl solution over the space of 7 days. Data is mean average from three measurements and error bars are standard deviation.

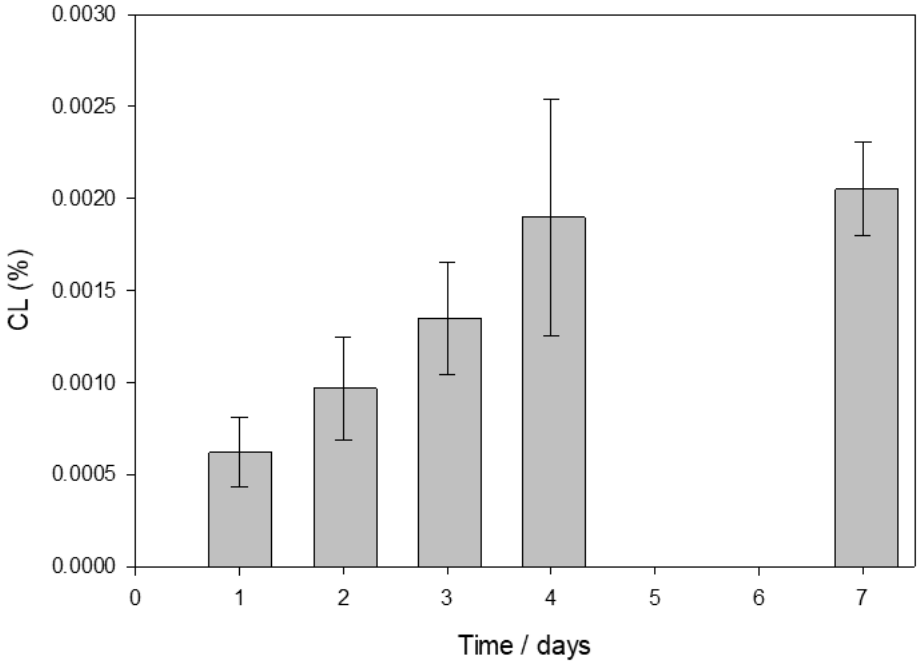

Figure 6.9 - Storage stability of paraffin wax capsules containing sodium hypochlorite bleach, manufactured using the freeze dropped method and stored in distilled water over the space of 7 days. Data is mean average from three measurements and error bars are standard deviation.

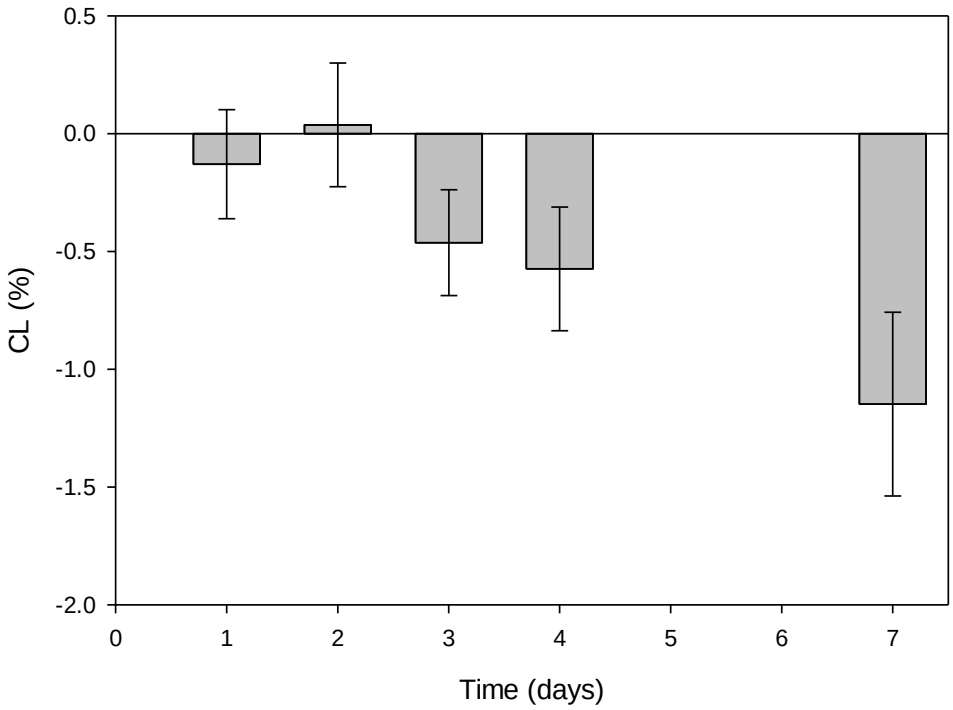

Figure 6.10 - Storage stability of paraffin capsules containing sodium hypochlorite bleach, manufactured using the moulding method and stored in 15% NaCl solution over the space of 7 days. Data is mean average from three measurements and error bars are standard deviation.

The storage stability of the moulded paraffin wax and soy capsules are given in Figure 6.7 and Figure 6.8. Over a period of 7 days, both capsules showed relatively good retention of bleach, showing only 1 – 3 % leakage on average over this time period. The same capsules stored in 15% NaCl solution showed a slight measured decrease in conductivity over the 7 day storage period. This indicates that very little-to-no bleach leaked from the capsules. The loss of conductivity could be due to slight recrystallisation of the salt from the saturated solution. Hence, these data indicate that osmotic pressure was a major driving force for leakage of bleach from

the moulded capsules, however the capsules showed good bleach retention, even in distilled water.

The storage stability data for the freeze dropped paraffin wax capsules are given in Figure 6.9 and Figure 6.10. Both of the storage experiments for the freeze dropped capsules showed that these capsules had improved stability compared to the moulded capsules: even when stored in water, the freeze dropped capsules leaked approximately 0.002% of its bleach over a 7-day period (essentially negligible given the accuracy of the measurement instrumentation), compared to 1 – 2% for the moulded capsules. For the freeze dropped capsules stored in 15% NaCl, a decrease in conductivity was seen, similar to that of the moulded capsules, hence it can be assumed that very little-to-no bleach was prematurely released from these capsules. It is not possible to definitively state the mechanism of leakage from the freeze dropped capsules were, as the leakage was so small to the point where it was practically negligible, however the osmotic pressure difference may have produced slight cracks in the wax microstructure which allowed diffusion of bleach. From these storage stability profiles, it can be stated that the freeze dropped method developed in this work produced capsules that were better sealed than those using the moulding method, as shown by the much slower rate of leakage during storage, and additionally the encapsulation efficiency was higher. The freeze dropped tablets may have been more effective at containing the bleach due to the fact that the manufacturing process forms the entire wax shell *in situ*, whereas for the moulding method it must be manufactured in two halves –

an initial hollow 'cup' followed by a 'lid'. It is estimated that the join between the 'cup' and the 'lid' for capsules produced using the moulding method was the primary escape route for the encapsulated bleach, as it would be very difficult to produce a seal between that is good enough to completely prevent the diffusion of such a small molecular weight molecule as bleach.

6.4.4.2 Release characteristics

Increasing the temperature of the capsules and logging the change in conductivity of the surrounding medium was used for examining the release characteristics of the capsules. The temperature(s) at which increases in conductivity are seen and the magnitude of the increase in conductivity indicated the melting point of the wax capsules. These data were recorded for moulded and freeze dropped paraffin wax/bleach capsules stored in water, and for moulded soy wax/bleach capsules stored in water, and the release graphs are shown in Figure 6.11, Figure 6.12, and Figure 6.13. Also included on the release graphs is the DSC melting curve for the wax used in the capsule, in order to examine if DSC was a good predictive tool for determining release temperature from these capsules.

It can be seen from the release curves that all three capsules exhibited temperature-mediated burst-type release, as shown by the large spike in release % (conductivity) at a temperature close to the melting temperature of the wax. The release % (conductivity) showed an initial large spike followed by a rapid drop and levelling off: this is simply because it took a few seconds for the bleach to become

evenly dispersed after release, so the conductivity probe, which was located near the wax capsules, gave an anomalously high conductivity reading until all the bleach become evenly dispersed.

For the moulded capsules, the release spike overlapped with the melting peak in the DSC thermogram, with the paraffin wax capsules showing burst release at approximately 57 °C, and the soy wax at approximately 51 °C. Hence, either capsule fulfils the aim originally set out for this work: to achieve burst-type release via a melting mechanism between a temperature of 50 – 60 °C. It can be assumed that the release occurred via melting as the release peak was very sharp, indicating a sudden breakdown of the capsules, and the location of the release spike was overlapping with the melting thermogram.

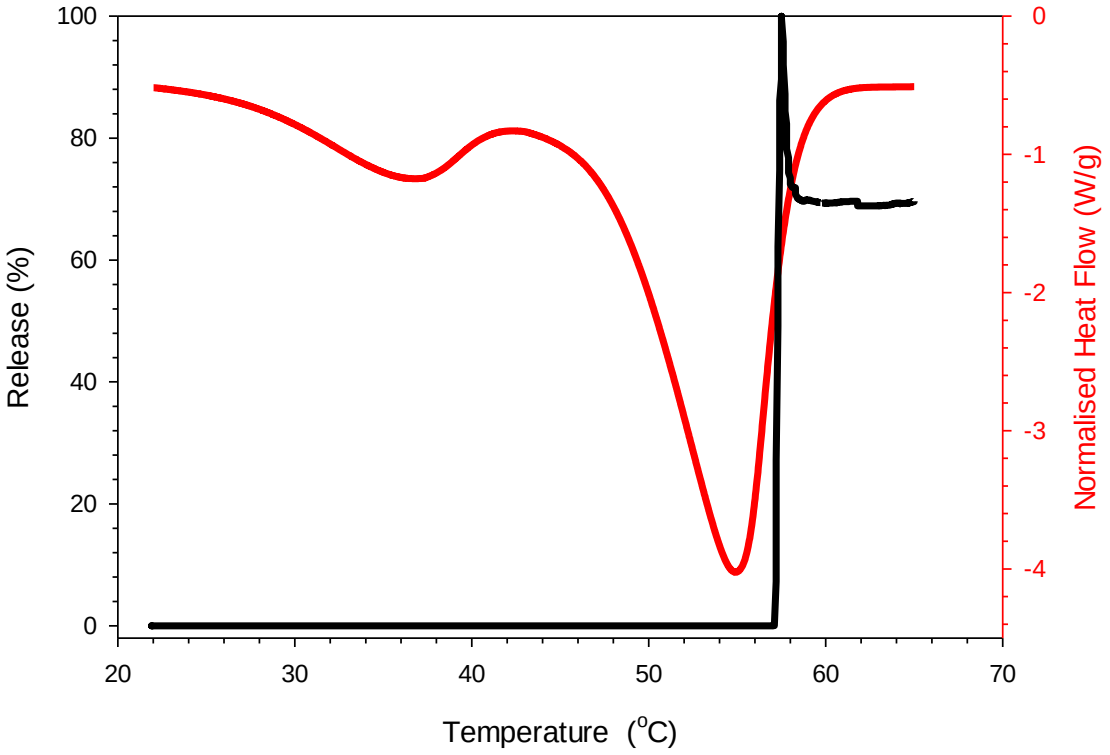

Figure 6.11 - Release curve of bleach from moulded paraffin wax capsules, stored for 7 days in DI water (black) alongside the DSC thermogram of paraffin wax melting (red). Data plotted are mean averages from three measurements.

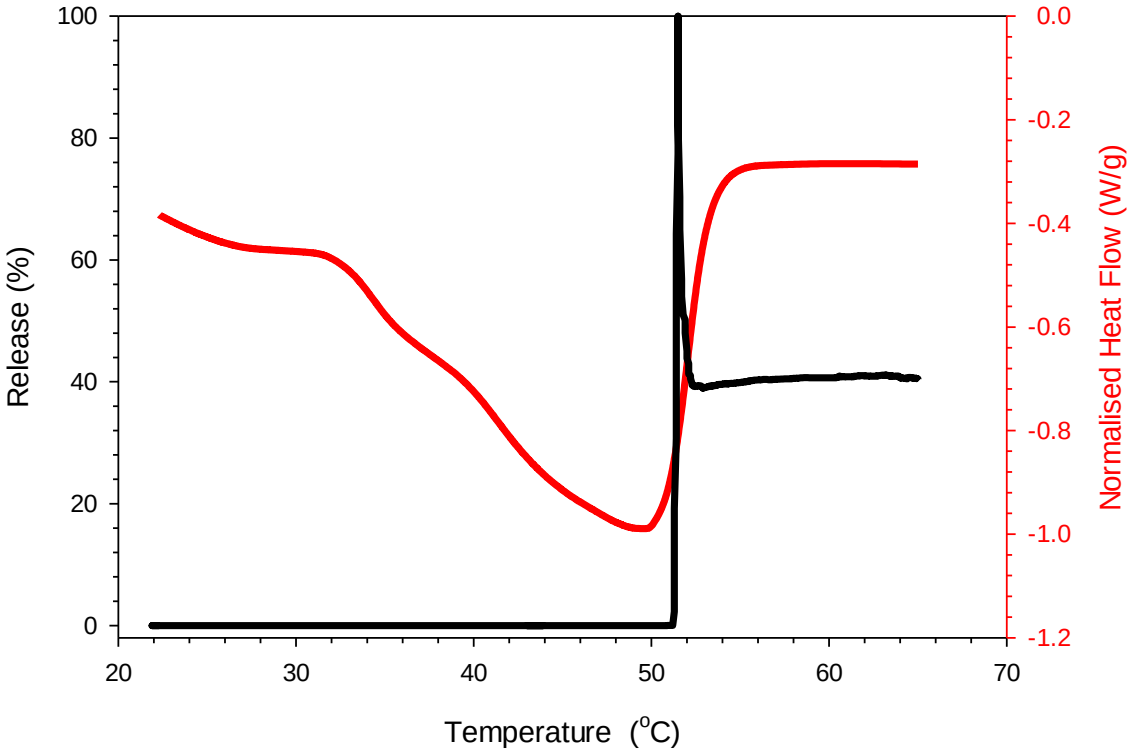

Figure 6.12 - Release curve of bleach from moulded soy wax capsules, stored for 7 days in DI water (black) alongside the DSC thermogram of soy wax melting (red). Data plotted are mean averages from three measurements.

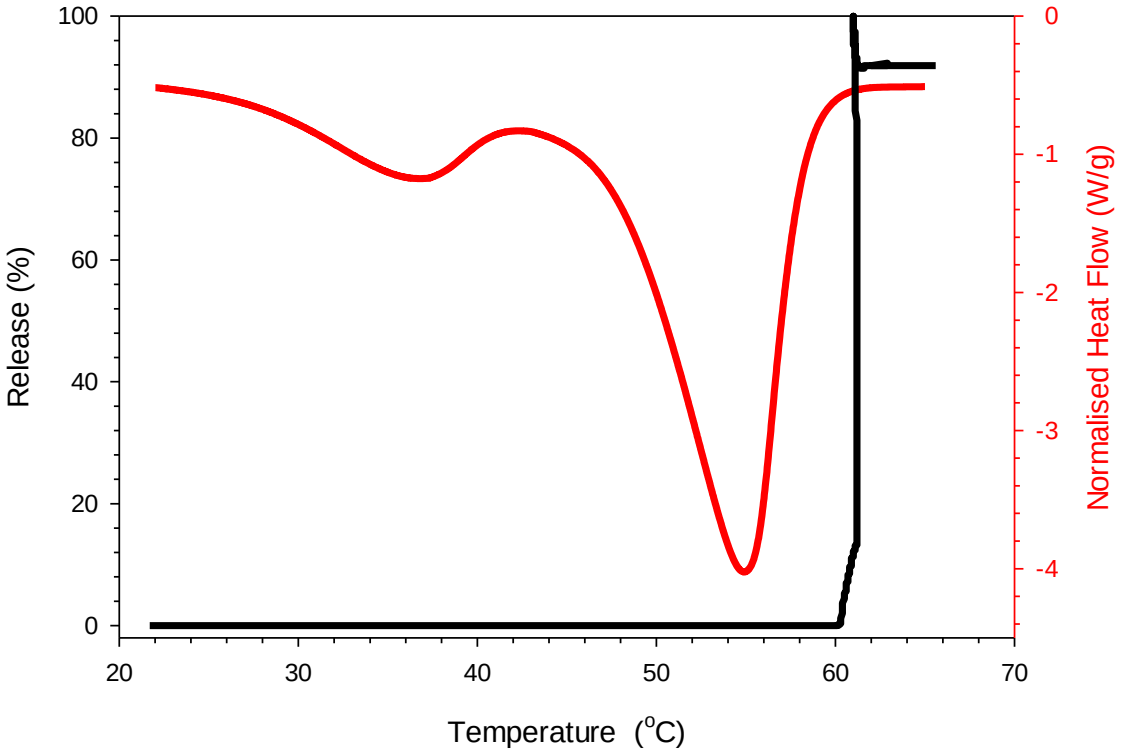

Figure 6.13 - Release curve of bleach from freeze dropped paraffin wax capsules, stored for 7 days in DI water (black) alongside the DSC thermogram of paraffin wax melting (red). Data plotted are mean averages from three measurements.

For the freeze dropped paraffin wax capsules, the release spike was seen at a slightly higher temperature compared to the moulded capsules – at approximately 61 °C instead of 57 °C. This could be that the crystal structure of the wax changed during the super-cooling in liquid nitrogen, which enhanced its thermodynamic stability and hence slightly raised the melting temperature. To confirm this, it would be pertinent to perform some additional DSC analysis on some paraffin wax that had been super-cooled in liquid nitrogen. However, the release temperature is still very similar to the target release temperature range, and hence the slight increase in melting temperature of the wax does not preclude its use as a controlled

release capsule. As with the other capsules, no leakage was seen up until the capsule melted and rapidly release its bleach payload, which was the target release mechanism.

6.4.5 Texture Analysis of Wax Capsules

Hardness analysis of the wax capsules was performed measuring by measuring the force require to compress the capsules using texture analysis, and these results are shown in Figure 6.14. The mechanical strength of the waxes can be important to characterise, as in many dishwashers the mechanical actions of the washing process can stress the tablets, possibly to the point where they mechanically break and release their payload prematurely. Additionally, a greater hardness will be more resistant to damage during transit and storage.

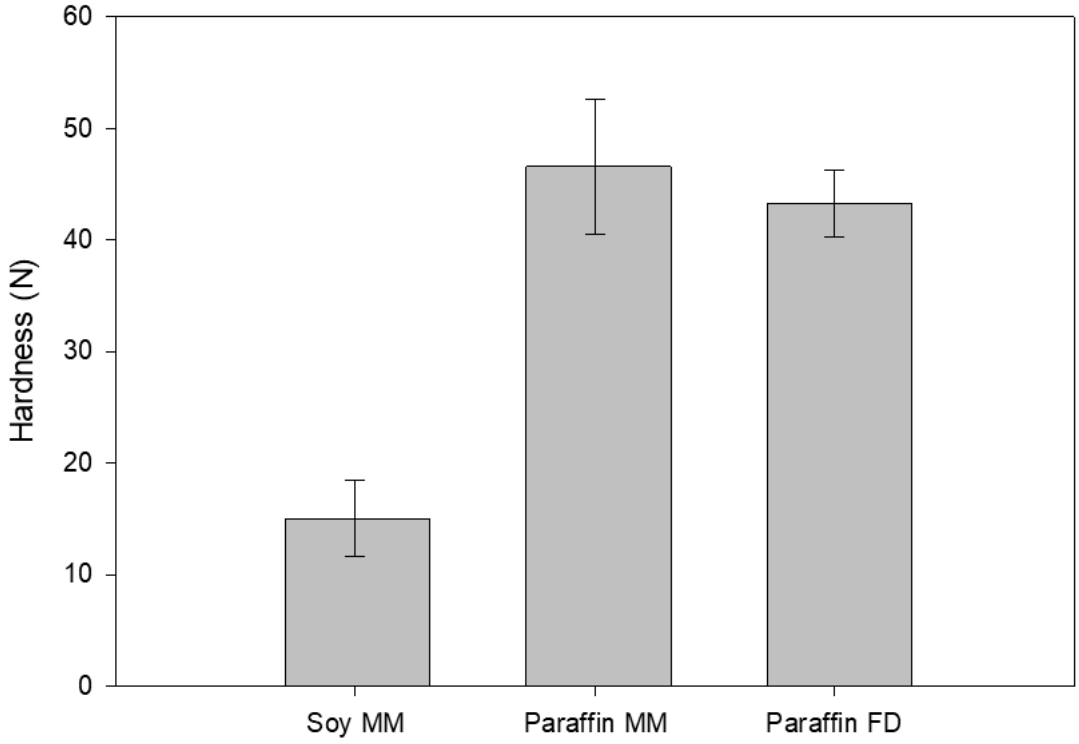

Figure 6.14 - Hardness of wax capsules measuring using TA. Each value is a mean average from at least three measurements, and error bars represent standard deviation.

The moulded soy wax capsules were measured to be significantly less hard than the moulded paraffin wax capsules, as these were measured to have a hardness of 15 N compared to approximately 45 N in the paraffin wax capsules. This is expected, as the DSC results showed a lower enthalpy of crystallisation and a lower temperature of crystallisation in the soy wax compared to the paraffin wax. These data indicated a lower degree of wax crystallisation in soy wax and the average chain length of the wax molecules in soy wax are shorter than in paraffin wax. Generally, shorter chain-length waxes have been shown to be less hard than longer chain-length waxes (Fei et al., 2018). When comparing the freeze dropped and

paraffin wax capsules, there was no statistical difference between the two methods, hence there was no mechanical advantage or disadvantage to producing capsules using either method.

6.5 Conclusions

Wax capsules containing sodium hypochlorite bleach were successfully manufacturing using two different methods and two different waxes. Encapsulation of smaller molecular weight molecules such as bleach requires special attention to ensure that the porosity is low enough to slow or stop diffusion of the bleach ions out of the capsules. It was shown that both the moulding method and freeze dropped method was successful at producing capsules which showed good storage stability, however the freeze dropped method was measured to have a higher encapsulation efficiency and better storage stability than the moulding method. Texture analysis showed that the use of paraffin wax gave capsules which were approximately three times harder than capsules producing using soy wax, however the choice of capsule production method had no measurable impact on the mechanical hardness of the capsules. Further work may involve refinement of the freeze dropping method to improve encapsulation efficiency and extending the choice of waxes and encapsulated payloads.

6.6 References

Chun, K. W., Theiler, R. F., Baumgarten, M. I., & Gabriel, R. (1990) *Machine Dishwashing Detergent Tablets,* United States Patent and Trademark Office, US5133892. Retrieved from https://patents.google.com/patent/US5133892A/en (Accessed: 1 April 2019).

Fei, T., Walker, J. A., Vickerman, K. L., Stanley, L. M., Jarboe, D., & Wang, T. (2018). Synthesis and characterization of soybean oil-based waxes and their application as paraffin substitute for corrugated coating. *Journal of Industrial and Engineering Chemistry*, *58*, 113–122. https://doi.org/10.1016/J.JIEC.2017.09.015

Gambogi, J., Kennedy, S., & Ambundo, E. (2009). Part E: Applications - Dishwashing with Detergents. In U. Zoller (Ed.), *Handbook of Detergency* (pp. 39–65). Boca Raton, FL: CRC Press Taylor & Francis Group.

Geonzon, L. C., Bacabac, R. G., & Matsukawa, S. (2019). Network structure and gelation mechanism of kappa and iota carrageenan elucidated by multiple particle tracking. *Food Hydrocolloids*, *92*, 173–180. https://doi.org/10.1016/j.foodhyd.2019.01.062

Goertz, J. P., Demella, K. C., Thompson, B. R., White, I. M., & Raghavan, S. R. (2019). Responsive capsules that enable hermetic encapsulation of contents and their thermally triggered burst-release. *Materials Horizons*, *6*(6), 1238–1243. https://doi.org/10.1039/c9mh00309f

Mellema, M., Van Benthum, W. A. J., Boer, B., Von Harras, J., & Visser, A. (2006). Wax encapsulation of water-soluble compounds for application in foods. *Journal of Microencapsulation*, *23*(7), 729–740. https://doi.org/10.1080/02652040600787900

Milanovic, J., Manojlovic, V., Levic, S., Rajic, N., Nedovic, V., & Bugarski, B. (2010). Microencapsulation of flavors in carnauba wax. *Sensors*, *10*(1), 901–912. https://doi.org/10.3390/s100100901

Olson, K. E. (1989) *Water insoluble encapsulated enzymes protected against deactivation by halogen bleaches*, United States Patent and Trademark Office, US4965012, Retrieved from https://patents.google.com/patent/US4965012A/en?q=~patent%2FUS20020137648A1&sort=new&page=2 (Accessed 1 April 2019).

6.7 Appendix

Table S7.1 – 3D printing parameters used for the manufacturing of PLA casts, as discussed in section 2.2.1.

Parameter	Value
First layer height	0.20 mm
Layer height	0.12 mm
Fill density	10 %
Fill pattern	Hexagonal
Perimeter shells	4
Top solid layers	4
Bottom solid layers	4
Resolution	High
Print speed	50 mm / s
Extruder temperature	200 °C
Platform temperature	65 °C

7

Conclusions & Future Work

7.1 Conclusions

The following section will seek to summarise the key findings of the previous experimental chapters, noting the importance of the findings in the context of this thesis and the wider scientific literature.

7.1.1 Biopolymer gels with non-ionic surfactants

In Chapters 3 and 4 of this thesis, work was presented in which biopolymer gels were formulated to encapsulate non-ionic surfactant. The aims were to: encapsulate a sufficient quantity of non-ionic surfactant inside the biopolymer gel for a detergency application; to produce gels which had a melting temperature between 30 and 40 °C and 'sufficient' gel strength to withstand handling; to understand the impact that the non-ionic surfactant had on the microstructure and properties of the biopolymer gel. From reviewing the literature on suitable gel systems, kappa carrageenan and low acyl gellan gum with tamarind seed xyloglucan were the two gel formulations tested in Chapters 3 and 4 respectively.

7.1.1.1 Kappa carrageenan with non-ionic surfactants

Rheology and DSC were initially used to identify which, if any, concentrations of kappa carrageenan would be suitable to form gels with a melting temperature between 30 and 40 °C - 0.6% w/w kappa carrageenan was identified as a suitable concentration. It was found that the introduction of non-ionic surfactant to the formulation resulted in an increase in gelling temperatures, melting temperatures

and gel strength, which indicates that the introduction of surfactant enhanced the helical aggregation of kappa carrageenan. The mechanism of the increase in helical aggregation was further elucidated using turbidity measurements, which showed a clear decrease in turbidity of the gel solutions upon addition of the non-ionic surfactant: this was estimated to be due to larger carrageenan aggregates forming, which reduced the number of overall carrageenan aggregates. The release measurements proved that the carrageenan gels were able to show burst-type release at 40 °C, however some gel erosion was measured at temperatures below the melting temperature, due to diffusion of the counter-ions from the gel structure. These findings proved that non-ionic surfactant could be encapsulated and released with a temperature trigger, hence providing one potential formulation for the proposed dishwasher detergent system.

7.1.1.2 Low acyl gellan gum and tamarind seed xyloglucan with non-ionic surfactant

Low acyl gellan gum and tamarind seed xyloglucan was identified as a gel formulation with relatively unique properties: good gel strength and low thermal hysteresis. Once again, rheology and DSC were used to study the properties of the gel system, with and without non-ionic surfactant. It was found that 0.5 wt% LAG with 1.5 wt% TSX was the most 'suitable' formulation tested, and the introduction of non-ionic surfactant led to small but measurable increase in phase transition temperatures and storage moduli. The release tests were performed by monitoring conductivity in water, as for the kappa carrageenan gels, and it was found that at

30 and 40 °C complete melting was achieved in several minutes, whereas at 20 °C the erosion of the gels took several hours. The gel strength was greater than that of the 0.6 wt% kappa carrageenan gels, and the gels were more resistant to erosion at temperatures below the desired melting point, hence it can be concluded that the LAG/TSX gels showed improved performance compared to the kC gels. This chapter, therefore, found a more "successful" encapsulation system than what was previously reported, which therefore has more potential as commercial detergent product.

7.1.2 Biopolymer gels with α-amylase

The two gel formulations previously studied – kappa carrageenan and low acyl gellan gum with tamarind seed xyloglucan – were investigated to see if they could encapsulate and selectively release α-amylase at a temperature of 35 – 40 °C. A photometric assay based on Benedict's reagent was used to measure the activity of the amylase enzyme, and it was found that melting-triggered release was obtained. The kappa carrageenan gels, when placed in the release medium below their melting temperature, showed significant erosion and subsequent premature release of the enzyme, however the LAG/TSX formulations were much more effective at retaining the enzyme at temperature below the melting point. The introduction of enzymes to the gel formulations led to small changes in the rheological properties and phase transition temperatures of the kappa carrageenan gels, however the LAG/TSX gels showed much larger changes. The mechanism of the interaction between the enzymes and biopolymer molecules was

not investigated and would be interesting to characterise. This chapter provided further evidence that a hydrocolloid gel system could be used as a detergent encapsulate, by showing successful retention and release of the amylase enzyme.

7.1.3 Wax encapsulation of bleaching salts

The work presented in this thesis suggested three different methods for manufacturing wax capsules, two of which were previously reported, and one was novel to this work. The freeze dropping technique, novel to this work, was found to have the highest encapsulation efficiency and lowest leakage during storage, indicating an improvement to incumbent wax encapsulation techniques. The method of manufacturing did not influence the mechanical properties of the capsules, whereas paraffin wax was shown to be much harder than soy wax. Thermoselective release of the bleach from the wax capsules was achieved in the target temperature range of 50 to 60 °C, and leakage was low in all capsules over a period of one week in water or salt solution. The osmotic pressure difference between the inside and outside of the capsule was shown to be a primary cause of leakage from the capsule. By combining a wax-encapsulated bleach system with a gel-encapsulated surfactant and enzyme system, three essential dishwashing detergent ingredients could theoretically be encapsulated together in a single product, and released with a temperature trigger, thus accomplishing real-life application of the initial inception. It is reasonable that an industrial product could be manufactured using the materials and methods outlined in this thesis, which

could theoretically provide greater detergency performance than incumbent products.

7.2 Areas for future work

The work presented in this thesis laid out some interesting and novel materials and techniques to encapsulate and selectively release dishwashing detergent ingredients at pre-determined temperatures. In the process of writing this thesis, several areas were identified as topics which could benefit from further scrutiny, and these topics will be discussed in the following section.

Firstly, it would be interesting to examine the exact mechanical requirements of a biopolymer gel to perform well during storage, handling and application. For example, the 0.6% kC gels were quite weak gels, and to be successful in application they must resistant mechanical breakage prior to the target release temperature. None of the formulations were inserted into a dishwasher, due to the inherent difficulties with measuring the tablet breakdown *in situ* inside a sealed dishwasher unit.

Additionally, although the mechanism of interaction between low acyl gellan gum and tamarind seed xyloglucan was suggested as a coupled biopolymer network, it would be prudent to perform some additional analysis which could directly

elucidate the microstructure of these gels, such as ^{1}H NMR, ^{13}C NMR, fluorescent tagging and microscopy or more in-depth rheological studies. By understanding the microstructure of the LAG/TSX system, better understandings can be gained of the effect that encapsulated molecules have on the microstructure and hence gel properties.

The novel freeze dropping method presented in this work was shown to produce well-sealed capsules at high encapsulation efficiency. Due to time constraints, only limited work was done on refining the technique. More time spent on this could produce capsules with greater encapsulation efficiency, and it could also be investigated the extent to which other waxes and payloads could be used to create capsules with this technique. Additionally, only one capsule size was tested using the freeze dropping method, and it could be interesting to examine the influence of capsule size on properties such as storage stability, encapsulation efficiency and mechanical strength.